Statically balancing using an elastic actuator that is efficiently adjustable in all positions

The Master Thesis of:

Jesse van Dongen

Delft University of Technology
Faculty of Mechanical, Maritime and Materials Engineering
Department of BioMechanical Engineering

Student Number: 1316125
Master Exam: Excie034-2013

Preface
This report shows my master exam paper on statically balancing using an elastic actuator that is efficiently adjustable in all positions. The results discuss the possibility of balancing a pendulum without a fixed vertical reference. Over the last year I learned a lot regarding building and creating prototypes, and searching and reading through scientific literature. It seems that a paper never feels completely finished, and if I could I would like to create a whole new second prototype and continue till everything is deemed perfect (if it ever is). This shows that even with a single assignment that the time always goes by quicker than you think.

I would like to thank Just Herder from TUdelft , together with everybody at InteSpring BV (especially Giuseppe Radaelli ,Emile Rosenberg and my supervisor Milton Aguirre) for their support in guiding me through the steps of my master thesis. Finally I would like to thank my exam committee for their patience with me handing in my report. Writing has never been my strongest asset, making the creation of this paper a big struggle for me, however I hope that I will take the readers on a pleasant and interesting journey.

CONTENTS

Statically balancing using an elastic actuator that is efficiently adjustable in all positions1

Excie034-2013

STATICALLY BALANCING USING AN ELASTIC ACTUATOR THAT IS EFFICIENTLY ADJUSTABLE IN ALL POSITIONS

Jesse van Dongen
Department of Mechanical Engineering, Faculty of
Mechanical, Materials and Maritime Engineering,
Delft University of Technology
Delft, The Netherlands
Email: Jesse.v.dongen@gmail.com

ABSTRACT

Technologies exist that equilibrate the effects of gravity; however there are limitations to these technologies. Spring based gravity equilibrators require an always present vertical reference, while in some cases, like on devices worn on the human body there is no part that is always vertical.

The goal of this paper is to conceptualize, build and evaluate a regenerative elastic actuator that can adjust its output force efficiently at any position, for the application of gravity equilibration.

A concept and eventual prototype was realized by adjusting perpendicular to the driving force, and dividing the problem into many sub problems. Results showcased, that the output force could be changed at any position, with the adjustment force being separated at the exception of friction.

Showcasing that it is possible to create an elastic actuator that is adjusted efficiently at any position, allowing for systems to be gravity equilibrated that otherwise cannot be.

NOMENCLATURE

x	position of the adjustment system [mm]
θ	deviation of a pendulum with the gravity vector [deg]
μ	mean value
σ	standard deviation
F_{out}	output force of the system [N]
F_{out_min}	minimum output force of the system [N]
F_{out_max}	maximum output force of the system [N]
F_{weight}	weight times the gravity constant [N]
η	energy efficiency [%]
s	slip [%]
t	time [s]

1. INTRODUCTION

Recent developments showcase an increased interest in energy efficient actuation. For example, vehicles are being equipped with Kinetic Energy Recovery Systems [1-3], and within the field of Robotics there is a search for actuators with recoverable energy [4-6]. Both in the field of Robotics and Prosthetics, gravitational forces generate a high energy cost to accomplish simple tasks, such as holding an object in space.

Technologies like statically balancing exist, which effectively equate the effect of gravity within a system; although current methods have various considerations and limitations that need to be taken into account. One of those limitations, in the special case of spring based balancers, is the requirement of an always present fixed vertical reference [7]. A second limitation lies in the energy efficient adjustability of such systems [1].

One application where a consistent vertical reference is not available is in the case of balancing on a non-fixed base, such as a human. In this example, this limits the utilization and functionality of spring balanced devices when used for exoskeletons and other systems where the base can change its orientation.

Similarly energy efficient adjustability at any moment or position, allows for the creation of a "Very Versatile Energy Efficient" actuator that is able to store energy for any force profile generating negative work on the load [4].

The goal of this paper is to design and evaluate an energy efficient elastic actuator (an actuator that utilizes an elastic energy source) capable of efficiently changing its stiffness

---

[1] A literature search (See Appendix O) found systems that could be energy efficiently adjusted at a single position, systems that could be energy efficiently adjusted when locked, but only 3 systems that could be energy efficiently adjusted in all positions. See appendix X

profile demonstrated by the example of statically balancing a pendulum on a sloped surface.

This paper will present a short introduction to the problem of statically balancing without a fixed reference, followed by a problem analysis and subdivision. This generates requirements, for the design and creation of a prototype, which will be built evaluated and discussed.

2. METHOD
Detailed Problem Description: Balancers Without Fixed Reference

When operating a device against external forces, such as those induced by gravity there will be energy costs. Balancing methods have been created to negate the influence of external forces on a system, lowering the operating energy costs of the system.

Two common methods to balance a system against gravity are balancers based on counterweights or spring mechanisms (See appendix A for more details)

While spring based balancers offer some big advantages over counterweight systems with regard to the systems overall size and weight, they require a fixed vertical gravity reference.

For example, in systems with multiple degrees of freedom, like adding pendula in series, when balanced with springs, a mechanism needs to be attached that passes through the reference of the gravity orientation for each individual pendula. The most common solution utilizes four-bar mechanisms [8].

Systems exist that work by balancing the effective center of mass (referenced through a bar linkage) [9]. However those systems still require a lot of parts when compared to mass balanced pendula, which can simply be stacked.

Secondly, in systems where there is no location fixed relative to the gravity vector, a new problem surfaces as there is no longer a direct location the balancer can be fixed to. An example of such a case is displayed in **Figure 1**, while a counterweight based balancer will continue to function when the base is rotated, a spring based balancer will lose its orientation with respect to gravity and lose its ability to balance.
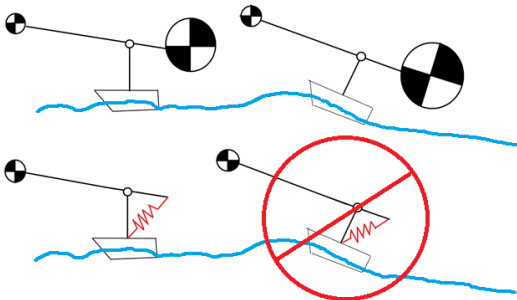

Figure 1. A showcase of a counterweight and spring based balancer when the base is rotated. As the base is a reference for the direction of gravity for a spring based balancer, it will stop functioning when the base is rotated.

A similar issue occurs with balancing systems that can be worn on the human body. A patent from Agrawal et al [10] balances the weight of a human's leg, the orientation of the torso is used as a vertical reference, meaning that if the torso is no longer straight up (e.g. bending forward) the device will no longer show the desired behavior of balancing the leg. As there is no part of the human body that is always vertical, currently having a spring balanced device that always balances correctly requires a connection to the outside world as seen in the patent of Ou Ma et al [11].

In general the advantages of a spring balanced system are often desired in applications where size, inertia or total mass play an important role. Similar criteria are often desired in systems that need to be able to move or be transported, and it is exactly those devices that often do not have a fixed reference to the ground. This creates the demand for a spring balanced system that can still operate without fixed reference.

With an understanding of the problem, it becomes important to define the design criteria. These are based on the requirements for the device to function and the ability for the device to be competitive against other balancing methods.

Requirements For Functioning

Comparing the required moments of an inverted pendulum starting in an upright position relative to the ground on both a horizontal and slanted surface (**figure 2**) it can be seen that the required sinusoidal balancing torque encounters a phase shift with respect to the ground. Notice that the moment curve of the pendulum relative to gravity direction remains unchanged.

With the possibility of a phase shift between 0 and 90° (for instance mounting the pendulum on a vertical wall instead of on the ground),for any angle between the arm of the pendulum and the ground surface, the applied torque should be able to vary from the minimal torque to the maximal torque.

This generates the first desired property:

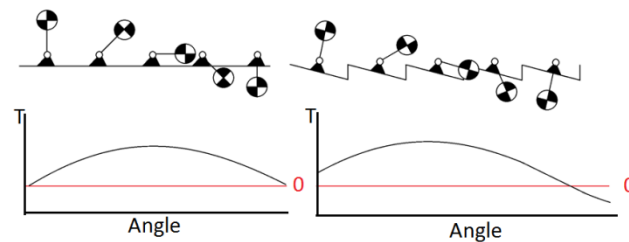1) At any position the balancer should be able to change between the minimal and maximal torque.

figure 2. Showcase of the required moments of an inverted pendulum at various positions relative to the ground underneath. On the left the case with a level ground is depicted, while on the right the case with a slanted surface is presented, the slanted surface showcases the need for a phase shift in the effective balancing force.

Desires For Competitiveness

The first main desire concerns one of the main advantages for statically balanced systems; the low force and energy requirements for operation.

If a statically balanced system would require big (energy consuming and heavy) actuators to adjust the system, it would undo its advantages. From which follows, that ideally the adjustment mechanism should adjust the applied torque without any energy cost. This leads to the main desire for such a system:

1) Changing the torque should be energy efficient and ideally force free [2]
2) The total system should be able to energy efficiently withdraw and store energy

The major advantage of a spring based balancer over a counterbalanced system is the size and weight. Therefor unless the device can continue to compete on these fields, the use of simpler counterbalanced system would always be preferred, generating the second desire for such a system.

3) The weight of the system should be smaller than the total balanced weight.

The final desire stems from the assumption that the system will likely become more complex and expensive than traditional methods of balancing. If the system is able to adjust the force output at any time, it would be nice if this could be utilized to not only change the phase of the balancing function but amplitude and shape as well. So that possible increases in complexity and cost could be covered by adaptability and added functionality of such a device.

4) Ability of adjustment of the balancing force at any point.

With the main property and desires defined, an overview can be generated, showcasing measurable design parameters.

Overview of the criteria and desires

Based on requirements and desires for the elastic actuator, and overview in **Table 1** and **Table 2** has been constructed.

The total efficiency is based on a personal desire to have an efficiency that is higher than most electric energy recovery devices. Slip is set at 0% to ensure no leakage from the energy storage. The gear ratio and range were added to the list to allow a pendulum to be offset 45° from a horizontal position for demonstrative purposes.

---

[2] A note should be made that a restriction exists on the ability to freely change the torque at any position without any energy costs. The average work done by the pendulum should remain zero, as otherwise the search for a perpetual motion device would be initiated.

Table 1. Requirements for the system

Property	Requirement
Ability for adjustment	$\forall \theta \quad x \in [x_{min}, x_{max}]$

Table 2. Desires of the prototype

Property	Desire
Total efficiency	$\eta > 75\%$
Slip	$s = 0\%$
Adjusting output force	$Corr(F\_Adjust, F\_output) = 0$
Adjusting output force	$F\_Adjust \ll F\_output\_max$
Total weight	$F\_weight < F\_out\_max$
Output range	$\angle \theta_{min} \theta_{max} > 90°$
Gear Ratio adjustment	$F\_out\_max / F\_out\_min > \sqrt{2}$
Ability to change profile	$f_x(\theta)_{t=0} <> = f_x(\theta)_{t=1}$

Main Process Diagram

In order to break down the design problem into multiple sub problems, the system was investigated using a closed feedback loop (**Figure 3**).

The total system was separated into 4 parts. The first part is an actuator that provides (or receives) energy from the pendulum when it changes its relative angle towards gravity. The second part is the pendulum itself. The third component is a sensor (electrical or mechanical) that measures the angle of the pendulum relative to the gravity vector. This device transfers the information of the pendulum to the fourth part; the controller that based on the angle of the pendulum provides the correct actuator setting to keep the pendulum balanced.
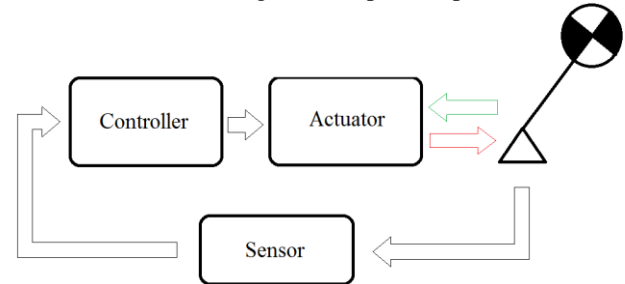

Figure 3. Closed loop block diagram showcasing a breakdown of components for balancing a pendulum using an elastic actuator. Double lines near the pendulum indicate the ability for the pendulum to provide and obtain energy to and from the actuator.

Both the sensor and controller could be mechanical or electrical; however the necessary controller and sensor depend on the functioning of the elastic actuator. As the actuator is the most critical component it was further broken down, into subdivisions.

Subdivision Into Energy Storage And Transfer

To break down the complexity of the elastic actuator its functioning is separated in 2 parts, Energy Storage and Energy Transfer (**Figure 4**).

The energy storage holds a buffer of energy that stores energy when the pendulum loses some of its potential energy, and releases energy when the pendulum needs to gain potential energy. The Energy transfer ensures that the energy from the Energy storage reaches the pendulum and vice versa.

To change the output towards and away from the pendulum, either the energy storage or the energy transfer need to change their throughput (**Figure 4**). To generate an overview of the possibilities, a search on literature has been conducted on these elements.
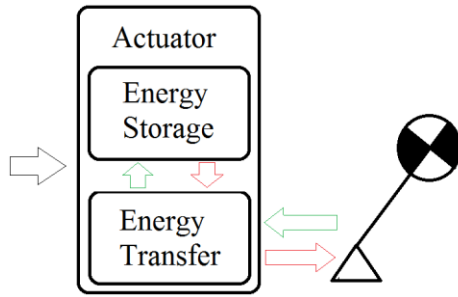
Figure 4. Zoom in on the actuator block of the closed loop block diagram, depicting a separation in energy storage and energy transfer as possible methods for altering the output torque.

As this papers focus is on an elastic actuator, only the utilization of elastic elements for energy storage was investigated (See appendix B). When using an elastic material as energy storage, the amount of energy stored is a function of the deformation and the material & geometric properties that give the energy storage element its stiffness. This generates the notion that the Energy Storage can be controlled by regulating the effective stiffness of the storage, and that the Energy Transfer can be controlled by changing and controlling the actual deformations applied on the elastic material (**Figure 5**).

Categories Of Adjustable Systems.

A search on literature (See Appendix O) allowed for the creation of the following subdivision. Systems that adjust the energy container can be grouped in the following categories

- Devices that adjust the pretension of a system [12-18]
- Devices that change the active part of the spring element [19-24]
- Devices that change how the system is loaded [25, 26]

Systems for changing the transmission ratio can be grouped in 4 categories

- Pendulum based adjustable balancers [6, 27-32]
- Path adjusting balancers [13]

- Lever CVT[3] based stiffness actuators [33-39]
- Other CVT[3] based stiffness actuators [40]

Within these categories the category of changing the energy storage through a CVT[3] showcased the most variety in technologies that could be utilized for energy efficient adjustment while under load. For this reason only the field of adjustable transmissions was used for concept generation.
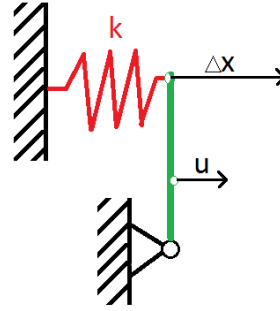

Figure 5: a simple demonstration of the separation in energy storage and energy transfer for a simple mechanism of a lever attached to a spring that follows hooke's law . The energy storage defines the spring stiffness (k) affecting the force generated for a certain spring deflection (δx) (in the figure the red spring element), while the energy transfer determines the amount of actual spring deflection (δx) based on an input displacement (u) (in the figure the green lever element).

Design And Prototype

With a defined set of criteria and desires, and a possible solution field for adjustability, concepts were generated. As all concepts follow the block scheme of **Figure 3**, for the sake of simplicity the final concept will be discussed based on the individual parts for the block scheme. The order of discussion will be about the energy transfer, energy storage, and finally the sensor and controller.

Energy Transfer.

Three concepts were generated for the function of altering the apparent output stiffness (**Figure 6**). 1.the Omniwheel CVT mechanism, 2.the   Ball CVT mechanism and finally 3. The Adjustable bar-linkage. For the used morphological table to generate the concepts please see Appendix N.

The omniwheel CVT mechanism showcases 2 friction wheels (**Figure 6** Top), changing the radius where the small wheel sits on the big wheel changes the transmission ratio.

However by using an omni wheel which is a special wheel that can move both laterally and transversally allows for

---

[3] CVT stands for Continuously Variable Transmission

moving the wheel (adjusting the transmission ratio) perpendicular to the direction of the applied force.

The ball CVT mechanism (**Figure 6** left), uses a friction ball between 2 rotating discs, by moving the discs away from each other the ball will roll (perpendicular to the driving force) towards new contact points on the discs. The ratio between the radius of contact on the lower disc and the upper disc generates the transmission ratio.

The adjustable bar mechanism (**Figure 6** right) got an input and an output link (the vertical links) that can transmit power to each other by rotation. Due to the ability to change the length of both the input and the top link, it is possible to change the transmission ratio between the in- and output-link without changing the position of these links, allowing for a theoretically energy free adjustment.
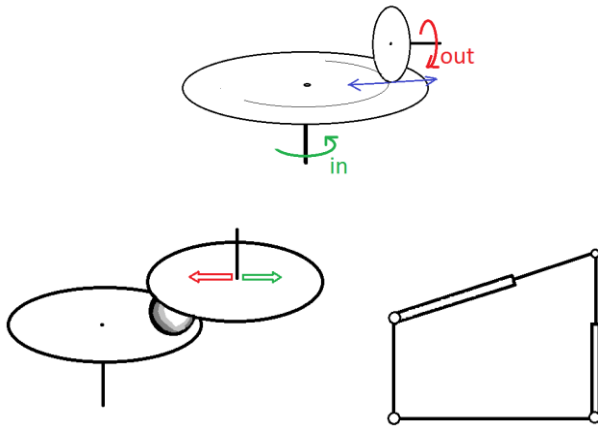
Figure 6. Showcase of 3 Concepts For Controlling The Effective Output Stiffness. Top figure shows the omniwheel CVT mechanism. The bottom left figure shows the ball CVT mechanism. The bottom right shows an adjustable bar-linkage

A comparison of the three concepts can be seen in **Table 3**, the usage of a linkages instead of friction, and planar operating space make the bar linkage the simplest concept. However the linearity and large range of motion add definite advantages for controllability for the ball and omni-wheel type CVT solutions. This easy controllability allows for the creation of a modular total system with exchangeable and individually testable parts. For this reason the decision was made to continue with the CVT concepts, the ballCVT was picked over the OmniwheelCVT due to expected issues with friction and roundness with most commercially available omni-wheels.

With energy transfer selected, an appropriate energy storage mechanism is needed to complete the elastic actuator.

Table 3. Comparison of different concepts

	Omniwheel	*BallCVT*	*BarLinkage*
Force transmission	Friction	Friction	Linkage
Dof for Adjustment	1	1	2
Constant input/output	Yes	Yes	no
Operating space	Spatial	Spatial	Planar
Range of Motion	360°	360°	~30°
Difficulties	Omniwheel roundness	Containing the ball	Correctly adjusting the double arms

Energy Storage.

The chosen energy transfer method provides a constant gear ratio between the in- and output shafts for a set adjustment setting. In order to keep this feature a desire is generated for an energy storage system that generates a constant output force.

Using mechanisms like linkages and snailcams [7, 27] it is possible to generate a constant output force out of any elastic element. Optimizing for low hysteresis, and high amounts energy storage per volume or weight unit [41-43] it becomes possible to pick the most ideal spring a system, for simplicity however an off the shelf constant force spring was used.

With both the energy transfer and the energy storage mechanism selected, the elastic actuator is now complete. The next parts in the block diagram are the sensor and controller.

Sensor & Controller – Mechanical or Electrical.

The sensor and controller could be mechanical or electrical. A mechanical system allows for a fully passive system, an electro-mechanical system requires a secondary power source, computational power and an actuator to adjust the elastic actuator. The main advantage of an electro-mechanical system is the possibility to change the force characteristic by making changes to the controller in software instead of hardware.

Electrical: With an electrical system (**Figure7**), an accelerometer is used as sensor to measure the pendulums position relative to the gravity vector, and a computer controlled linear actuator that adjusts the elastic actuator in generating the correct balancing torque for the pendulum.
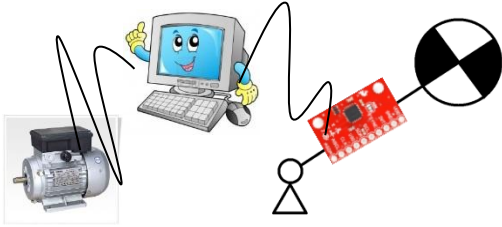
Figure 7. Simplified showcase of an electrical setup, an accelerometer measures the position relative to gravity; a computer interprets the results and sends it to an actuator that will adjust the system controlling the output torque for balancing the pendulum.

Mechanical: When balancing an inverted pendulum mechanically without knowledge over the gravity direction, a mechanical sensor is needed that senses the relative position of the gravity vector compared to position of the pendulum. This could be free floating measuring pendulum, which through a linkage references the difference between the pendulum and the reference, as seen in the example of **Figure 8**. Using computer based optimization ideal linkage lengths for generating the correct sinusoidal output can be found, together with ability to predict individual sensitivities to mass and friction changes for the complete connected mechanical system.
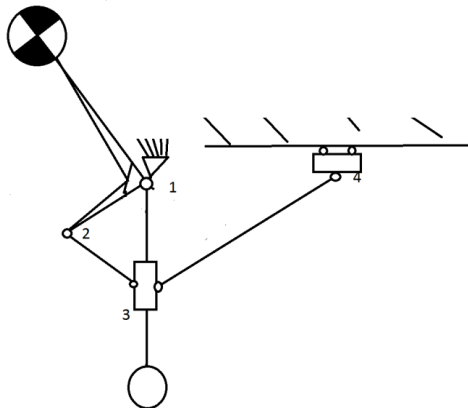
Figure 8. Showcase of a sensor and control system for a pendulum. The big pendulum, is referenced through a smaller pendulum, of which the difference is output through the slider on the right hand side (note the slide should be perpendicular to the direction of motion of the pendulum, but for simplicity is drawn in a 2d fashion).

Selection: The choice was made to continue with an electrical solution. An electrical system uses its own power source, making it less likely to be influenced by other parts.

Secondly, the ability to completely adjust the stiffness curve at any moment makes it possible to use this device for a broader range of applications than only balancing a pendulum,

and allow for more freedom in fine-tuning after a prototype has been build.

With this all components have been selected, allowing for the creation of designs (**Figure 9**) leading to a prototype.
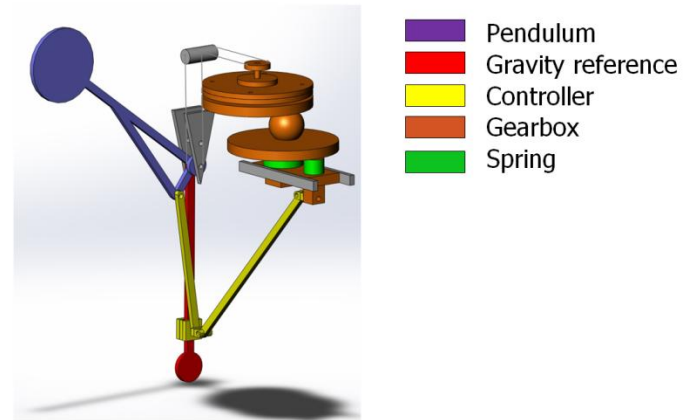
Figure 9. Conceptual drawing of the complete system. The figure shows a mechanical sensor and control system, which can be replaced with an electrical setup.

Experimental Evaluation

To verify if the theoretical concept and considerations were correct, a prototype was built (Apendix H) of the elastic actuator (**Figure 10**).

Materials & Building method.

As this prototype would only be used for demonstrative purposes about the working principle, materials were selected that are readily available, and allow for quick iterations when necessary. The system was modularly built allowing for testing of individual parts. To desire for low total weight was dropped to allow for easier construction with more modularity and adjustability.

The base frame to which all parts were connected was constructed out of aluminum ITEM profiles, these profiles contain a rail mounting system allowing for easy adjustment of all parts connected to it.

The majority of the custom components were made out of laser-cut stacked plates of acrylate (Appendix G). The primary reason for this is the quick turnover rate to fabricate new parts. Everything was assembled using bolts to allow for disassembly.

To minimize friction, all rotating parts were supported by ball bearings. For sliding parts drawer hinges (to save on costs) modified for lower friction were utilized. Teethed belts were used to couple mechanical connections over longer distances.

Bouncing balls and computer mouse balls were used for the power transfer between the top and bottom plate due to their relatively high friction coefficients yet low hysteresis, requiring a lower normal force to generate enough traction, and in turn requiring a lower stiffness of other components.

Sensor & Controller.

For the electronics the following components were used.

Sensor: MPU-6050; this 6-axis (Gyro + Accelerometer) motion tracking device senses the position of the pendulum in relation to the gravity vector. The sensor was mainly chosen for its ease of implementation and its relatively cheap costs.

Actuator: Alps RSA0N11M9 motorized slide potentiometer. To move the elastic actuator to a desired position preset, to generate the desired output force, a motorized slide potentiometer was used. Motorized slide potentiometers are used as audio faders in mixing boards making them cheap and readily available linear actuators.

Control interface: Arduino & Simulink, arduino's are affordable readily available prototyping boards to make a computer interact with electrical sensors and actuators. Due to personal preference Matlab Simulink was used as control interface. The sensor and actuator were controlled through a simple PID controller. For a total overview of the purchased parts see appendix D, for an overview of the electrical specs and wiring scheme see appendix E and F.

With the parts of elastic actuator defined, it becomes important to look into the evaluation method of the prototype.

Testing equipment.

Testometric M250-2.5CT; The testometric material/tensile/compression testing machine was used to conduct nearly all tests (Appendix I), it was used to: obtain detailed details about hysteresis, mechanical properties of components and for measuring the overall performance of the elastic actuator.

Other measurements were done with regular measurement tools such as a measurement lint, caliper, and a cellphone photo- and video camera.

Conducted Tests.

A series of tests was conducted to obtain detailed information about the correct functioning of the prototype and the quality of operation.

Ability to adjust the transmission ratio: To test the different transmission ratios the system was tested 3 times with four different conditions (1:1, 2:3, 1:3 and 0:1 gear ratios).

By connecting the output shaft of the elastic actuator with a pulley to the testometric tensile tester, hysteresis graphs were obtained from the different testing conditions. These graphs provided the following information:

- Range of adjustment of the transmission
- Efficiency of the transmission under different settings.

Force free adjustment of the transmission: As the ability to adjust the system freely at any position is an important desire for the overall design. 3 tests were performed based on the adjustment of the transmission. The slide controlling the output force was connected to the testometric tensile tester, measuring the forces required to move the slide by itself without the ball, with the ball but without the spring, and with both the ball and the spring. These graphs provided the following information:

- Indication of friction of the slide itself
- Indication of the additional friction due to the ball between the interfaces
- Indication of the additional friction introduced due to the forces applied on the ball.

Finally a series of tests was conducted to evaluate the individual force losses of components. To help the identification of main factors causing energy losses, and pin point the key areas for future development. Friction was measured for the individual parts in an unloaded case, slip measured over the top and bottom disc, and finally a hysteresis plot created on compressing the interfacing ball to investigate the viscoelastic effect to indicate rolling friction. These graphs provided the following information:

- Contribution of every part towards the total energy loss of the system.
- Identification of the main energy losses in the system

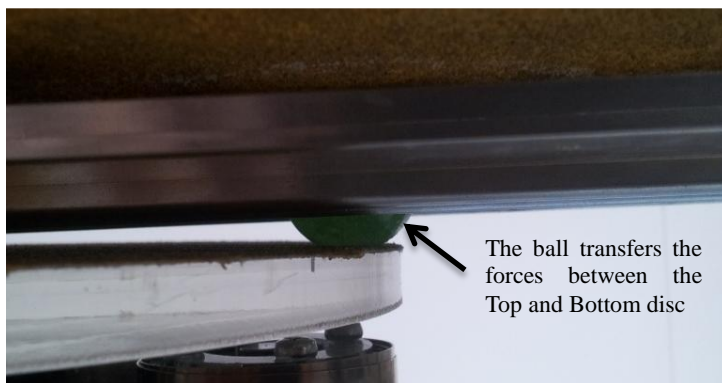A teethed belt connects the output shaft with the top disc
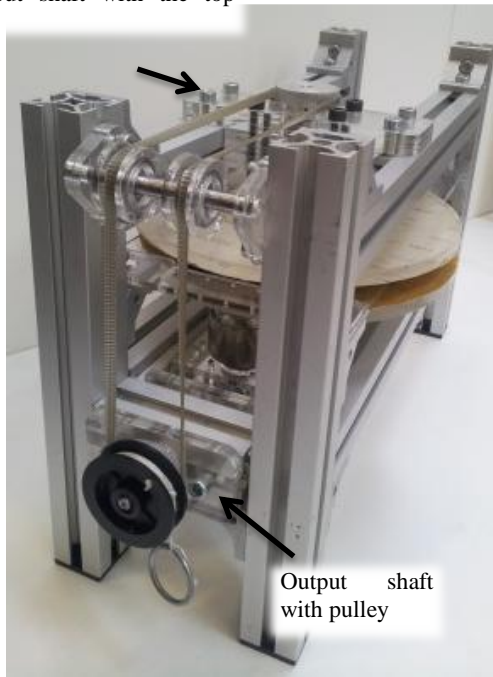
Top Disc

Output shaft with pulley
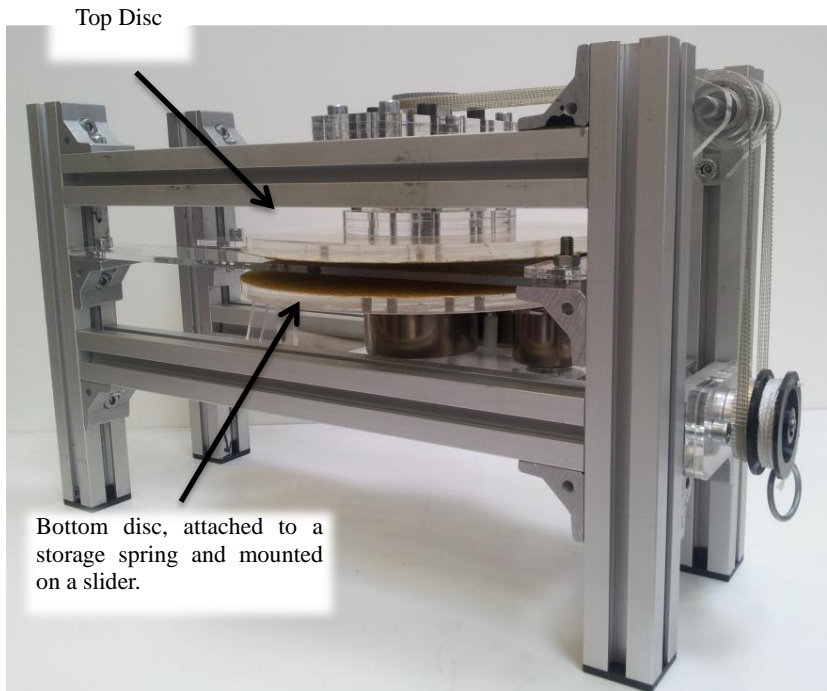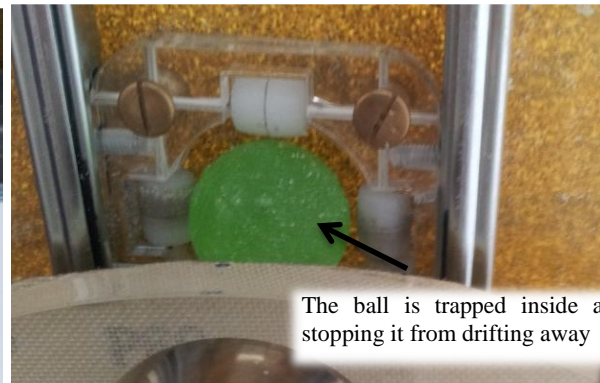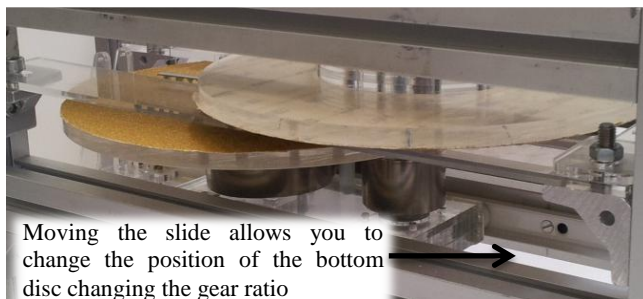
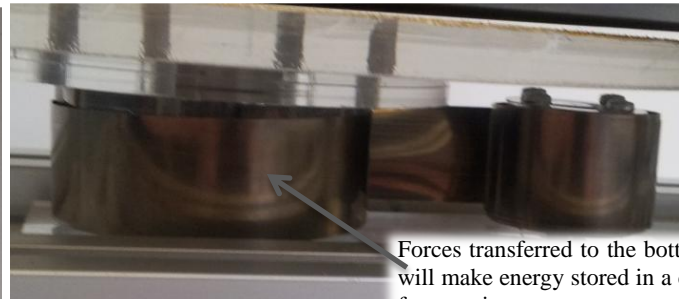Bottom disc, attached to a storage spring and mounted on a slider.

The ball transfers the forces between the Top and Bottom disc

The ball is trapped inside a cage stopping it from drifting away

Moving the slide allows you to change the position of the bottom disc changing the gear ratio

Forces transferred to the bottom disc will make energy stored in a constant force spring

Figure 10. Experimental test setup of the elastic actuator
- **Top figures: overview of the entire test setup, showcasing the output shaft (with attached pulley in the figure), top disc, bottom disc and spring assembly.**
- **Middle figures: to transfer forces between the top disc and the bottom disc, a caged ball acts as transfer medium.**
- **Bottom left: the bottom disc assembly is attached to a rail allowing the top and bottom disc to slide apart from each other, this changes the position of the ball on the discs and adjusts the transmission ratio between the top and bottom disc.**
- **Bottom right: close-up of the constant torque spring assembly attached to the bottom disc.**

3. RESULTS

Transmission Performance

The elastic CVT was tested in four positions, with a gear ratio varying from 1:1 to 1:0 (**Figure 11**). The resultant average output forces and their standard deviation have been plotted in **Figure 12** (raw measurement data can be found in Appendix J). The information in this figure can be used to create all sorts of different shapes like for instance that of a sinus for balancing a pendulum (**Figure 13**)

The found standard deviation originates mostly from the increased normal pressure due to the slightly inconsistent diameter of the ball (the raw data shows a periodic pattern equivalent to a half rotation of the ball). Measured efficiency for different gear ratios and the with measured slip for a full cycle can be found in **Table 4**.
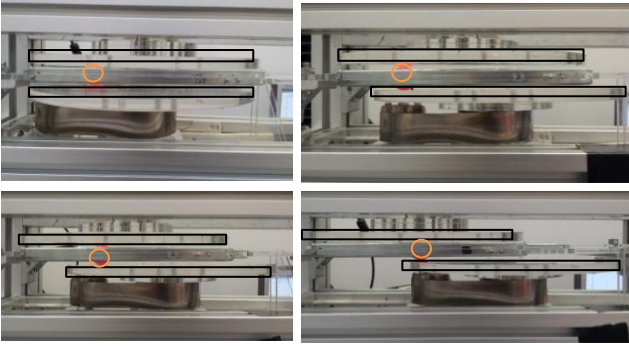
Figure 11. Testing efficiency of the system in 4 different positions
- **Top left the 2 discs are position vertically above each other generating a 1:1 gear ratio.**
- **Top right slight horizontal movement of the bottom disc, generating a 3:2 gear ratio.**
- **Bottom left figure depicts bigger movement of the bottom disc, generating a 3:1 gear ratio.**
- **Bottom right, in this figure the ball is directly above the shaft of the top disc, generating an 1:0 gear ratio aka freewheeling, for the top disc while the bottom spring system is locked.**

Table 4. Overview of the efficiency of the elastic actuator in different gear ratios

Gear Ratio	1:1	2:3	1:3	1:0
Efficiency	51%	50%	40%	0%
Slip	8%	0%	0%	100%
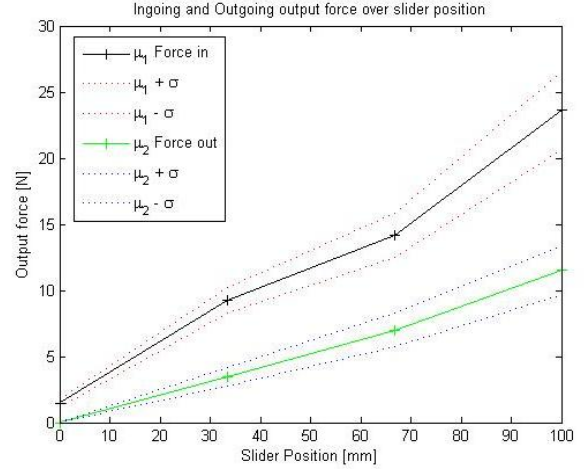
Figure 12. Showcase of different required in and output forces of the elastic actuator for different slider positions (100 stands for a 1:1 gear ratio, while 0 stands for a 0:1 gear ratio)
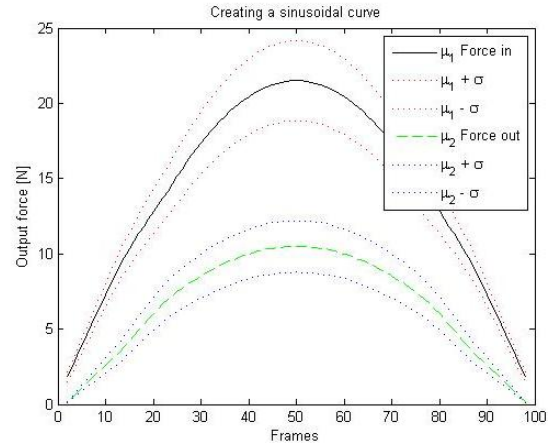
Figure 13. Changing the position of the force adjustment slider over time allows you to generate a different stiffness curve, in this case a sinusoidal curve was generated.

Performance Of the Force Adjustment Slider

The second series of tests evaluated the forces required to adjust the slider position (which changes the actuators output forces). The results of these tests and their conditions have been summed up in Table 5 (raw measurement data can be found in Appendix K)

Table 5: Friction Forces When Changing Gear Ratio

Slide Condition	μ	σ
Free sliding	0.89N	0.17N
Sliding with ball	1.41N	0.31N
Sliding with ball & spring	3.12N	0.76N

The stiffness of the discs is lower on the outer radius than inner, creating a difference in normal pressure and rolling friction depending on the balls location when moving the slide as seen in y1 in **Figure 14**. Adding the spring to the system shows another declining slope y2. Subtracting these from each other leaves slope y3.

As the additional force transmitted over the ball due to the spring varies between 5.8N and 2.9N, while the compression on the ball to generate enough friction lies in the order of 15N (2.5mm compression see **Figure 15**) means that the added pressure on the ball likely does not cover the Force difference. Instead the slope of line y3 is most likely caused by the spring force acting sideways on the slide assembly, making the slide pressed against the side increasing the friction.
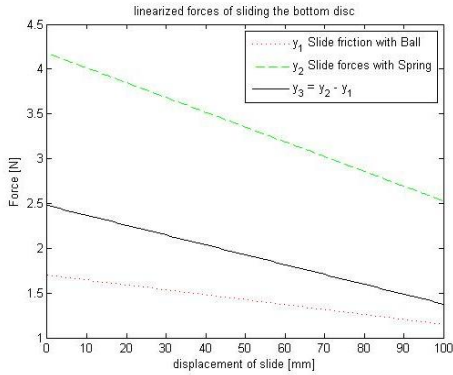
Figure 14. Measured linearized forces for different conditions when changing the force adjusting slide from one position to the other.

Force Losses Breakdown

The final section of the results aims to generate an overview of the force losses due to individual components, for this purpose a wide selection components have been measured as can be seen in **Table 6** (raw measurement data can be found in Appendix M). Based on the results from this table a rough overview of the losses for four different gear ratios has been constructed in **Table7**.
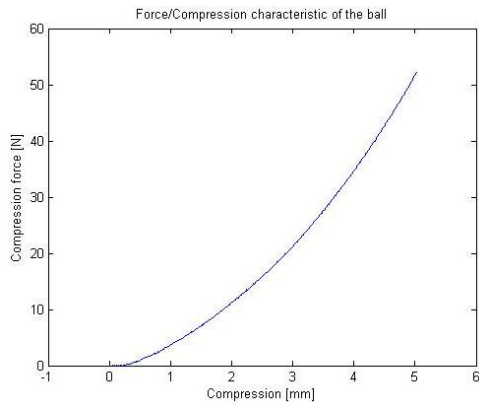
Figure 15. force/compression characteristic of the force it takes to compress the ball between the top and bottom disc. Table 6. Overview of individual forces of sectioned parts

System Components	μ	σ
belt + topdisc	0.7N	0.2N
top + ball (center) no cage	2.6N	1.4N
Top + ball (3/4th) no cage	2.2N	1.0N
Top + ball (end) no cage	1.8N	1.0N
bottom disc + spring upper	18.2N	0.6N
bottom disc + spring lower	15.8N	0.9N
Ball rolling friction	~0.3N[4]	NA
Full System 1:1 ratio upper	23.6N	3.0N
Full System 1:1 ratio lower	11.5N	1.9N
Full System 1:1 8% slippage losses	~3N[4]	NA
Full system 2:3 ratio upper	14.2N	1.7N
Full system 2:3 ratio lower	6.7N	1.3N
Full system 1:3 ratio upper	9.3N	1.0N
Full system 1:3 ratio lower	3.5N	0.7N
Full System 0:1 ratio	1.5N	0.3N

Table 7: Overview Of The Force Losses Per Gear Ratio

Ratio	Force loss	Belt & Top	Ball Roll	Ball Slip	Spring & Bottom	Deficit
1:1	12N	-1.4N	-3.8N	-3N	-2.4N	1.4N
2:3	7.5N	-1.4N	-3.4N	0	-1.6N	1.1N
1:3	5.8N	-1.4N	-2.6N	0	-1N	0.8N
0:1	1.5N	0.7	0	0.8N	0	0

These tables show that the forces of adding the ball, take away the biggest percentage of efficiency, followed by the actual elastic element.

Rolling friction of a ball is primarily caused by slip and viscoelastic hysteresis [44], with the slip already known the viscoelastic loss of the ball was measured (Appendix L) and calculated (Appendix C), however the calculated rolling resistance was an order of magnitude lower.

This means that the losses of the ball must be attributed to something else.

The 1:1 ratio measurement got 2 full rotations of the discs and multiple full rotations of the ball, meaning that losses due to gap difference or ball fluctuation should balance each other except for the rolling friction.

The forces for operation in the 0:1 ratio are pretty low, making it unlikely that normal forces on the bearings are the cause of this friction.

The most likely causes for the losses would either be the moments transferred through the discs during off centric loading or hysteretic deformation losses of the discs themselves. Finally the deficit losses of **Table7** are most likely the result of forces lost over the cage assembly that holds the ball in place.

---

[4] Denotes calculated estimations, not direct measurements

4. DISCUSSION

This research started with a desire to create an elastic actuator that is able to create any elastic characteristic at no energy costs for the purpose of statically balancing.

Although the statement of no energy cost is an utopian premise, a prototype has been created that shows a new "Very Versatile Energy Efficient" actuator.

Using the concept of a modified traditional Continuously Variable Transmission that always adjusts perpendicular to the driven force, an adjustable elastic actuator has been created that is different from other designs that use lever based designs [33, 38].

One of the main differences of this concept is that the adjustment of the output stiffness is always perpendicular to the output force. This means that there is only need for a single degree of freedom when adjusting the system. Secondly unlike other systems this elastic actuator is able to provide a full 360 degrees of rotation, and a linear relation between control input and system output.

As this system shows that it is possible to adapt and modify traditional CVTs intended for the transport industry, for operation as an elastic actuator. A new field is generated for possible collaborative research.

In terms of performance, while the efficiency was on the low end operating around 50% efficiency, while ball CVTs can obtain efficiencies as high as 97% (Appendix B). The elastic actuator did show that for a constant control setting a constant output force is generated, and that a max ratio change of nearly 16x can be attained. The high ratio change enables the device to generate sinusoidal curve with a range of nearly 180 degrees.

The adjustment from a low gear to a high gear is not fully energy free or fully independent from the output force. With currently $1/4^{th}$ of the max output force being required to drive the slide. However as the measured forces in the slide are a result of friction and not a decomposition of forces, better bearings should provide a better result.

While the friction in the slide is dependent on the normal forces applied to the slide, it is fully independent to the total energy transferred over the system. The ability for the elastic actuator to rotate over 360°, allows for lowering the forces transmitted through the actuator (and with that lowering the forces needed for adjustment), while keeping the total amount of transferred energy high.

A clear pitfall in the design resulted to be in the precision, which is partly attributed to the construction method and material selection. Slight deviations in the roundness of the interfacing ball or the spacing between the discs resulted big fluctuations of the output force, and even leading towards the addition of slip in the drivetrain. However as the construction method and material selection were based on modularity, ease of modification and making new iterations, a lot of improvements could easily be made by focusing on high stiffness, accuracy and precision.

Overall despite shortcomings the concept showcased the functioning of the concept. Although the system is not efficient enough and too big and heavy, there are a lot of opportunities for scaling the design down and increasing the efficiency.

The concept and design path investigated in the paper, show a lot of potential for future research. Devices like this could in the foreseeable future generate solutions for balancing devices with periodic movements that cannot be balanced with the current conventional solutions.

5. CONCLUSION

This paper shows the full process of designing and creating an elastic actuator. This paper describes a new set of criteria and desires for using an elastic actuator for the application of statically balancing.

As criteria the device would need to be able to adjust its output force at any position over its working range.

As desire the device would need to be competitive against other balancing devices, meaning energy efficient, lightweight, and able to change its force profile at any moment.

To allow for adjustment at all positions in an energy efficient fashion, 3 concepts were generated, that could adjust the output force at any position, perpendicular to the driving force. Based on the winning concept a prototype was built, and evaluated.

The evaluation of the prototype showed that the system could always be adjusted over its full range. Secondly the system successfully separated the energy needed for adjustment, from the energy that passes through its output. Making the prototype one of the, if not the, first elastic actuator, where the force adjustment is by design always perpendicular to the output, and thus energy efficient.

The functioning of this prototype shows that it is possible to adapt and modify traditional continuously variable transmissions, for the usage of elastic actuators, generating a large field for future research.

The linear relation between the adjustment setting, and the output force, allow for the ability to easily control the system. This ease of control could bring birth to a completely passive solution in the future.

The ability to rotate over 360 degrees, allows gears to be used to increase the amount of rotations, this means that a high amount of energy can be transferred at relatively low forces. This property, together with the usage of stiffer materials, make it likely to assume, that within a few years, a product could be made, that is competitive with other technologies, allowing for systems to be balanced that cannot be today.

In a world where energy efficient actuation is obtaining more awareness and importance every day, this device could potentially inspire the creation of a new branch of statically balanced energy efficient devices, with functionalities considered improbable till now.

REFERENCES

1. Boretti, A., *Comparison of fuel economies of high efficiency diesel and hydrogen engines powering a compact car with a flywheel based kinetic energy recovery systems.* International Journal of Hydrogen Energy, 2010. **35**(16): p. 8417-8424.

2. Boretti, A.A., *Improvements of vehicle fuel economy using mechanical regenerative braking.* International Journal of Vehicle Design, 2011. **55**(1): p. 35-48.

3. Walsh, J., T. Muneer, and A.N. Celik, *Design and analysis of kinetic energy recovery system for automobiles: Case study for commuters in Edinburgh.* Journal of Renewable and Sustainable Energy, 2011. **3**(1).

4. Stramigioli, S., G. van Oort, and E. Dertien, *A concept for a new Energy Efficient Actuator.* 2008 Ieee/Asme International Conference on Advanced Intelligent Mechatronics, Vols 1-3, 2008: p. 671-675.

5. Visser, L.C., R. Carloni, and S. Stramigioli, *Energy-Efficient Variable Stiffness Actuators.* Ieee Transactions on Robotics, 2011. **27**(5): p. 865-875.

6. Van Ham, R., et al., *Compliant Actuator Designs Review of Actuators with Passive Adjustable Compliance/Controllable Stiffness for Robotic Applications.* Ieee Robotics & Automation Magazine, 2009. **16**(3): p. 81-94.

7. Herder, J.L., *Energy-free systems: theory, conception and design of statically balanced spring mechanisms.*, in *Department of Biomechanical Engineering*2001, Delft University of Technology: Mekelweg 2, 2628 CD Delft, The Netherlands.

8. Lin, P.Y., W.B. Shieh, and D.Z. Chen, *Design of a Gravity-Balanced General Spatial Serial-Type Manipulator.* Journal of Mechanisms and Robotics-Transactions of the Asme, 2010. **2**(3).

9. Agrawal, S.K. and A. Fattah, *Gravity-balancing of spatial robotic manipulators.* Mechanism and Machine Theory, 2004. **39**(12): p. 1331-1344.

10. Agrawal, S., *Gravity balanced orthosis apparatus*, 2005.

11. Ou Ma, J.W., *Apparatus and method for reduced gravity simulation*, 2009.

12. Wolf, S. and G. Hirzinger, *A new variable stiffness design: Matching requirements of the next robot generation.* 2008 Ieee International Conference on Robotics and Automation, Vols 1-9, 2008: p. 1741-1746.

13. Nam, K.H., B.S. Kim, and J.B. Song, *Compliant actuation of parallel-type variable stiffness actuator based on antagonistic actuation.* Journal of Mechanical Science and Technology, 2010. **24**(11): p. 2315-2321.

14. Palli, G., et al., *Design of a Variable Stiffness Actuator Based on Flexures.* Journal of Mechanisms and Robotics-Transactions of the Asme, 2011. **3**(3).

15. Wang, R.J. and H.P. Huang, *An Active-Passive Variable Stiffness Elastic Actuator for Safety Robot Systems.* Ieee/Rsj 2010 International Conference on Intelligent Robots and Systems (Iros 2010), 2010.

16. Migliore, S.A., E.A. Brown, and S.P. DeWeerth, *Biologically inspired joint stiffness control.* 2005 IEEE International Conference on Robotics and Automation (ICRA), Vols 1-4, 2005: p. 4508-4513.

17. Hurst, J.W., J.E. Chestnutt, and A.A. Rizzi, *The Actuator With Mechanically Adjustable Series Compliance.* Ieee Transactions on Robotics, 2010. **26**(4): p. 597-606.

18. Kilic, M., Y. Yazicioglu, and D.F. Kurtulus, *Synthesis of a torsional spring mechanism with mechanically adjustable stiffness using wrapping cams.* Mechanism and Machine Theory, 2012. **57**: p. 27-39.

19. Hollander, K.W., T.G. Sugar, and D.E. Herring, *Adjustable Robotic Tendon using a 'Jack Spring'(TM).* 2005 Ieee 9th International Conference on Rehabilitation Robotics, 2005: p. 113-118.

20. N. Vrijlandt, J.L.H., *Seating Unit for supporting a body or part of a body*, L. Hoffman & Baron, Editor 2004: NL.

21. van Dorsser, W.D., et al., *Energy-free adjustment of gravity equilibrators by adjusting the spring stiffness.* Proceedings of the Institution of Mechanical Engineers Part C-Journal of Mechanical Engineering Science, 2008. **222**(9): p. 1839-1846.

22. Rodriguez, A.G., N.E.N. Rodriguez, and A.G.G. Rodriguez, *Design and validation of a novel actuator with adaptable compliance for application in human-like robotics.* Industrial Robot-an International Journal, 2009. **36**(1): p. 84-90.

23. Wang, R.J. and H.P. Huang, *Mechanically stiffness-adjustable actuator using a leaf spring for safe physical human-robot interaction.* Mechanika, 2012(1): p. 77-83.

24. Tonietti, G., R. Schiavi, and A. Bicchi, *Design and control of a variable stiffness actuator for safe and fast physical human/robot interaction.* 2005 IEEE International Conference on Robotics and Automation (ICRA), Vols 1-4, 2005: p. 526-531.

25. T. Sugar, K.H., *Adjustable stiffness leaf spring actuators*, USPTO, Editor 2009: US.

26. Wisse, B.M., et al., *Energy-free adjustment of gravity equilibrators using the virtual spring concept.* 2007 Ieee 10th International Conference on Rehabilitation Robotics, Vols 1 and 2, 2007: p. 742-750.

12

27. Duval, E.F., *Mechanical Arm Including A Counter-Balance*, USPTO, Editor 2008: USA. p. 1-82.

28. Barents, R., et al., *Spring-to-Spring Balancing as Energy-Free Adjustment Method in Gravity Equilibrators.* Journal of Mechanical Design, 2011. **133**(6).

29. Barents, R., et al., *Spring-to-Spring Balancing as Energy-Free Adjustment Method in Gravity Equilibrators.* Proceedings of the Asme International Design Engineering Technical Conferences and Computers and Information in Engineering Conference, Vol 7, Pts a and B, 2010: p. 689-700.

30. Van Ham, R., et al., *MACCEPA: the actuator with adaptable compliance for dynamic walking bipeds.* Climbing and Walking Robots, 2006: p. 759-766.

31. Vanderborght, B., et al., *MACCEPA 2.0: Adjustable Compliant Actuator with Stiffening Characteristic for Energy Efficient Hopping.* Icra: 2009 Ieee International Conference on Robotics and Automation, Vols 1-7, 2009: p. 179-184.

32. J.L. Herder, R.B., B.M. Wisse, W.D. van Dorsser, *Efficiently variable zero stiffness mechanisms.* Workshop on Human-Friendly Robotics, 2011. **2011**.

33. Visser, L.C., et al., *Modeling and Design of Energy Efficient Variable Stiffness Actuators.* 2010 Ieee International Conference on Robotics and Automation (Icra), 2010: p. 3273-3278.

34. Visser, L.C., R. Carloni, and S. Stramigioli, *Variable Stiffness Actuators: a Port-based Analysis and a Comparison of Energy Efficiency.* 2010 Ieee International Conference on Robotics and Automation (Icra), 2010: p. 3279-3284.

35. Kim, B.S. and J.B. Song, *Hybrid Dual Actuator Unit: A Design of a Variable Stiffness Actuator based on an Adjustable Moment Arm Mechanism.* 2010 Ieee International Conference on Robotics and Automation (Icra), 2010: p. 1655-1660.

36. Jafari, A., N.G. Tsagarakis, and D.G. Caldwell, *A Novel Intrinsically Energy Efficient Actuator With Adjustable Stiffness (AwAS).* Ieee-Asme Transactions on Mechatronics, 2013. **18**(1): p. 355-365.

37. Ghorbani, R. and Q. Wu, *Adjustable stiffness artificial tendons: Conceptual design and energetics study in bipedal walking robots.* Mechanism and Machine Theory, 2009. **44**(1): p. 140-161.

38. Rao, S., R. Carloni, and S. Stramigioli, *A novel energy-efficient rotational variable stiffness actuator.* 2011 Annual International Conference of the Ieee Engineering in Medicine and Biology Society (Embc), 2011: p. 8175-8178.

39. Tsagarakis, N.G., I. Sardellitti, and D.G. Caldwell, *A New Variable Stiffness Actuator (CompAct-VSA): Design and Modelling.* 2011 Ieee/Rsj International Conference on Intelligent Robots and Systems, 2011: p. 378-383.

40. Cicchitti, L., *Design and Implementation of a variable stiffness actuator*, in *Construzione di Macchine Automatiche e Robot LS*2009, Universita di Bologna: Italy.

41. Dieter Muhs, H.W., Manfred Becker, Dieter Jannasch, Joachim Voßiek, *Roloff / Matek Maschinenelemente*. 4th ed2005, Den Haag: Academic Service. 270-310.

42. Beek, A.v., *Advanced engineering design, lifetime performance and reliability*2006, Delft: Delft University of Technology. 500.

43. Cool, J.c., *Werktuigbouwkundige Systemen*2003, Delft: DUP Blue print.

44. Yung, K.L. and Y. XU, *Non-Linear Expressions for Rolling Friction of a Soft Ball on a Hard Plane.* Nonlinear Dynamics, 2003. **33**(1): p. 33-41.

45. Tolou, N., et al., *Stiffness Compensation Mechanism for Body Powered Hand Prostheses with Cosmetic Covering.* Journal of Medical Devices-Transactions of the Asme, 2012. **6**(1).

46. Soemers, H., *Design Principles for precision mechanisms*2010, Enschede: T-pointprint.

47. Hibbeler, R.C., *Mechanics of Materials, Sixth Edition*2005, Singapore: Prentice Hall.

48. Norman H. Beachley, A.A.F., *Continuously variable transmissions: Theory and practice*1979: Lawrence Livermore Laboratory.

49. Cuypers, M.H., *Continu variabele transmissies. Deel 1 : theoretisch en praktisch bekeken.* Aandrijftechniek, 1985. **8**(1): p. 10-15.

50. Chen, T.F., D.W. Lee, and C.K. Sung, *An experimental study on transmission efficiency of a rubber V-belt CVT.* Mechanism and Machine Theory, 1998. **33**(4): p. 351-363.

51. Chen, T.F. and C.K. Sung, *Design considerations for improving transmission efficiency of the rubber V-belt CVT.* International Journal of Vehicle Design, 2000. **24**(4): p. 320-333.

52. Francis, R., *Pushing Belt Drive Efficiency.* PTdesign, 1998. **March 1998**: p. 33-36.

53. Lee, D.W. and C.K. Sung, *On the efficiency analysis and improved design of a rubber V-belt CVT.* International Journal of Vehicle Design, 1997. **18**(2): p. 119-131.

54. Zhu, C., et al., *Experimental investigation on the efficiency of the pulley-drive CVT.* International Journal of Automotive Technology, 2010. **11**(2): p. 257-261.

55. Michael A. Kluger, D.R.F., *An Overview of Current CVT Mechanisms, Forces and Efficiencies.* SAE Technical Paper 970688, 1997.

56. Benford, H.L. and M.B. Leisling, *The Lever Analogy: A New Tool in Transmission Analysis.* SAE Technical Paper, 1981(810102): p. 429-437.

57. Cuypers, M.H., *Continu variabele transmissies. Deel 2 : theoretisch en praktisch bekeken.* Aandrijftechniek, 1985. **8**(2): p. 33-35.

58.   Cuypers, M.H., *Continu Variabele transmissies. Deel 3.* Aandrijftechniek, 1985. **8**(3): p. 49-53.

59.   Yamamoto, T., K. Matsuda, and T. Hibi, *Analysis of the efficiency of a half-toroidal CVT.* Jsae Review, 2001. **22**(4): p. 565-570.

60.   Carbone, G., L. Mangialardi, and G. Mantriota, *A comparison of the performances of full and half toroidal traction drives.* Mechanism and Machine Theory, 2004. **39**(9): p. 921-942.

61.   Younes, Y.K., *A Design Scheme for Multidisk Beier Traction Variators.* Journal of Mechanical Design, 1992. **114**(1): p. 17-22.

62.   Takaki, T. and T. Omata, *100g-100N finger joint with load-sensitive continuously variable transmission.* 2006 Ieee International Conference on Robotics and Automation (Icra), Vols 1-10, 2006: p. 976-981.

63.   Takaki, T. and T. Omata, *Load-sensitive continuously variable transmission for robot hands.* 2004 Ieee International Conference on Robotics and Automation, Vols 1- 5, Proceedings, 2004: p. 3391-3396.

APPENDICES

Appendix A: Basic Information about static balancing

Static Balancing and its advantage

An ideal statically balanced device is in static equilibrium throughout its working range, got a constant level of energy and can be moved energy free in a quasi-static situation [7]. A visualization to obtain a better understanding of the subject can be made using marbles under the effect of gravity.
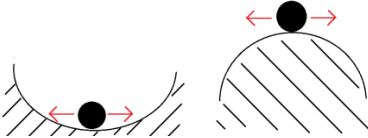
Figure 16: A visualization of marbles in a stable (left) and unstable (right) equilibrium.
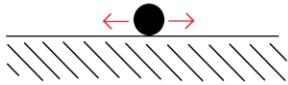
Figure 17: A visualization of a marble in equilibrium that is neither stable nor unstable.

When a marble is placed on top of a hill (**Figure 16**) it won't immediately fall down. However if a small perturbation occurs the marble will fall down the hill. If a marble is in a gully (**Figure 16**) and a small perturbation occurs it will move back to its original position.

This preference for the marble to go towards or away from a certain position means that marble is not in static equilibrium at all positions, in this case due to the influence of gravity. The energy levels of the marble are not constant either due to the different heights over the trajectory meaning that there are different states of potential energy.

When a marble is placed on flat ground (**Figure 17**) it can be placed anywhere without wanting to change to a different position, meaning it's always in a static equilibrium. A constant height over the trajectory ensures a constant potential energy level. In quasi static movement where the velocity and acceleration are effectively zero, it won't require any force to move the system from the left to the right.

The ability to move an object without any force allows for higher precision, smaller actuators, and lower power consumption [7], generating the desire to modify and create systems that are statically balanced. As gravity is a common phenomenon that gives devices a preferred position, gravity balancing is a popular and commonly applied method of statically balancing. If there would be no gravity then the marbles in all 3 pictures could be placed anywhere in the figure and stay there. Although this research will focus on the case of gravity equilibration all sorts of forces can be balanced, like for instance undesired internal stiffness'[29, 45].

For simplicity most forms of balancing will be described through the usage of an inverted pendulum with one degree of freedom (**Figure 18**). With an inverted pendulum, a moment

should be created around its base that counteracts the moment generated by the forces of gravity.

Figure 18: An inverted pendulum under the influence of gravity, including a balancing equation for the required torque (M) with respect to the pendulums angle with gravity (ϕ) to keep the pendulum from having any preferred position.

Balancers utilizing counterweights

There are multiple ways to compensate against gravity but the most popular way throughout history has been through counterweights. Typical applications (Figure 19) range from big devices such as bridges, cranes and elevators to smaller devices such as desk lamps and pick-up arms.

Figure 19: Various systems that are balanced against gravity by the usage of counterweights.

Balancing by counterweights (**Figure 20**) works by mounting a mass (m2) such that it generates a force or moment that counteracts the force or moment generated by gravity on the original mass (m1).
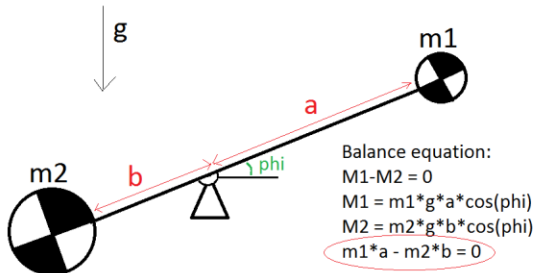
Figure 20: An inverted pendulum under the influence of gravity, counterbalanced by a secondary mass, including a balancing equation for the required ratios of mass and distance.

This means that counterweights require an additional mass for the counterbalance, meaning that the total mass and inertia of the moving system increases which means a higher force is required for acceleration. Counterweight balanced systems are generally bulky compared to the unbalanced system as there needs to be additional space for the counterweight.

However the simplicity of such a system requiring no addition of energy to place it in any position makes it a popular and often cheap choice for gravity equilibration. If the downfalls are not a problem for a desired application then it's mostly advised to go for this method.

Spring balancers with a fixed reference

Another way to statically balance devices is through the usage of elastic elements such as springs. Although more complex in its execution, spring based balancers can often store more energy in their spring within a smaller size and weight package, than equivalent counterbalanced systems.

Balancing by the use of springs (**Figure 21**, **22**Figure 22), generally works through the utilization of special zero-free-length springs that have a linear relation between force and its actual length rather than just its extension. This allows for the creation of a sinusoidal torque curve that counteracts the gravity induced torque (**Figure 18**). In order to obtain the correct phase in the counter torque placement of the spring attachment points relative to the pendulum joint and the gravity vector is critical (For example in **Figure 21** the mounting point should be perfectly vertical above the pendulum joint)
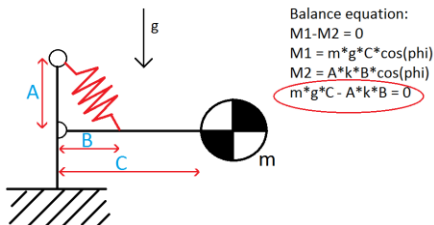
Figure 21: A pendulum counterbalanced by a zero-free-length spring, including a balancing equation for the required mounting position and spring stiffness.
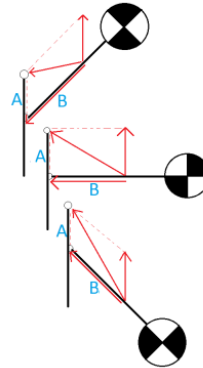
Figure 22: On the left a figure is shown of an inverted pendulum in multiple positions.

If a zero-free-length spring is used, the spring force becomes:

F = k*Lspring

Decomposing the forces into a force alongside the arm (b) and a force parallel to (a). Will then be

F∥a= k*a
Fb = k*b

Although springs with absolutely no initial size in any plane do not exist, Zero-free-length springs can be created through multiple methods

1) Adjusting the pretension (**Figure 23**) of the spring such that its force/length graph crosses the zero.
2) Placing the spring at a different location (**Figure 24** a-b) then where its force is exerted.
3) Using special materials (**Figure 25**) that initially show a nonlinear force deflection relationship.
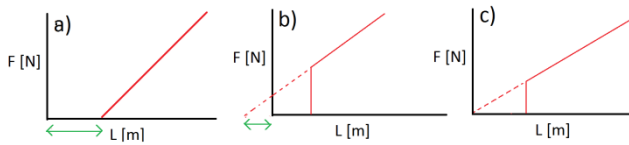
Figure 23: A showcase of 3 (red) force/length characteristics with their appropriate zero-force lengths (green) [7]
- a) a regular spring without pretension and a positive zero-force-length.
- b) a pretensioned spring with a negative zero-force-length
- c) a pretensioned spring where the pretension is such that it generates a zero-force-length of zero
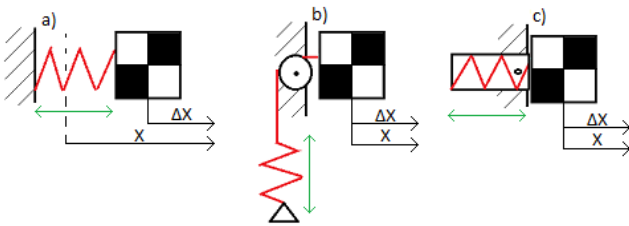
Figure 24: A showcase of 3 different configurations of a 1-dof, mass-spring system. [7, 46]
- a) The spring is directly attached to the mass, making the initial spring length add up to the total length.
- b) Using a pulley system the spring is hidden away making the initial length not affect the total length.
- c) By placing the spring attachment points on the same plane even though there is an excess length elsewhere, can make a spring act like as if it got zero-free length
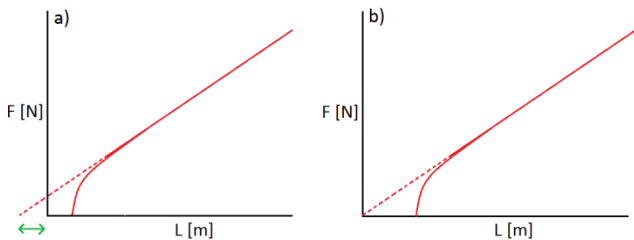
Figure 25: Showcase of two force deflection curves of rubber springs. [41]
- a) Natural rubber initially shows a big decrease in stiffness, giving it an effective negative free length.
- b) Adding some stiff material in series with rubber allows for the creation of an effective zero-free-length spring.

Appendix B: Background Research On Energy Storage And Transfer Mechanisms

Elastic elements and their properties

Parameters affecting the stiffness

Before looking at various mechanisms that manipulate the stiffness of elastic mechanisms, it is important to overview various types of springs and their working principles in order to understand what variables can be adjusted to manipulate the stiffness.

An overview of different types of springs and their loading conditions is shown in **Figure 26** [41].Although the overview is for metal springs different materials could be used to generate similar shapes.
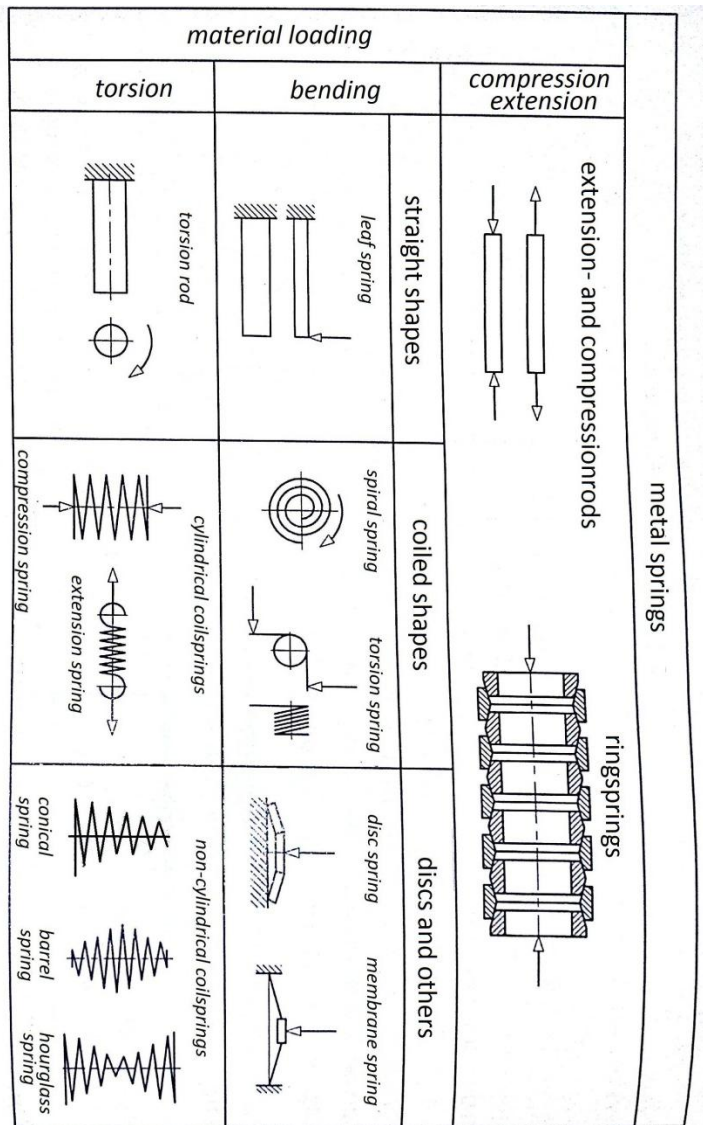
Figure 26: Grouping of metal springs to material load [41]

Combining the basic formulae for force and deflection for some of the coiled and disc shapes generates **Table 8** [42]. From the different equations it can be seen that the stiffness can be modified by changing the amount of coils (n), wire dimensions (d), coil radius (r), shear modulus of elasticity (G), modulus of elasticity (E) and in the case of a spiral spring the effective spring length (l) and for the disc spring the disc width δ.

Table 8: Approximate formulae for spring stiffness's of some coiled shaped and disc type springs. [42]

Spring	Stiffness
Cylindrical coilspring Round wire	$F = \dfrac{\pi}{16}\dfrac{d^3}{r}\tau$ $f = \dfrac{64\,n\,r^3\,F}{d^4\,G}$
Cylindrical coilspring Square wire	$F = \dfrac{d^3}{4.8\,r}\tau$ $f = \dfrac{44.9\,n\,r^3\,F}{d^4\,G}$
Conical coilspring Round wire	$F = \dfrac{\pi}{16}\dfrac{d^3}{r_1}\tau$ $f = \dfrac{16\,n\,(r_1+r_0)(r_1^2+r_0^2)\,F}{d^4\,G}$
Torsion spring Round wire	$F = \dfrac{\pi}{32}\dfrac{d^3}{r}\sigma$ $\varphi = \dfrac{2\,D\,\pi\,n}{E\,d}\sigma\dfrac{180}{\pi}$ φ [deg.]
Spiral spring Round wire	$F = \dfrac{\pi}{32}\dfrac{d^3}{r}\sigma$ $f = \dfrac{2\,r\,l}{E\,d}\sigma$ $l = \text{eff spring length}$

19

Disc Spring

$$F = \frac{\delta^2}{1 - 2/3\, r_0/r}\, \sigma$$

$$f = \frac{0.65\, r^2}{E\, \delta\, (1 - 2/3\, r_0/r)}\,$$

Table 10: Some examples of the bending moment of inertia for popular shapes over either the x- or y-axis. [47]

Shape	Moment of Inertia $I_x = \int y^2\, dA$
Rectangular area	$I_x = \frac{1}{12}bh^3$ $I_y = \frac{1}{12}hb^3$
Triangular area	$I_x = \frac{1}{36}bh^3$
Semicircular area	$I_x = \frac{1}{8}\pi r^4$ $I_y = \frac{1}{8}\pi r^4$
Circular area	$I_x = \frac{1}{4}\pi r^4$ $I_y = \frac{1}{4}\pi r^4$

The relationship between force and deflection of a transverse loaded leaf spring can be found in Table.2 [42]. The I in **Table 9**, stands for the second moment of inertia for which the general formula and some examples of cross-sections can be found in **Table 10** [47].

From the relationship between force and deflection it can be seen that the stiffness can be modified for this type of spring by changing either the length (L), modulus of elasticity (E) or the moment of inertia (I)

Table 9: Linear formulae of deflection and slope for a transverse loaded beam. [42]

Loading	deflection	slope
	$\delta_b = \frac{FL^3}{3EI}$	$\theta = \frac{FL^2}{2EI}$

The relationship between force and deflection of a normally loaded beam can be found in **Figure 27** [42].

$$\sigma = E\varepsilon \qquad \varepsilon = \frac{\delta}{L} \quad : \quad \delta = \frac{FL}{AE}$$
$$\sigma = \frac{F}{A}$$
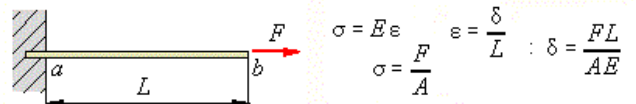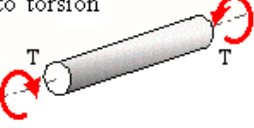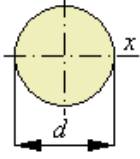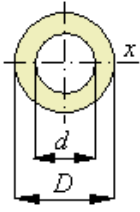
Figure 27: Simple calculation of the extension of a normally loaded tension bar.

From this relationship it can be seen that the beam length (L), area (A) and modulus of elasticity (E) all linearly relate towards the stiffness of the leaf spring.

The relationship between torque and rotation of torsionally loaded beam can be found in **Table11** [42]

From this it can be seen that the stiffness is determined linearly by the Shear modulus of elastiticity (G), rotational moment of inertia (Ip) and the length of the torsion rod (L).

Table 11: Torsion bar and the appropriate formulae to calculate the torque necessary to obtain a certain output [42]

Cross section	Torsion
Elementary equations for uniform beams subjected to torsion	$T = S_t \, \tau_{max}, \quad S_t = \dfrac{I_p}{r}$ $I_p = I_x + I_y$ $\varphi = \dfrac{TL}{G I_p}, \quad G = \dfrac{E}{2(1+v)}$
(solid circular cross section, diameter d)	$I_p = \dfrac{\pi}{32} d^4$ $S_t = \dfrac{\pi}{16} d^3$
(hollow circular cross section, diameters d, D)	$I_p = \dfrac{\pi}{32}(D^4 - d^4)$ $S_t = \dfrac{\pi}{16} \dfrac{D^4 - d^4}{D}$

Weight based efficiency on elastic elements

One of the properties for the ideal statically spring balanced pendulum without a fixed reference is that the total size and weight should be smaller than an equivalent mass balanced system.

Although in some cases the weight of springs can be negligible to the total weight of a system, when the amount of energy that needs to be stored in the system increases, generally the weight of the system will increase, which is why this section focusses on the weight based efficiency of different elastic elements.

When looking at elastic elements a separation can be made on the intrinsic properties of the used material, and how the material is shaped and loaded as a spring. Which follows from that the amount of energy per volume can be calculated with: W/V = α *σ²/E,

"α" gives an indication of how efficiently the material is used, the Young's modulus (E) is an intrinsic property of utilized material, the material stress (σ) depends on the loading condition and is limited by the elastic limits of the material. The energy per volume can easily be transformed into the energy to weight ratio through dividing by the density (δ) of the material.

A showcase of different utilizations of material for a few common spring types can be seen in **Figure 28** [43]

Figure 28: Comparison of different spring types and the amount of energy per volume W/V = a*σ²/E. [43]

In the energy to weight ratio, the young modulus, maximum allowable stress and density depend on the material. **Table 12** [43] shows a comparison of some different configuration of springs and material and their respective energy to weight ratio.

Table 12: Comparison table showcasing the energy to weight ratio (W/m = (α *σ²)/(E*δ)) in spring steel and some non-metal spring materials. Note: for the leaf springs a triangle shaped leaf spring is assumed, for composites it is assumed that only 50% is filled with fibers hence the halving of α [43]

material	springtype	α	σ max [MN/m²]	E [GN/m²]	ρ [kg/m³]	W/m [J/kg]
Springsteel	coilspring	1/4	1200	210	7800	200
wood	leafspring	1/6	120	27	600	150
rubber	tensile rod	1/2	2.5	0.0015	1200	1800
carbonfiber	leafspring	1/12	2000	110	1500	2100
aramidfiber	leafspring	1/12	2000	100	1500	2100
glassfiber	leafspring	1/12	2000	54	2500	3000

From **Table 12** it can be seen the energy to weight ratio can improve tenfold over regular steel coil-springs, by carefully selecting materials. This means that if there is a desire to maximize the amount of energy with a weight constraint that

alternative materials such as rubber and glass-fiber should be looked at over traditional coil springs.

Continuously Variable Energy Transfer mechanisms

Before looking at various elastic mechanisms that manipulate their output force through an adjustable transmission ratio, it is important to have an understanding on various types of existing continuously variable transmissions.

CVT's can get divided in five categories [48] [49]
1. Hydrostatic

2. Traction drive (V-belt and Rolling contact)

3. Overrunning clutch (Lever types)

4. Electric

5. Slipping clutch

With these categories it is important to note that for a passive system that energy losses must generate an increased operating effort (e.g. friction), rather than utilizing energy from the finite energy storage and possibly depleting it. This makes the usage of Hydrostatic, Electric and Slipping clutch designs undesirable. For that reason only Traction and Overrunning clutch designs will be discussed further. (Although it should be noted that the energy losses could possibly be counteracted by accounting for the inefficiencies by charging more energy than necessary)

Traction Drive CVTs
Traction drive is a term applied to any device which transmits power through adhesive friction between two objects loaded against each other [48].
The group of traction drives can be further separated into 2 groups, rolling contact traction drives and belt traction drives [48].

Belt Drive CVTs
The most famous belt drive CVTs are the variating pulley (**Figure 29**) and double cone (**Figure 30**) drives.
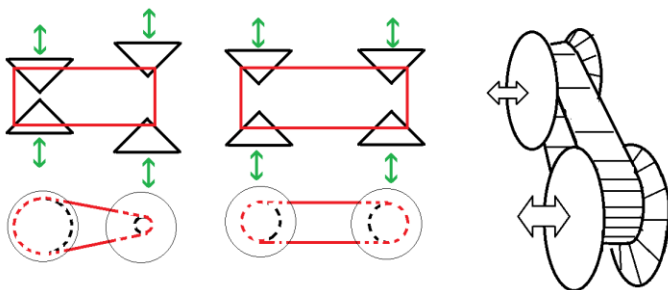
Figure 29: Variating pully CVT belt drive
The variating pulley belt drive is able to adjust the generated input and output force by moving sets of conical pulleys further apart or closer together. This makes the drive belt catch on to the pulley at different diameters allowing for adjustment of the transmission ratio.
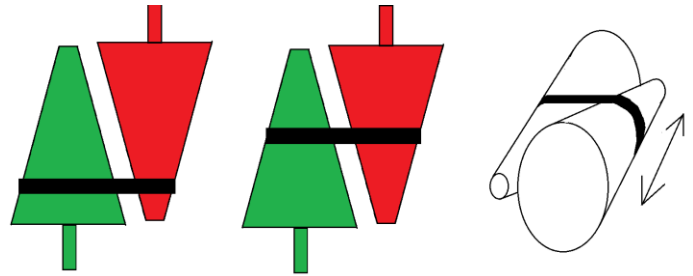
Figure 30: Double cone CVT belt drive
The Double Cone belt drive is able to adjust the generated input and output speed by adjusting a drive belt over 2 conically shaped pulleys. This means that the effective used diameter of the input and output shaft changes allowing the adjustment of the transmission ratio.

Efficiency:
Normally during power transmission, the belt undergoes cyclic tension and compression deformation when it is bent on and off the pulleys. This results in torque loss due to the bending hysteresis, that depends on the elastic properties and the magnitude of flexure of the belt [50, 51].
These effects make the selection of belts highly dependent on different load cases, pulley sizes as well as maintenance [52]. Overall the efficiency of a well set up belt driven CVT ranges from 90-97 % efficiency [50, 52-55] .

Amount of necessary parts:
The minimum amount of parts for variating pulley system to function equals 8. 4 conical pulleys, 2 shafts, a housing and a belt. For a double cone belt drive in the most simple form 6 parts are necessary: Input cone, output cone, 2 shafts and a housing, connecting belt. However once again that does not include the parts necessary to actually adjust the gear ratio.

Ability to adjust ratio when the device is not rotating
Belt drives adjust their ratio by applying a force on the belt, which makes the belt slowly shift towards a desired set point. For this to work the CVT's should be rotating.

Range:
Both belt type CVT's allow for full 360° rotations. Although they do not allow for one wheel to freewheel (an infinite ratio). If that would be desired a power split could be added to the system (more on that later)

Lever equivalent

Every transmission can be analyzed using lever analogy. Which can make the the torque and speed calculations easy and improves the ability to visualize the results and effects of gear tooth ratios [56]. For that reason the lever equivalent of every discussed CVT will be displayed.

Figure 31 shows the lever equivalent of the variating pulley belt drive and the double cone drive.
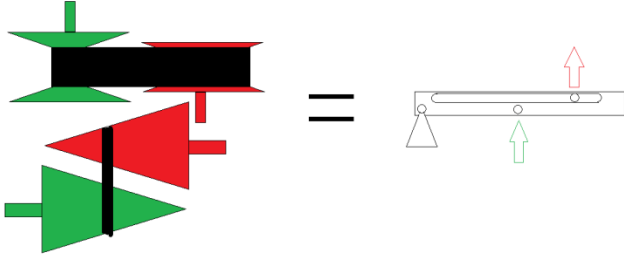
Figure 31: lever equivalent of the variating pulley belt drive and the double cone belt drive.

Rolling contact traction drives

Rolling contact traction drives transmits power through adhesive friction between two objects loaded against each other [48]. The difference between belt drive CVT's is that rolling traction CVT's utilize traction wheels or balls instead of a belt. Unlike traction drives with a set transmission ratio, there is a lot of diversity with continuously variable traction drives [57]. For this reason only a small selection of all the different rolling contact traction drives will be shown here. The chosen selection are CVT's that seem to reoccur the most in literature [48, 49, 55, 57, 58] Namely: Wheel CVT (**Figure 32**), Ball CVT (**Figure 33**), Half Toroidal CVT (**Figure 34**), Full toroidal CVT(**Figure 35**), Milner CVT (**Figure 36**), Kopp CVT (**Figure 37**), Nutating traction drive (**Figure 38**), Beier CVT drive (**Figure 39**).
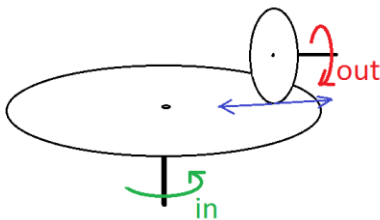
Figure 32: Wheel CVT
The wheel CVT works through a set of double wheels with one wheel placed 90° ontop of the other. By variatating the distance of one wheel towards the center of the other wheel the effective gearing ratio can be adjusted.
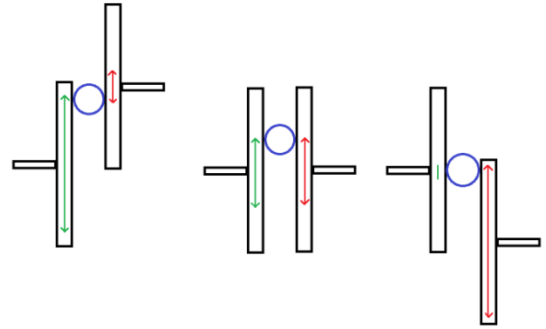
Figure 33: Ball CVT
The ball CVT works by placing a ball between two wheels connected to an in and output shaft. By moving one shaft up or down the relative position of the ball on the wheels changes, generating a different gearing ratio between the in and output wheel.
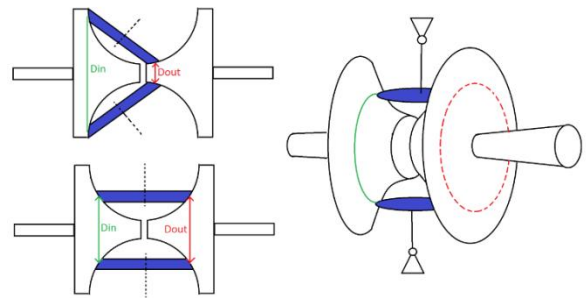
Figure 34: Half Toroidal CVT
The half toroidal CVT works by moving a disc between 2 wheels. Those wheels are shaped such that from a single point of rotation the disc can contact both wheels at different diameters allowing for a change of transmission ratio without having to move the actual driven wheels.
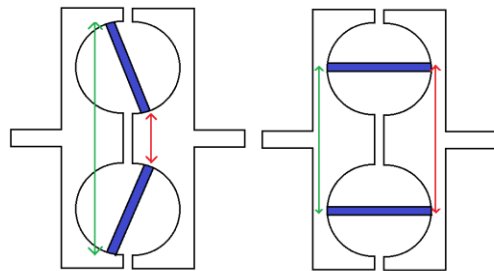
Figure 35: Full toroidal
The half toroidal CVT works by moving a disc between 2 wheels. Those wheels are shaped such that from a single point of rotation the disc can contact both wheels at different diameters allowing for a change of transmission ratio without having to move the actual driven wheels.
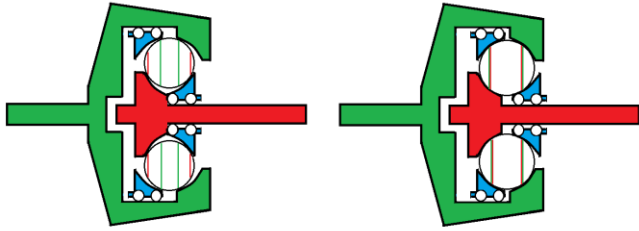
Figure 36: Milner CVT
The milner CVT works by moving moving little widges (blue in the drawing) to the left or the right. This pushes the balls up or down on the structure, making the inner and outer shaft effectively connect to the ball at a different circumference changing the output ratio. Of the CVT.
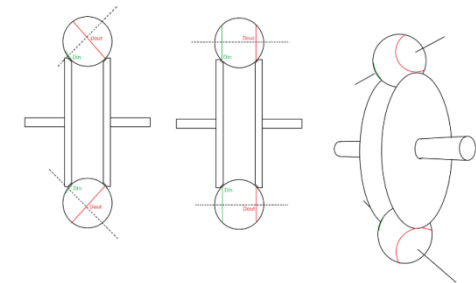
Figure 37: Kopp CVT
The kopp CVT functions by changing the center of rotation on a ball that connects an input and output wheel. Rotating the center of rotation effectively changes the radius around the ball that the in and output shaft follow, and with that change the transmission ratio.
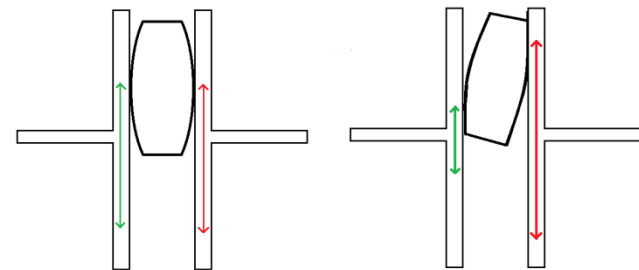
Figure 38: Nutating Traction drive
By placing a barrel shaped object between two wheels, and adjusting the angle of rotation of said barrel it becomes possible to alternate the contact point on the wheels effectively connecting the wheels at different diameters which changes the gearing ratio.
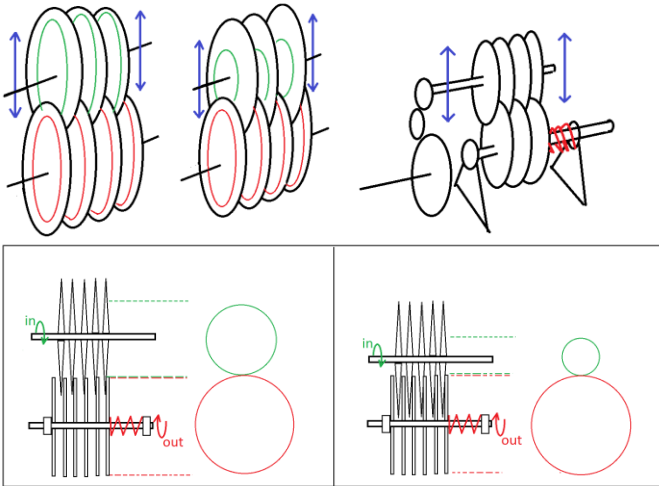
Figure 39: Beier CVT drive
The beier CVT drive works by meshing one set of wheels into another set of wheels changing the effective radius on one of the wheels and with that the gear ratio. The speciality of the concept lies in the utilization of multiple discs, that for a single compressive force generates multiple contact points. Allowing for high torque throughput for a relativel low compression force.

Efficiency
The key components introducing non-negligible energy losses with a friction CVT are spin and slip losses and not neglect able losses in bearings [57]

Since there is no relative speed difference between the in- and output shaft when operating quasi-statically spin should be neglect able.

Table 13 gives a general overview of efficiencies of various rolling contact traction drives. Formulae that can be used to predict the efficiency can be found in [57].

Table 13: Showcase of various efficiencies of rolling traction drives. *Due to the similar functioning of the Milner and the Kopp traction drive it is assumed that the efficiency of the Milner traction drive will be approximately the same as the Kopp CVT.

Traction Type	Efficiency
Wheel	93-96% [49]
Ball	75-90% [57]
Half Toroidal	90-97% [55, 59] [60]
Full Toroidal	88-97% [57] [60]
Milner	75-90%*
Kopp	75-90% [57]
Nutating	75-96% [55]
Beier	93-96% [61]

Range:

All of the noted CVT's can be used for a range of over 360° degrees. Although only the wheel and ball CVT by default allow for the usage of an infinite range. To obtain an infinite range with the others the addition of an additional device such as a power split mechanism should be utilized to generate an infinitely variable transmission.

Amount of necessary parts

To generate an overview of the amount of necessary parts **Table 14** has been set up.

Table 14: Showcase of a summation of parts for various rolling contact traction drives.

Type of CVT	# parts			
Wheel	4	2 shafts	2 wheels	
Ball	5	2 shafts	2 wheels	1 ball[5]
Half Toroidal	5	2 shafts	2 toroidal wheels	1 disc[5]
Full toroidal	5	2 shafts	2 toroidal wheels	1 disc[5]
Milner	6	2 shafts	2 balls	2 guides
Kopp CVT	5	2 shafts	2 balls	1 ball[5]
Nutating	5	2 shafts	2 wheels	1 barrel[5]
Beier	5	2 shafts	3 wheels[5]	

Ability to adjust ratio when the device is not rotating

For all devices beside the ball type CVT, adjusting happens by putting a force on the adjustment mechanism which changes the ratio over a certain range of rotation. Instantaneous change would require for the force transmitting member to slip, requiring high forces as these CVT's are designed to transmit energy through traction.

Lever equivalent

Every transmission can be analyzed using lever analogy. Which can make the the torque and speed calculations easy and improves the ability to visualize the results and effects of gear tooth ratios [56]. For that reason the lever equivalent of every discussed CVT will be displayed. **Figure 40** shows the lever equivalent for a wide selection of rolling contact traction drives.
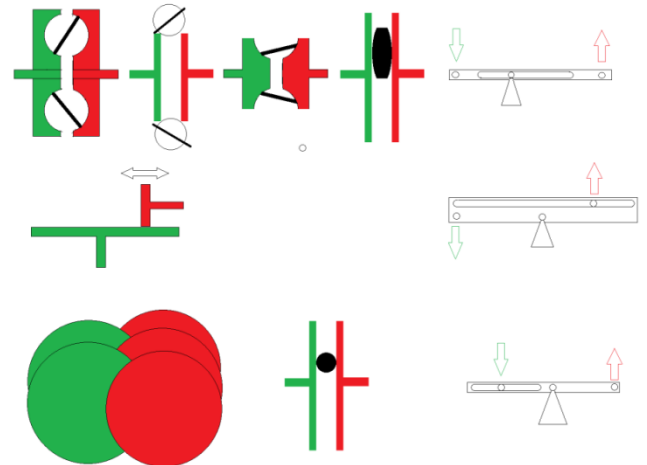
Figure 40: Overview of the lever equivalent for various rolling contact traction drives.

Overrunning clutch CVTs

Overrunning clutch or Epicyclic CVT's make use of adjustable mechanisms with a limited range, and through a ratchet or a swashplate generate a full cyclic motion. Some popular examples within this category are the Zero-max CVT (**Figure 41**) and the Benitez's ratcheting CVT (**Figure 42**).
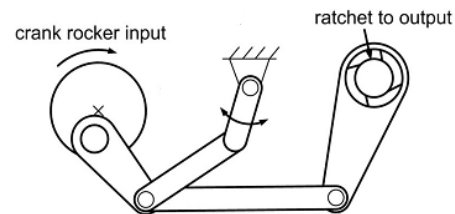
Figure 41: The zero-max CVT utilizes an adjustable four-bar mechanism to transfer an adjustable force from input to output. A ratcheting mechanism changes the small stroke of the four-bar mechanism into a single forward motion. By adding multiple devices together at an offset phase will allow for the generation of an output that will approach linearity. However due to the ratchet the system only works in a single direction.
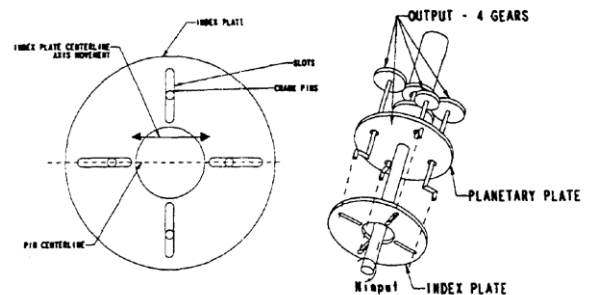
Figure 42: The benitez ratcheting CVT. The index plate rotates in a swirling motion off centered from the input shaft. This makes the pins in the index plate move up and

---

[5] **The number denotes a minimum amount to function. Adding more parts, generates more contact points, and with the same normal force allows for a higher torque throughput.[5]**

down similar to a scotch-yoke, a ratcheting gear set at the back transforms this sinusoidal motion back in a roughly linear output speed.

Efficiency:

The advantage of variable geometry CVT's is the lack of slip due to all parts being fixed. However to generate a linear output there is often a requirement for a lot of devices put together in parallel.Besides that variable geometry CVT's are often not dynamically balanced, causing various vibrations into the system. Literature for variable geometry based CVT's showcases an efficiency of 85-93% [55]

Range:

The range of epicyclic and overrunning clutch designs is 360° The range of adjustment of a zero-max CVT is in the order of 4x.

Amount of necessary parts:

The zero-max CVT requires 1 input wheel, 5 links and a ratcheting bearing. Making for a total of 7 parts

Ability to adjust ratio when the device is not rotating:

Overrunning clutch or Epicyclic CVT's can be adjusted when the device is not running. As it generally relates to adjusting the length of a lever arm.

Lever equivalent:

Every transmission can be analyzed using lever analogy. Which can make the the torque and speed calculations easy and improves the ability to visualize the results and effects of gear tooth ratios [56]. For that reason the lever equivalent of every discussed CVT will be displayed. **Figure 43**, shows the lever equivalent for the overrunning clutch CVT's.
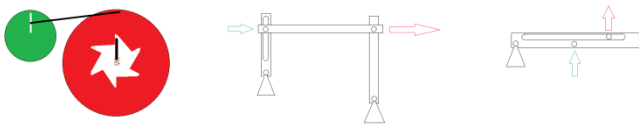
Figure 43: Overview of the lever equivalent for both the zero max and benitez overrunning clutch CVT's.

An direct utilization of a lever equivalent of the zero-max CVT can be found in the five bar linkage CVT (**Figure 44**) that has been discussed by Takaki et Al [62, 63]
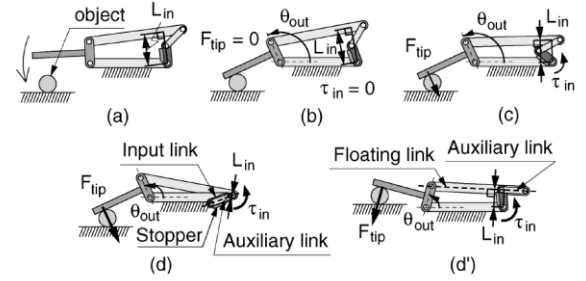
Figure 44: Showcase of the Five-bar linkage CVT under various positions and transmission ratios.

CVT Evaluation:

The ability of a CVT to match any input speed to a desired output speed generated a lot of research and products within the Production and Transport industry, the previous showcase is only a very small selection of all the patents and products created.

These devices however are often designed to operate in a continuous motion and at a high speed, with their primary competition against multi-gear gearboxes.

In the case of a spring balanced inverted pendulum, the competition is against a simple counterweight, in terms of mass, complexity and weight. And unlike the vehicular and production industry it should be possible to change the ratio even when the device operates in a quasi-static operation rather than in continuous fashion.

From the above solutions none of the previously shown CVTs are directly applicable; however this does not mean that existing CVTs cannot be modified or adopted for quasi-static operation. The different set of requirements and goals could generate completely different solutions.

The requirements for simplicity and limited weight could point into the direction for lever type CVT's. The requirements for energy free adjustment could point in the direction of a ball type CVT's.

Appendix C: Estimation of the Rolling Friction

To obtain a rough estimate of the rolling friction due to the ball a number of tests have been conducted.

In a simplified model a rolling ball under pressure can be compared with Figure 45.

When a ball is rolling part of the material gets loaded and unloaded (red part in the drawing), as not all energy from the loading is recovered friction will be felt.
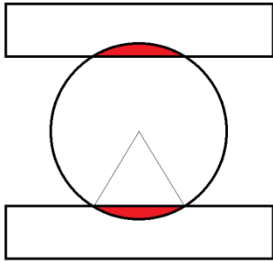
Figure 45: Concept of a ball compressed between two plates

By measuring the area in the hysteresis loop from different compressions of the ball, a plot can be made for energy losses of a single compression. (tests were done at a high speed of 150mm/min and slow speed of 10mm/min)
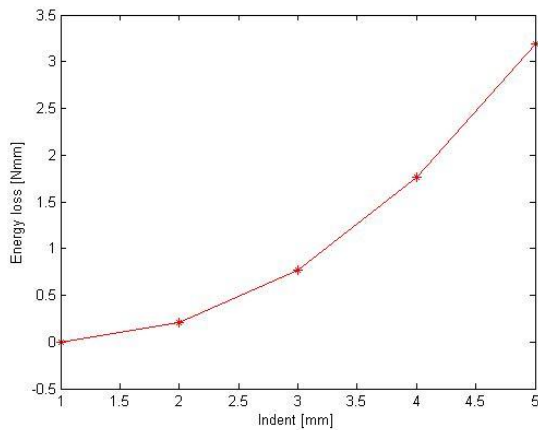
Figure 46: Viscoelastic energy losses for a single cycle of compressing of the ball

In the elastic actuator the ball of 26 mm was compressed to 23.5 mm. At this point the diameter of the circular contact point at the top was measured at 10mm this means that a full rotation of the ball got roughly 7 cycles of loading and unloading.

Considering that at a 1:1 gear ratio the ball makes roughly 10 full cycles for a full cycle of the top disc.

So a full cycle of the topdisc (145mm on the pulley) corresponds to an energy loss of 35Nmm or a frictive force of 0.25N Making it unlikely that the direct rolling friction of the ball causes the main gap in efficiency

Appendix D: Component/Cost list

Table 15. Overview of the different components used for construction of the elastic actuator and their comparative price

Part	Amount	Total Cost
50x50x10 acrylate plate	1	€69,90
50x50x5 acrylate plate	2	€39,90
radial Ball bearing	8	€29,52
axial Ball bearing	2	€8,60
Alps Motorized Slide	3	€52,8
arduino Mega	1	€33,02
MPU6050 Sensor	1	€27,90
9 Volt battery	2	€7,90
14 bouncing Balls	1	€5,99
50T2.5 Gears	2	€19,98
950 380T2.5 Belt	1	€9,99
large linear slide	1	€6.95
lmall linear slide	1	€7,95
1m Aluminum ITEM profiles	2	€27,40
wiring & solder	1	€5
bolts&bits	~30	€10
Total Accumulative	-	€348,93

Appendix E: Electrical wiring schematics

Figure 47 Depicts the used wiring scheme for the actuator. By grounding Switch 1 and 2 the motor doesn't do anything, enabling either switch 1 or switch 2 will then make the motor rotate in a direction. The speed of the motor is controlled by pulse width modulation, or in other quickly switching a switch on or off, the amount of time it is on average on and off then determines the average output voltage.

This system allows the use of a low voltage control signal (in this case 3.3v from the Arduino), to control a higher output voltage (9V from a battery).
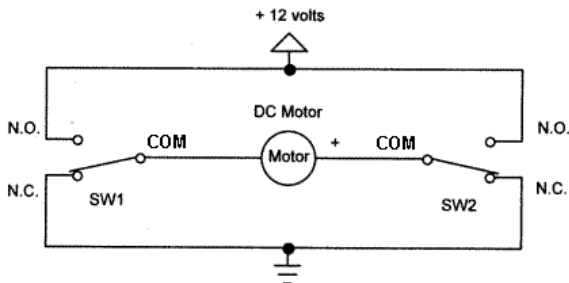
Figure 47. A showcase of the electrical wiring of the H-Bridge which allows the motor of the slide actuator to be powered by an external battery while controlled by the arduino board

In order to be able to control the position of the DC motor a slide potentiometer was used to measure the output (**Figure 48**).

Connection 3 was hooked up to the power source, with connection 0 being connected to ground, finally connection 2 was connected to the Arduino's analog input giving a reading from 0 to 1023 depending on the position of the wiper on the slide.
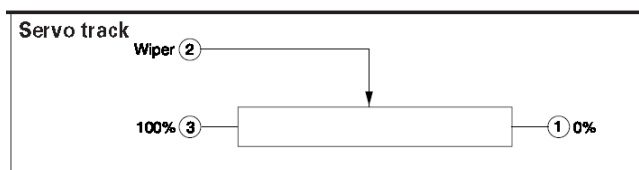
Figure 48. Showcase of the potentiometer connection to obtain feedback on the actuators position

Simulink Control Scheme

To change the output force based on the angle of the pendulum Simulink was used. A pretty standard PID controller in a closed feedback loop was used for this (**Figure 49**).

The reference was set using the accelerometer, the output force went through a small script that transferred an input signal between -1 and 1 to make the DC motor move in the correct way, and generate a pulse width modulated signal, which was output on the Arduino. Finally to track the error the position signal from the potentiometer was fed back to an analog input port.

To communicate with the Arduino the default Simulink arduino library was used. A custom library from minseg.com was used to communicate with the MPU-6050 gyro and accelerometer.
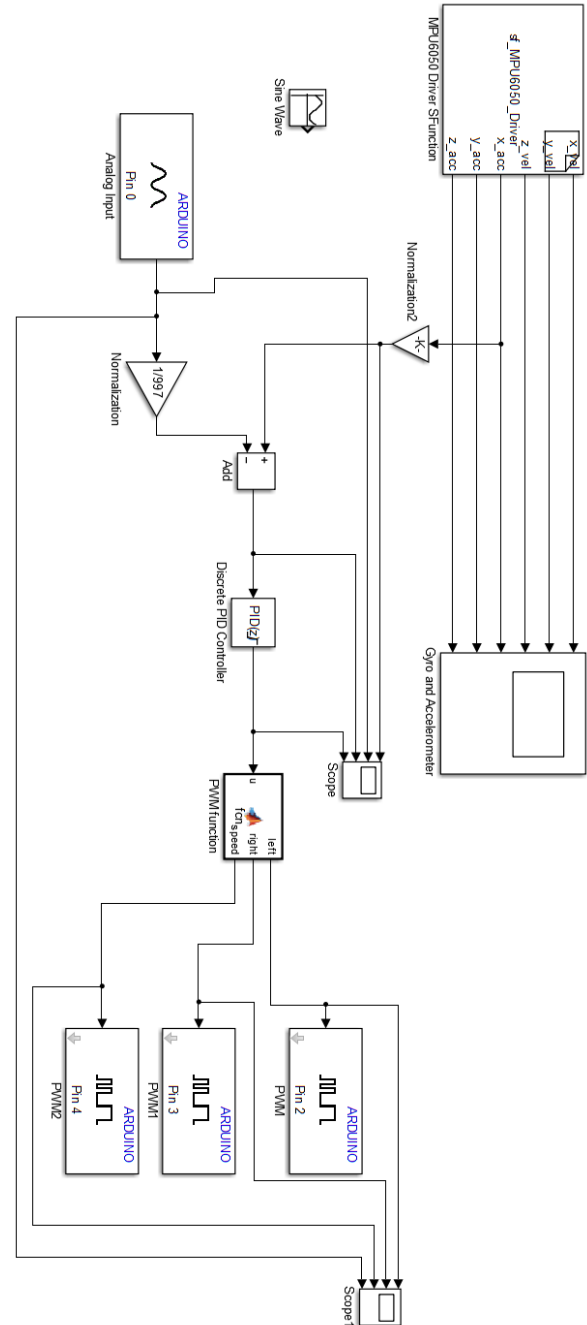
Figure 49. Simulink block diagram used to control the elastic actuator.

28

Appendix F: Electronic component overview

Alps Motorized slide potentiometer RRSA0N11M9A06

The alps motorized slide potentiometer (**Figure 50**), was used as a cheap linear actuator. As these devices are made as audio faders they are not made for heavy loads, which can be seen by the lack of gears in the system, the electrical DC motor is directly connected to the slide.

This means that the system only got a low maximum force (**Figure 51**). Because of this 3 slide potentiometers were used, however as the DC motors are required to operate close to their stall torque the efficiency will be very low.

An overview of the wiring scheme can be found in **Figure 52**.

Figure 50. Image of the Alps motorized slide potentiometer

Figure 51. Specsheet of the Alps motorized slide potentiometer

Figure 52. Wiring schematic for the motor and the potentiometer of the alps motorized slide potentiometer

Triple Axis Accelerometer & Gyro Breakout - MPU-6050

The MPU-6050 (**Figure 53**) is a 3-axis Accelerometer and 3-axis Gyro combined in a single package, and put on a breakout board so it becomes possible to solder. Even though this is a 6-axis chip the price of €27,90 is in the same order as single axis chips on a breakout board, while the specs aren't worse either.

The needed wiring schematic can be found in **Figure 54**, while the website minseg.com allows for the download of a Simulink based driver (**Figure 55**). Some specifications are listed below:

- VDD Supply voltage range of 2.375V–3.46V; VLOGIC at 1.8V±5% or VDD
- Tri-Axis accelerometer with a programmable full scale range of ±2g, ±4g, ±8g and ±16g
- Tri-Axis angular rate sensor (gyro) with a sensitivity up to 131 LSBs/dps and a full-scale range of ±250, ±500, ±1000, and ±2000dps

Figure 53. Image of the MPU-6050 mounted on the sparkfun breakout board
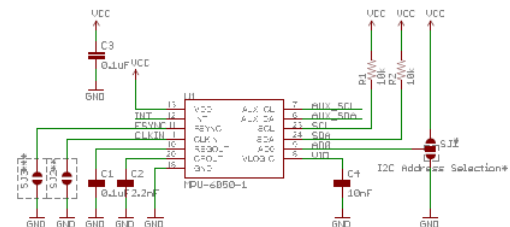
Figure 54. Wiring schematic of the MPU-6050
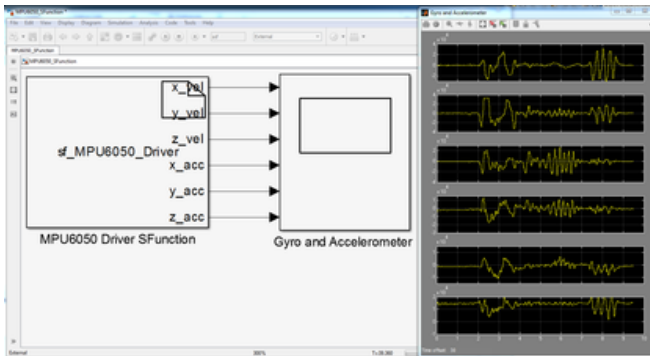
Figure 55. Figure showcasing the simulink driver from minseg.com when connecting the MPU6050, through an arduino mega 2560 using the Simulink platform

Arduino mega 2560
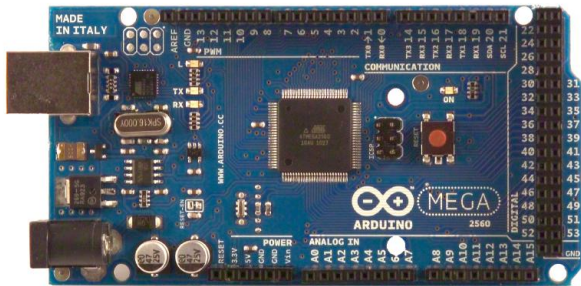
Figure 56. Picture of the arduino mega 2560

Description from arduino.cc

The Arduino Mega 2560 (**Figure 56**) is a microcontroller board based on the ATmega2560 . It has 54 digital input/output pins (of which 15 can be used as PWM outputs), 16 analog inputs, 4 UARTs (hardware serial ports), a 16 MHz crystal oscillator, a USB connection, a power jack, an ICSP header, and a reset button. It contains everything needed to support the microcontroller; simply connect it to a computer with a USB cable or power it with a AC-to-DC adapter or battery to get started. The Mega is compatible with most shields designed for the Arduino Duemilanove or Diecimila.

Specs	
Microcontroller	ATmega2560
Operating Voltage	5V
Input Voltage (recommended)	7-12V
Input Voltage (limits)	6-20V
Digital I/O Pins	54 (of which 15 provide PWM output)
Analog Input Pins	16
DC Current per I/O Pin	40 mA
DC Current for 3.3V Pin	50 mA
Flash Memory	256 KB of which 8 KB used by bootloader
SRAM	8 KB
EEPROM	4 KB
Clock Speed	16 MHz

Appendix G: Solidworks drawings

Main components of the system were made out of stacked pieces of laser cut acrylate (**Figure 57**).
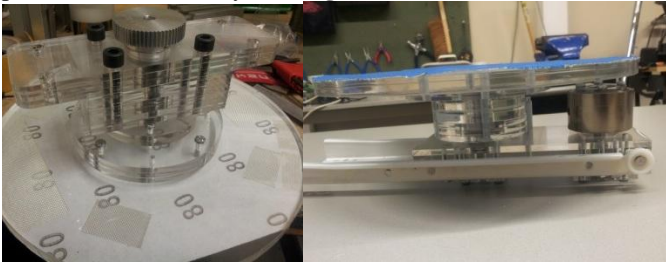
Figure 57. Showcase of stacked lasercut acrylate plates

To be able to cut the different components, drawings were needed. For this purpose it was necessary to learn how to use SolidWorks to generate DXF drawings, that could be fed into the laser cutter. An overview of all the cut parts can be seen below and to the right (**Figure 58-61Error! Reference source not found.**).
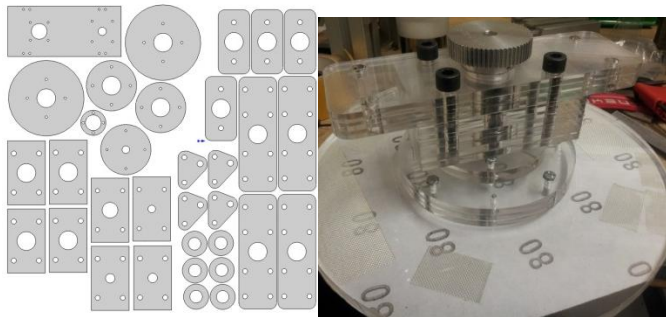
Figure 58. Showcase of laser cut parts of 5mm thickness, the main parts in this assembly are for the top disc, the bigger holes showcase bearing connections, while the smaller holes are generally assembly using bolts.
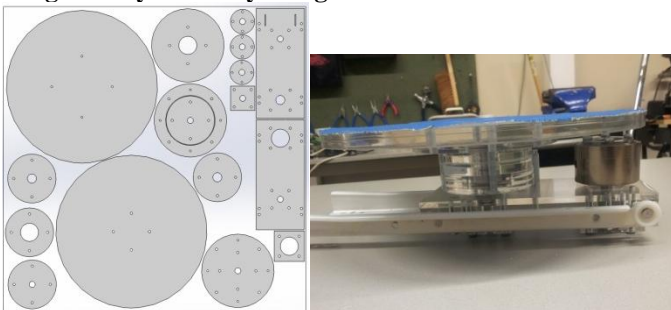
Figure 59. Showcase of laser cut parts of 10mm thickness, this figure shows the main discs for the elastic actuator, and the smaller discs for mounting the spring assembly of the bottom disc. The top right of the left figure shows the base slide assembly that allows the system to change its stiffness.
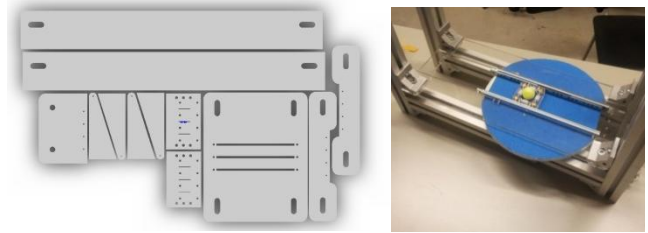
Figure 60. Here at the top we see the mounting plates that keeps the cage which holds the ball between the top and bottom disc in place. The bottom shows the mounting plate for the actuators which is placed below the slide to move the system. The other parts which got tiny holes in them are there for the springs that act as a proportional controller to keep the ball cage in place.

Figure 61 Showcase of the ball cages used to ensure that the ball cannot move away from its desired position.

Appendix H: Pictures of putting together the system

Figure 62. First the top disc gets assembled
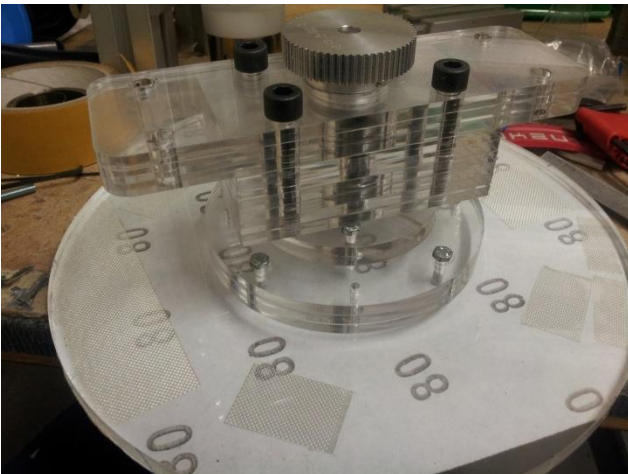
Figure 63. After the top disc is assembled the base that holds the bearings can be assembled
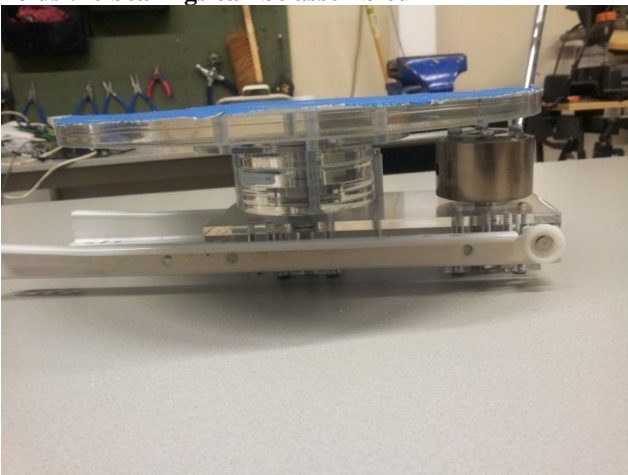
Figure 64. The bottom disc assembly gets assembled in a similar fashion
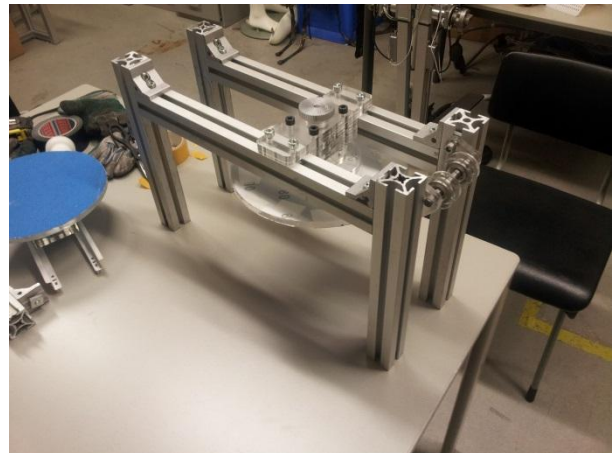
Figure 65. After the individual parts have been assembled the frame can be put together and the top disc attached to it
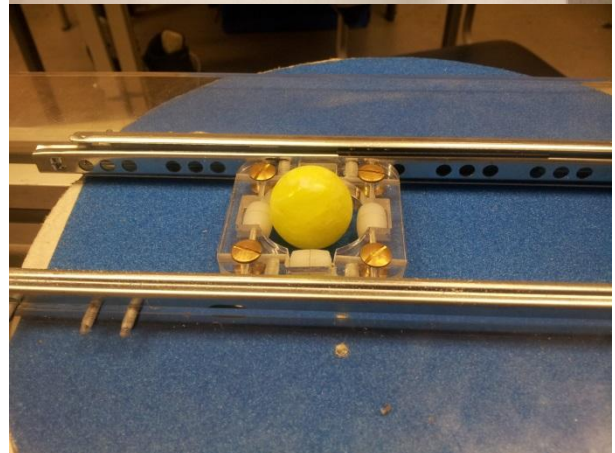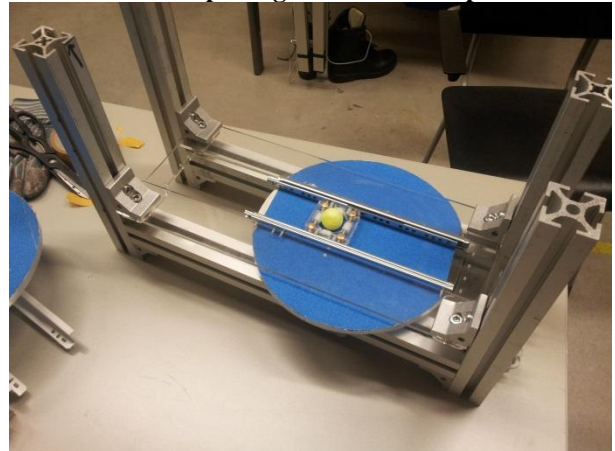
Figure 66. Turning the system upside down the rail system that keeps the ball in place can be attached
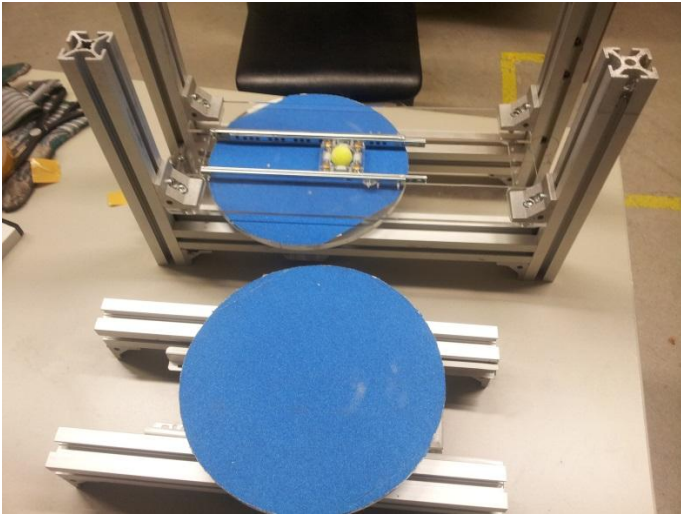
Figure 67. The next step consists on mounting the bottom disc assembly on its slide.
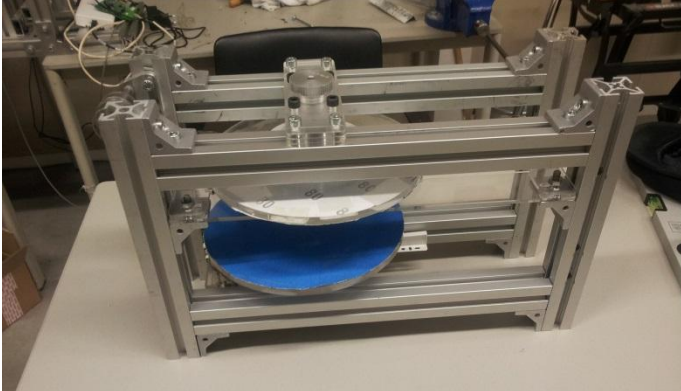
Figure 68. Slide component holding the bottom disc is slid into the rest of the framework
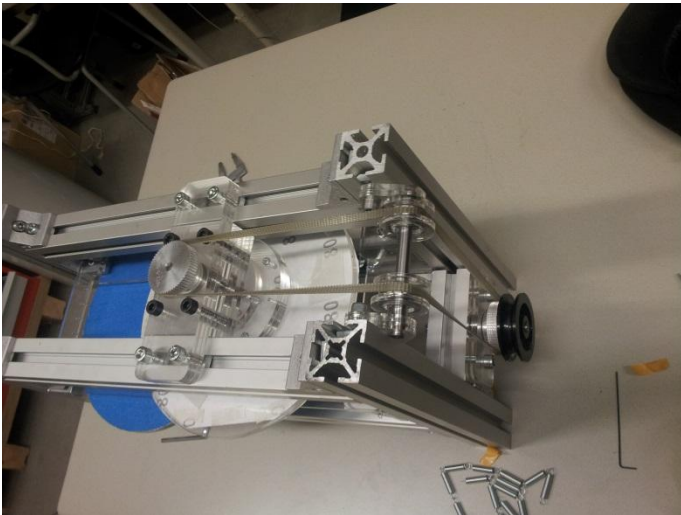
Figure 69. In this final picture the output shaft with pulley is added to the system together with the belt connecting it to the top disc.

Appendix I: Pictures of testing with the system

Figure 70. To generate hysteresis curves the Testometric M250-2.5CT tensile testing machine was used.

Figure 71. Forces for different gear ratios were measured by pulling on a rope that is attached to the pulley connected to the output shaft of the elastic actuator.

Figure 72. To measure the viscoelastic hysteresis curve of the ball that sits between the top and bottom disc, it was compressed and released a few times.
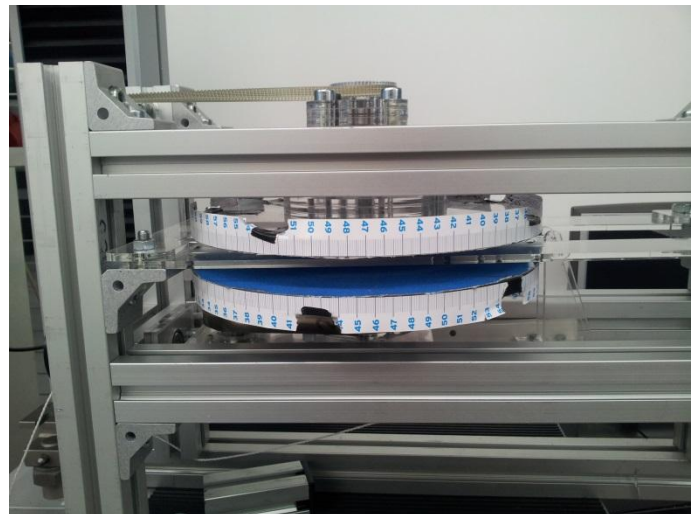
Figure 73. To measure the slip that exists within the system a paper measuring lint was attached to the discs, allowing for the measurement of the position of the discs at the beginning of a cycle and at the end of a cycle.
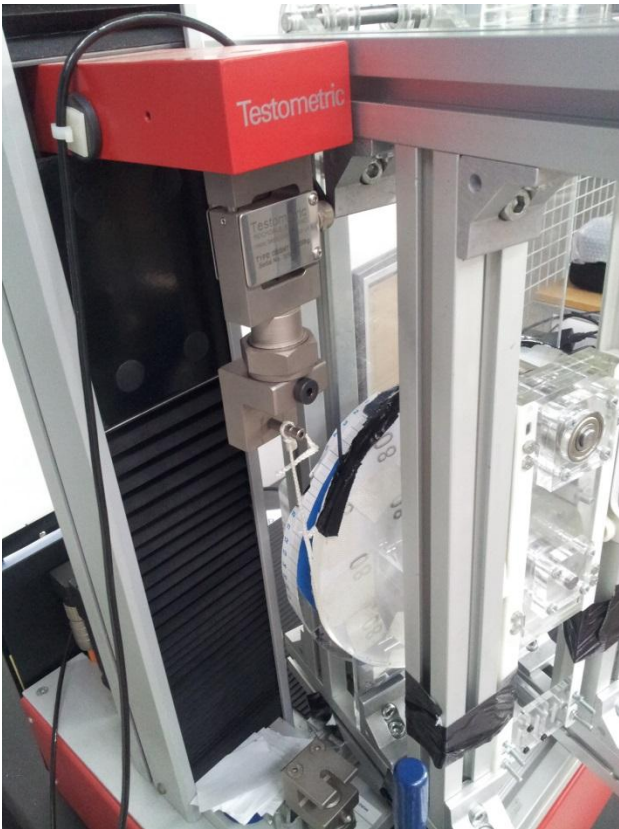
Figure 74. To measure the hysteresis curve of only the bottom spring assembly, the system was placed on its side, with a rope wound over the bottom disc. Pulling the rope rotated the spring assembly (note the difference in radius between the pulley and bottom disc were compensated in the actual table showing the measurements).

Figure 75. Showcase of the system used for measuring the forces of moving the bottom slide assembly. A pulley at the base of the tensile tensing machine redirects the rope to the slide (Note: although in the picture the rope pulls the slide at an angle during the actual measurements this was not the case).

Appendix J: Measurement data of the Performance Of Different Gear Ratios

0:1 - Gear ratio
With a 0:1 gear ratio all the forces required are those that generate losses in the top disc and the slip of the ball. The high frequency spikes showcase a stick slip effect within the ball. While the fluctuation could be slight variations in ball thickness, or gap between the discs. The measurement data can be seen in **Figure 76-78**)
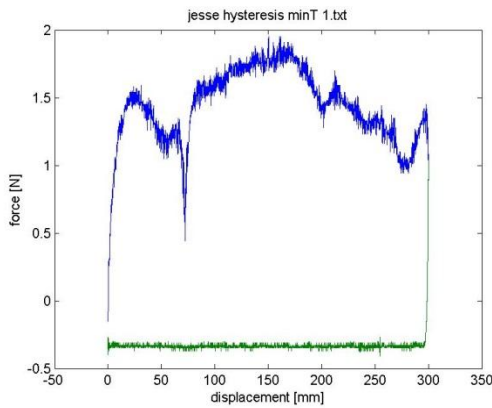
Figure 76. Hysteresis plot when the ball is right underneath the center of the topdisc, as the ball is purely slipping there is no energy recovery in the return path
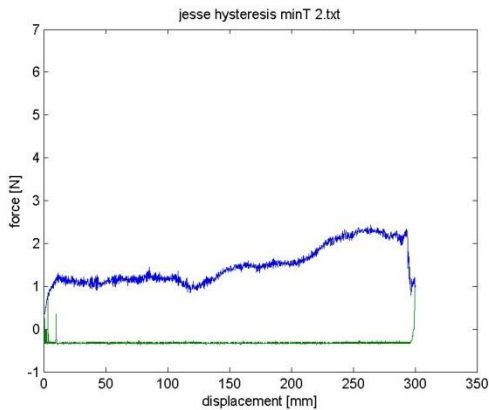
Figure 77. Hysteresis plot when the ball is right underneath the center of the topdisc, as the ball is purely slipping there is no energy recovery in the return path
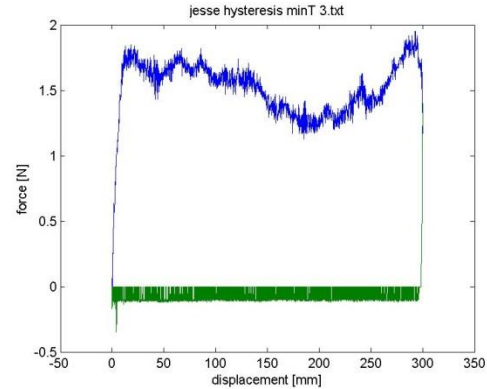
Figure 78. Hysteresis plot when the ball is right underneath the center of the topdisc, as the ball is purely slipping there is no energy recovery in the return path

1:3 - Gear Ratio
The results of the 1:3 gear ratio showcase more interesting result, there is a periodic sawtooth like pattern that corresponds with a half rotation of the interfacing ball between the top and bottom disc. This is likely due to imperfectness of the roundness of the ball generating a slight change in thickness, making the ball compressed more and less. At a lower frequency another slight pattern can be seen which corresponds to a slight variation in height over the discs. Overall about 40% efficiency is obtained. The measurement data can be seen in
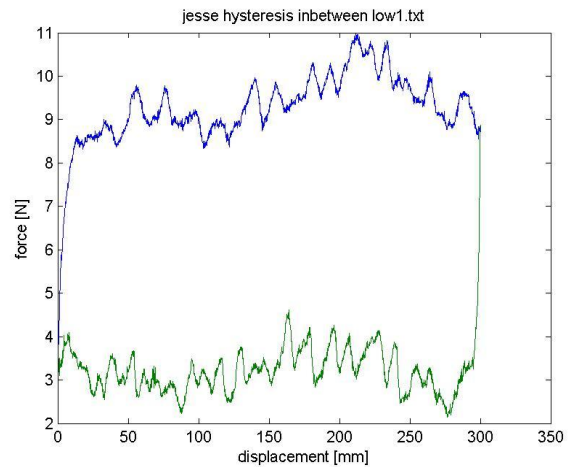
Figure 79. Hysteresis plot for a 1:3 gear ratio
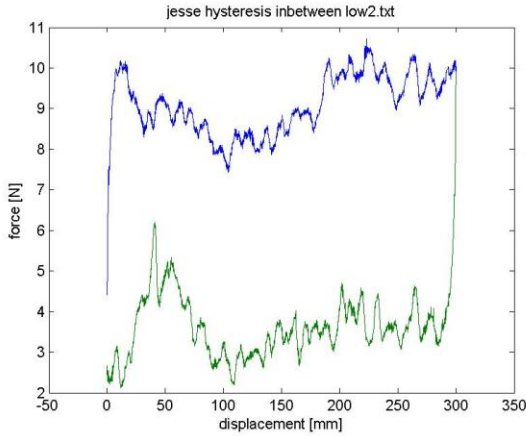
Figure 80. Hysteresis plot for a 1:3 gear ratio
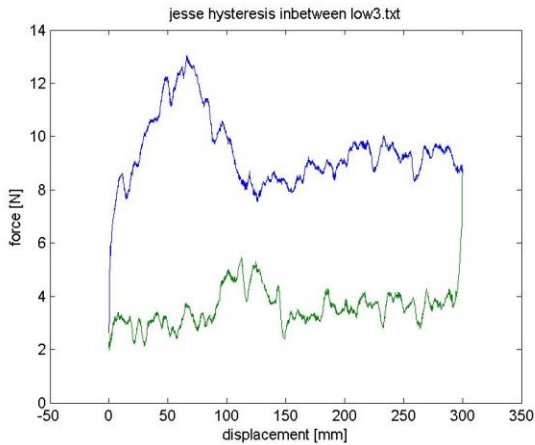
Figure 81. Hysteresis plot for a 1:3 gear ratio

Figure 82. Hysteresis plot for a 2:3 gear ratio
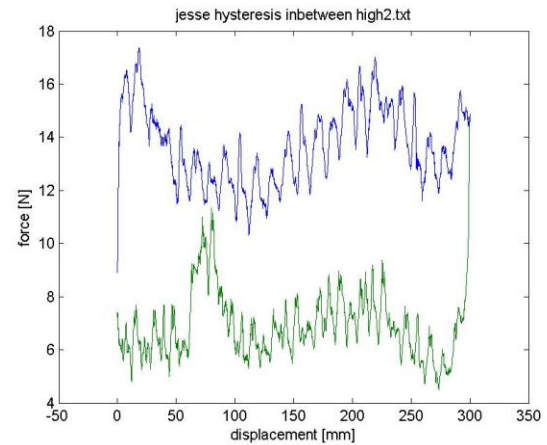
Figure 83. Hysteresis plot for a 2:3 gear ratio
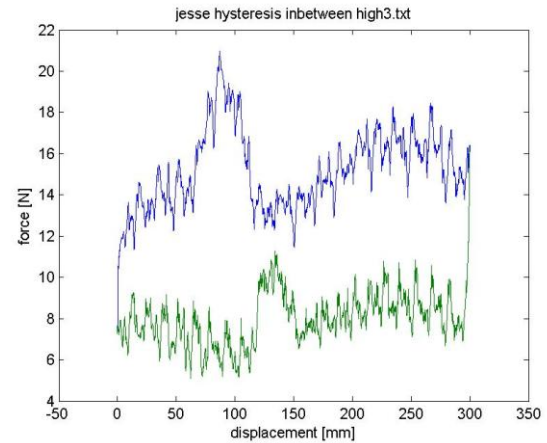
Figure 84. Hysteresis plot for a 2:3 gear ratio

2:3 - Gear Ratio
With the 2:3 gear ratio the efficiency is increased towards 50%, it can be noted that the periodic spikes due to the ball get lower in frequency and higher in amplitude. The reason for this is that the ball is getting closer to the center of the top disc but closer to the edge on the bottom disc, where the effective stiffness of the top disc is higher meaning the ball is compressed more making deviations generate higher force peaks. Overall beside the change in efficiency the results are very similar to those with a 1:3 gear ratio. The raw measurement data can be found in **Figure 82-84**.

1:1 - Gear Ratio
Finally with the 1:1 gear ratio the efficiency remains at around 50% in terms of ratio between the ingoing and outgoing path. However additional losses were measured in terms of slip.
Like seen with the 2:3 gear ratio, with the 1:1 gear ratio the frequency of the ball rotations has increased and with it the

height of the peaks. The raw measurement data can be found in **Figure 85-87**.
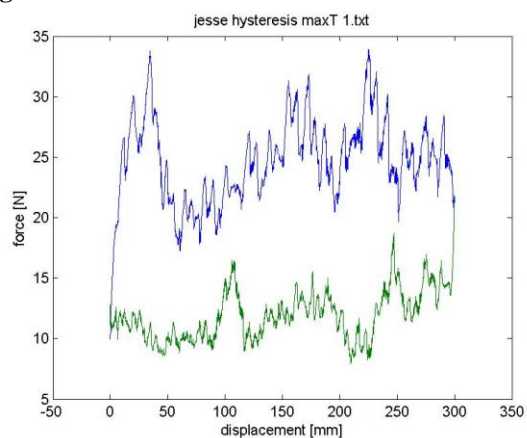
Figure 85. Hysteresis plot for a 1:1 gear ratio
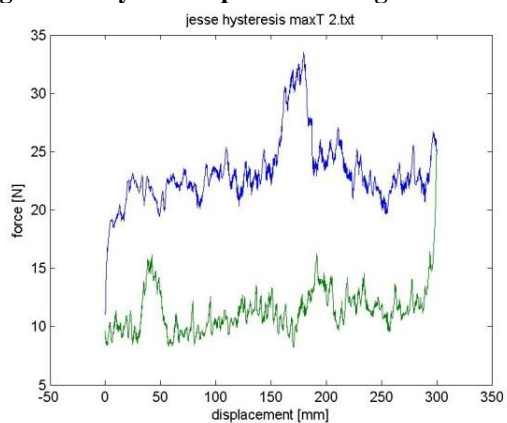
Figure 86. Hysteresis plot for a 1:1 gear ratio
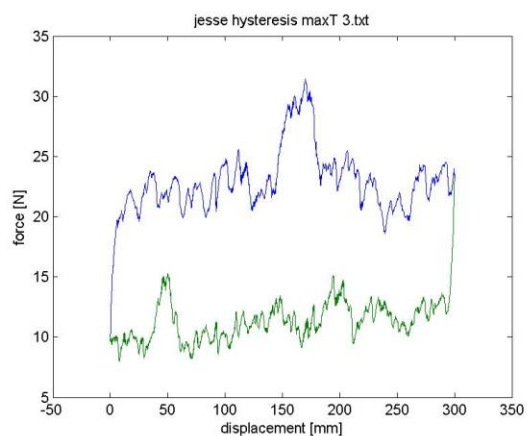
Figure 87. Hysteresis plot for a 1:1 gear ratio

Appendix K: Raw Measurements of the forces for adjusting the gear ratio

For measuring the forces of moving the slide which adjust the apparent output stiffness 3 tests were conducted, one test with only the slide (Figure 88), one test with the slide and a ball (Figure 89) adding additional rolling friction and normal pressure, and one with the ball and the attached spring system enabled (Figure 90). As with this data the effects of the position on the ball on the discs was investigated a linearization of the measurement data happens, with every first picture showing cutting location of the complete data set with the second picture showing the raw data of the cut and a linearization. Forces for moving the slide without the addition of a ball
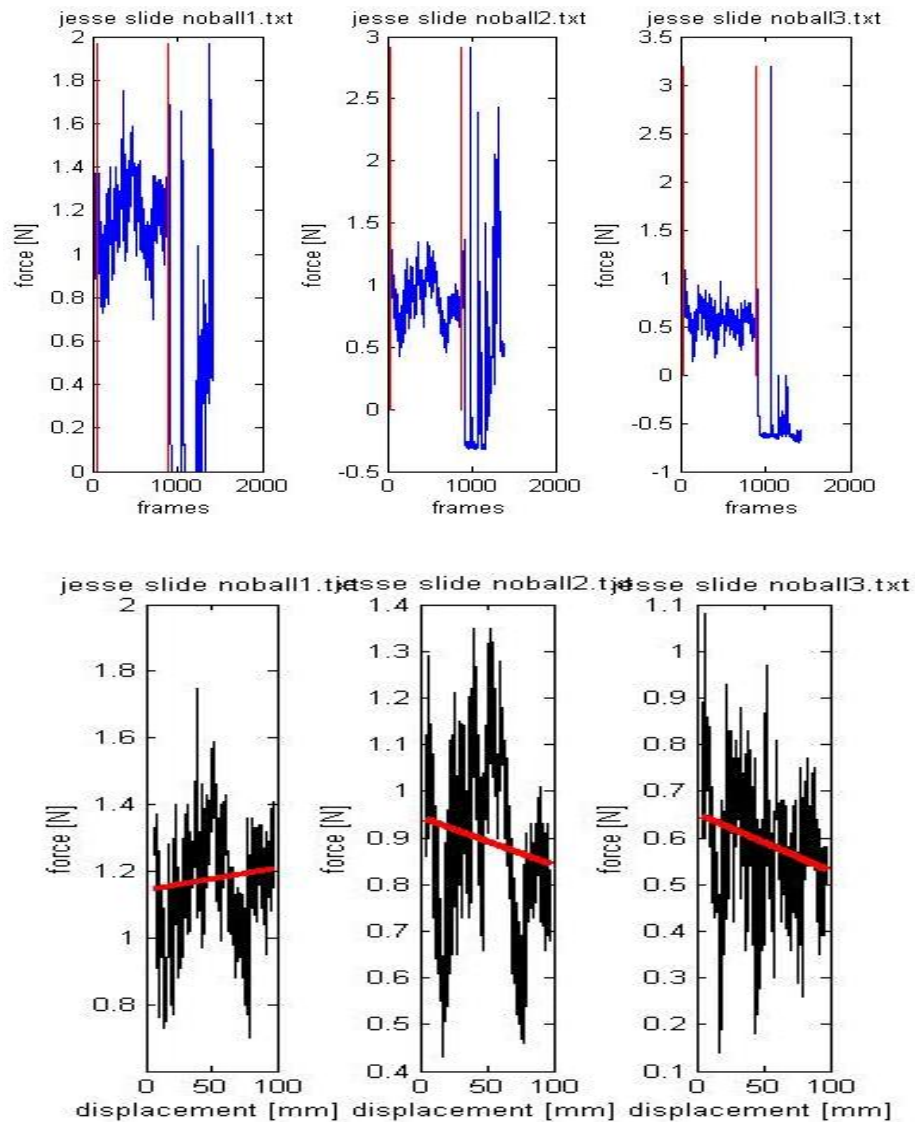
Figure 88. Raw measurement data of moving the slide without the ball, the top pictures show locations for cutting, the bottom pictures show the resulting dataset

**Figure 89. Raw measurement data of moving the slide with the ball,
the top pictures show locations for cutting, the bottom pictures show
the resulting dataset, the red line in the bottom figures is equivalent
to $Y = 1.7097 - 0.0057*X$**

Forces For Moving The Slide, While The Ball Is Added To The System Together With The Spring
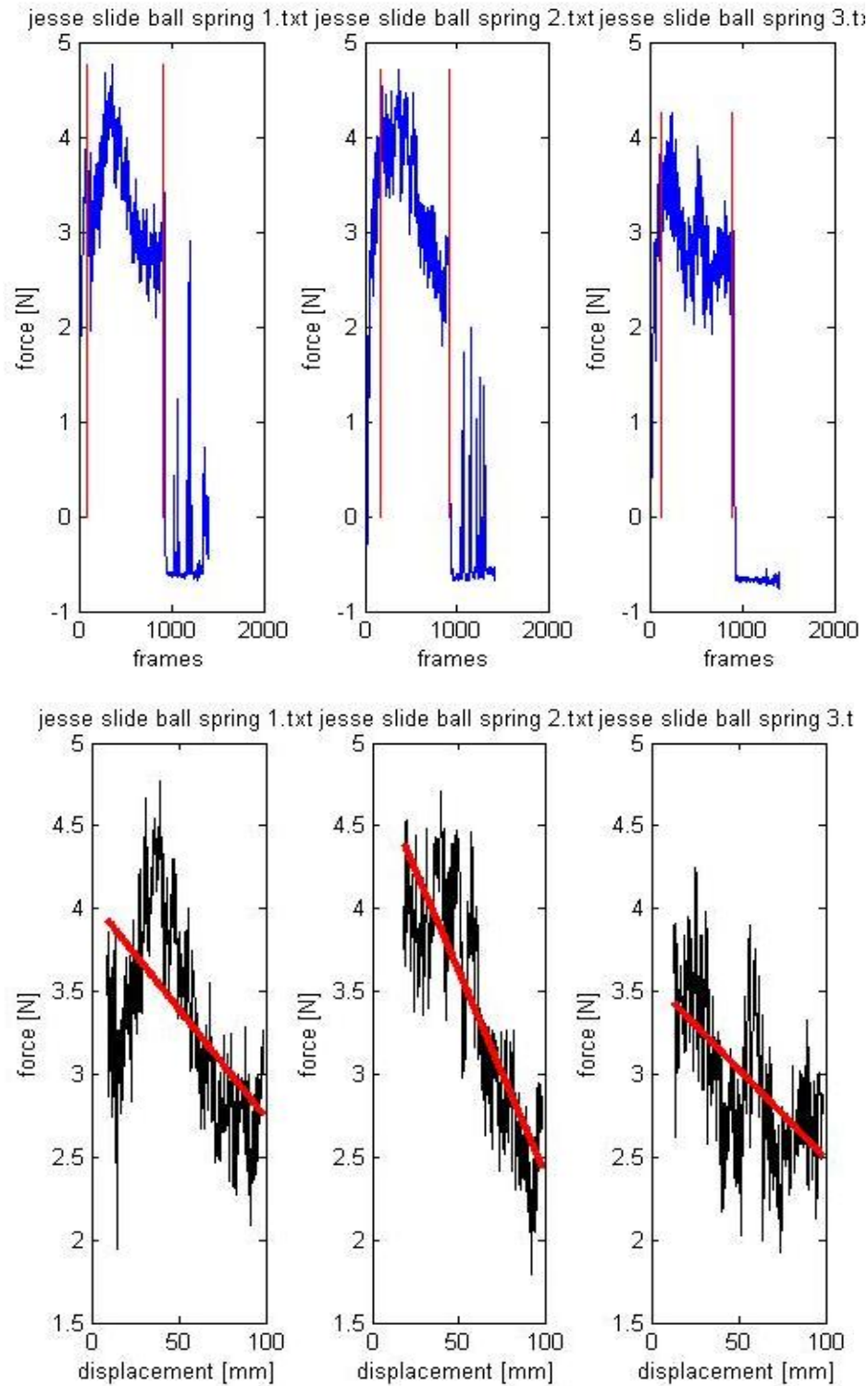
Figure 90. Raw measurement data of moving the slide with the ball and the spring, the top pictures show locations for cutting, the bottom pictures show the resulting dataset, the red line in the bottom figures is equivalent to Y=4.15 – 0.016*X

Appendix L: RAW Measurements With The Interfacing Ball

To measure the viscoelastic energy losses of the ball that sits between the top and bottom disc, a compression test was held at different speeds (150mm/min and 10mm/min). By comparing the area beneath the 2 different paths in the hysteresis plot a figure can be plotted for the energy losses for different indents. (no difference was found between the different speeds)

Data Cutting Points For Compressing The Ball
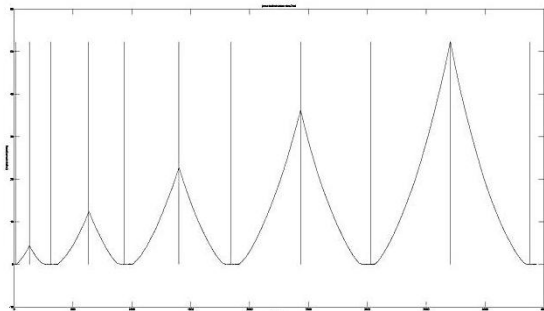
Figure 91. Vertical lines showcase where the dataset was cut, 5 peaks can be found corresponding 5 different indents on the ball varying from 1 to 5 mm
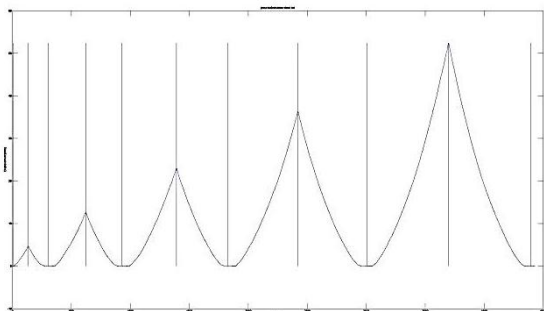
Figure 92. Vertical lines showcase where the dataset was cut, 5 peaks can be found corresponding 5 different indents on the ball varying from 1 to 5 mm
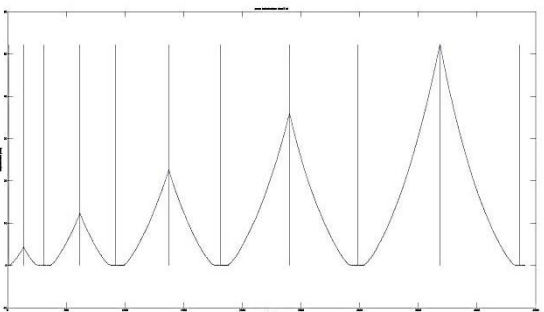
Figure 93. Vertical lines showcase where the dataset was cut, 5 peaks can be found corresponding 5 different indents on the ball varying from 1 to 5 mm

Energy Loss For Different Ball Indents
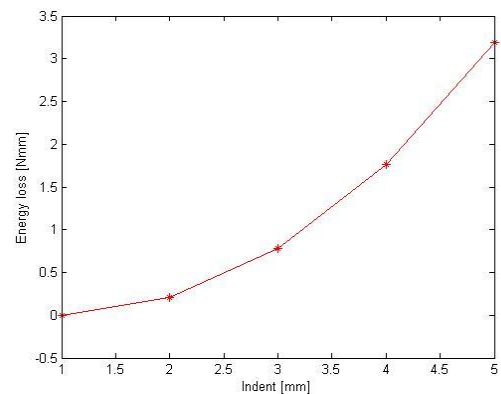
Figure 94. Overal showcase of the energy losses for different compression indents on the ball ranging from 1 to 5 mm

Ball Hysterese Curves
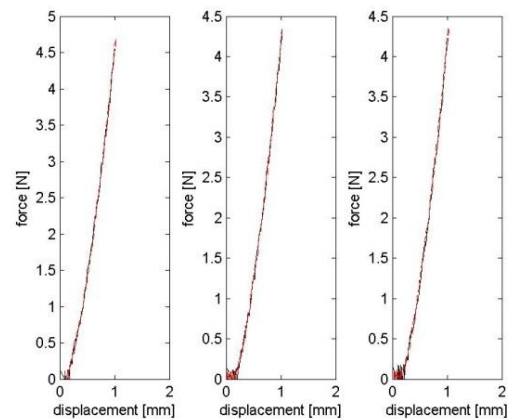
Figure 95. Ball compression hysterese curve for an indent of 1mm
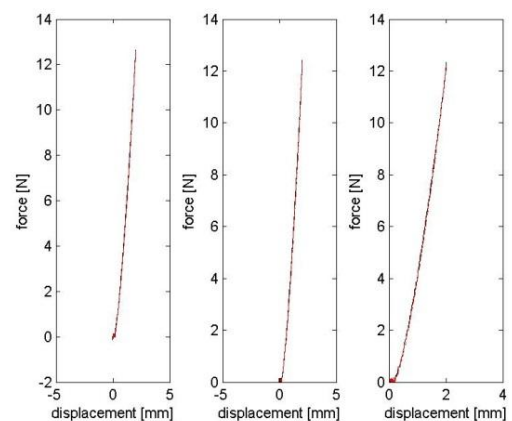
Figure 96. Ball compression hysterese curve for an indent of 2mm
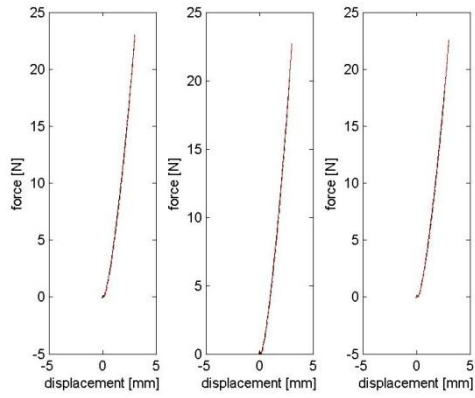
Figure 97. Ball compression hysterese curve for an indent of 3mm
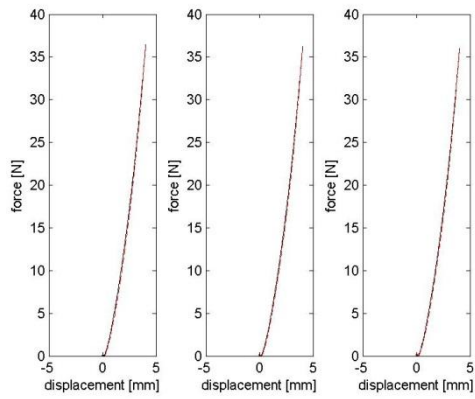
Figure 98. Ball compression hysterese curve for an indent of 4mm
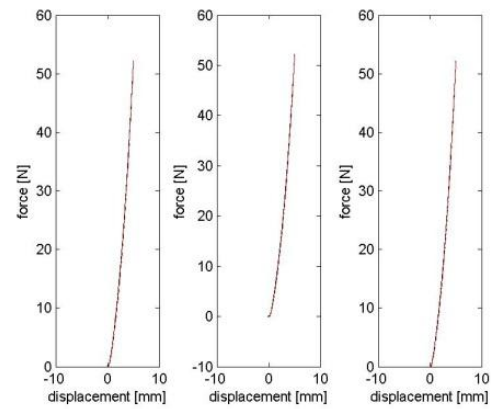
Figure 99. Ball compression hysterese curve for an indent of 5mm.

Appendix M: Other RAW Measurement Data Of The System

Bottom Assembly Together With Constant Force Spring

Measuring the bottom disc spring assembly separately from the rest of the system showcases nothing special, a very high frequency stick slip phenomenon can be noticed, as well as a slight deviation from a straight line due to the mounting screw on the spring.
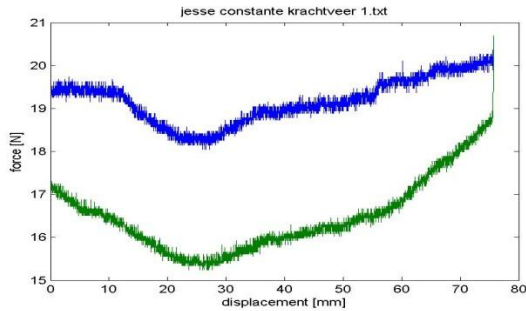
Figure 100. Hysterese plot of the bottom spring assembly
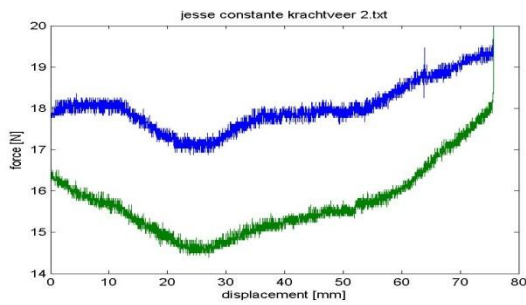
Figure 101. Hysterese plot of the bottom spring assembly
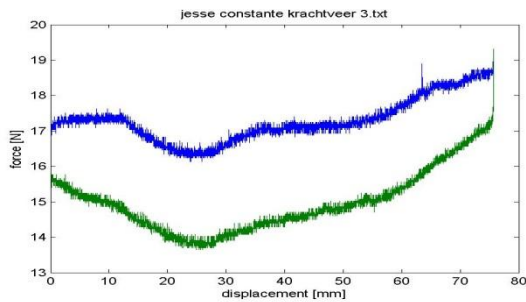
Figure 102. Hysterese plot of the bottom spring assembly

Max friction of the system

When looking at the max friction the system can deliver in the 1:1 ratio, it can be seen that the values get pretty close to the required forces for actuation in the 1:1 ratio. This likely explains the slip that can be found under this ratio. As increasing the normal force will increase the peaks due to the ball non

roundness, there is not much tweaking that can be done to improve this beside higher precision balls and stiffer discs.
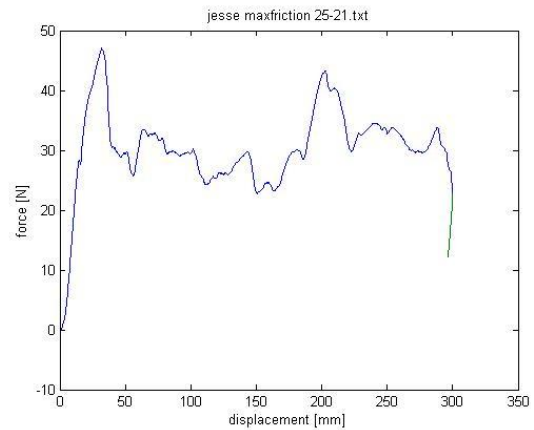
Figure 103. Overview of the max friction in the system when the bottom disc is hold still, around 144mm corresponds to a single rotation of the top disc, notice the double peaks occurring indicating denoting a friction increase once per rotation.

Force required to rotate the top disc with ball, without cage

These measurements show the forces required for the top disc to rotate without any spring attached to the system. The most interesting part of these figures is that they give is a less diluted overview of the periodic variations of the ball itself and variations due to the top disc.
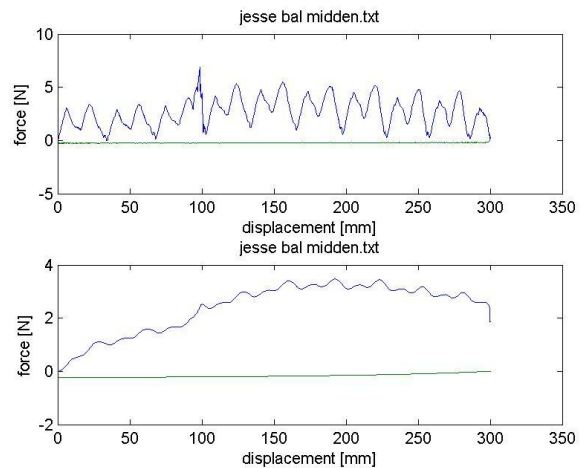
Figure 104. Top System with Ball (No Cage) at 50% of disc diameter
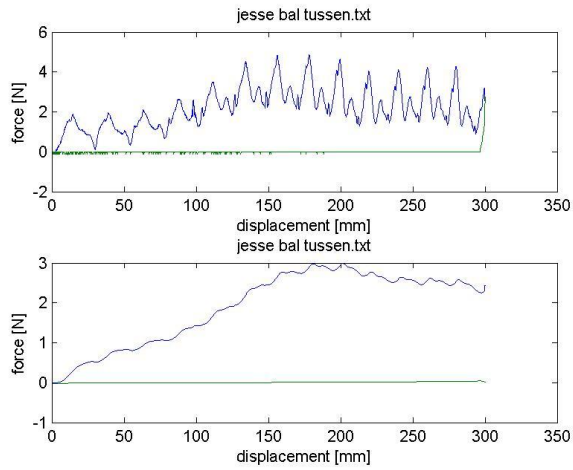
Figure 105. Top System with Ball (No Cage) at 75% of disc diameter
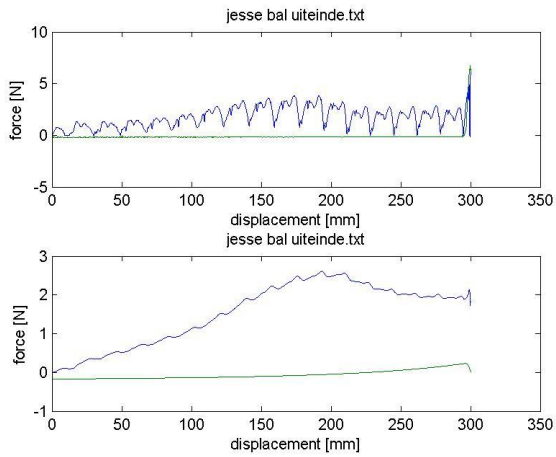
Figure 106. Top System with Ball (No Cage) at the tip of the disc diameter

Top System with no ball

When measuring the forces over the belt and the top disc, it is interesting that there appears to be a spike in the friction that corresponds with the period of 144mm of a single rotation of the top disc, likely caused due to an unevenness of the top disc.
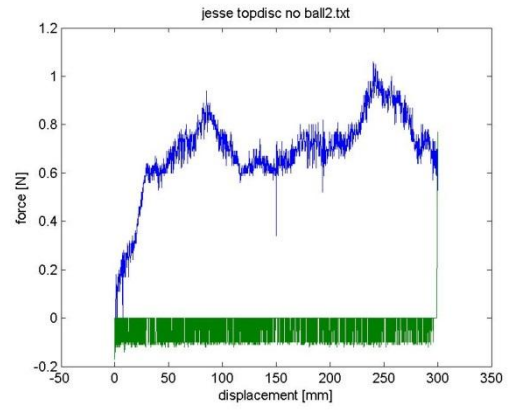
Figure 107. A plot showing the raw data of the friction when rotating the top disc
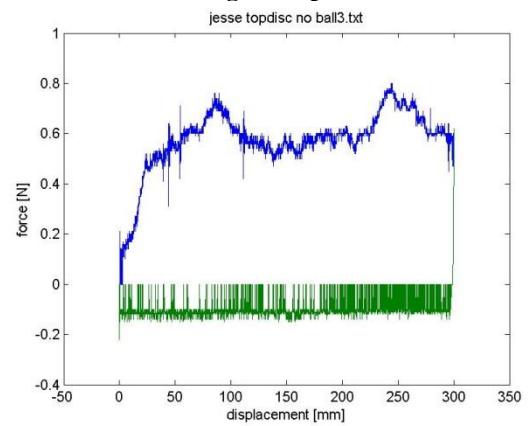
Figure 108. A plot showing the raw data of the friction when rotating the top disc
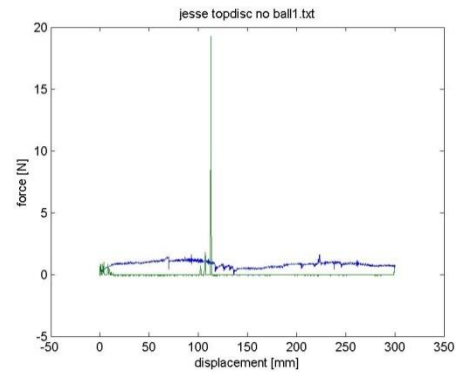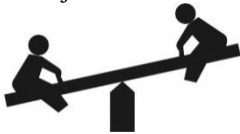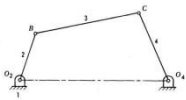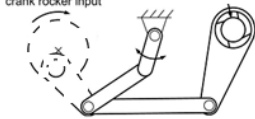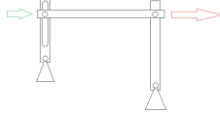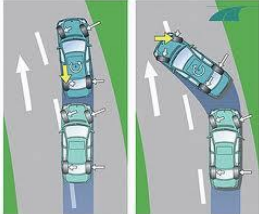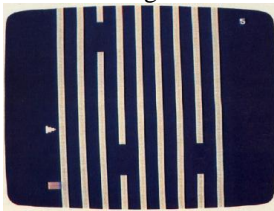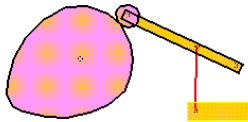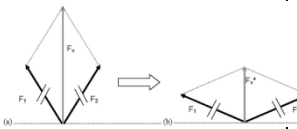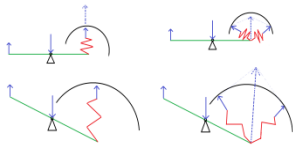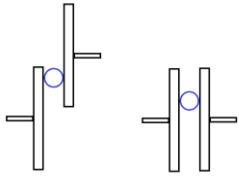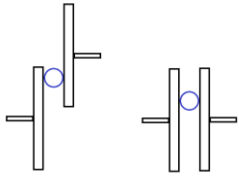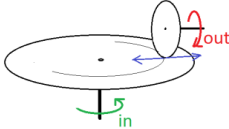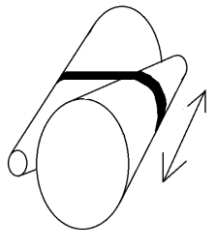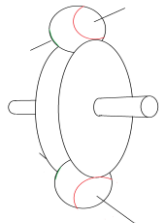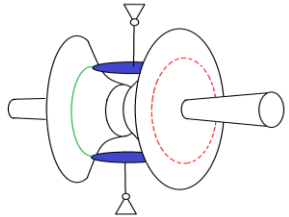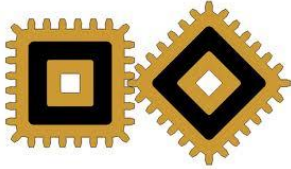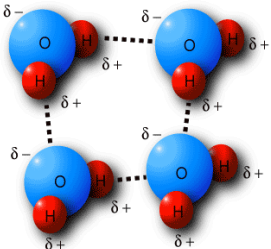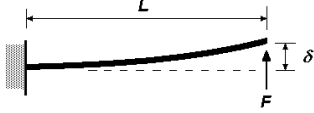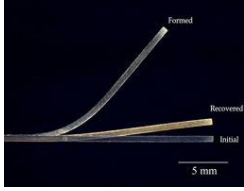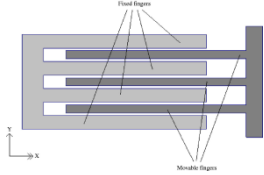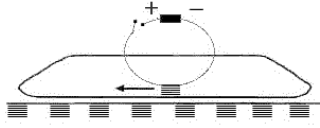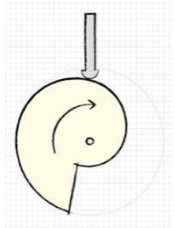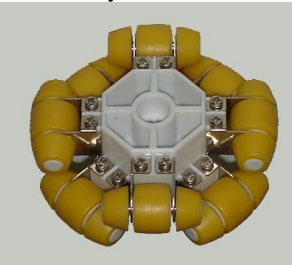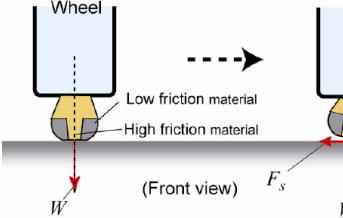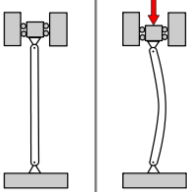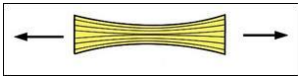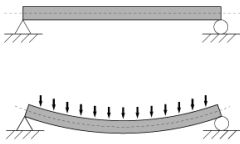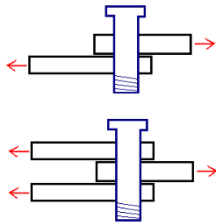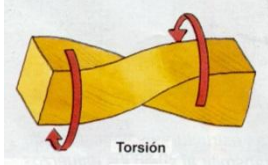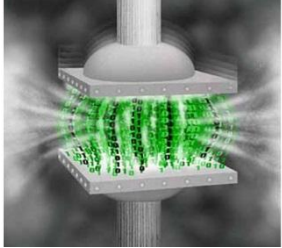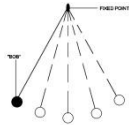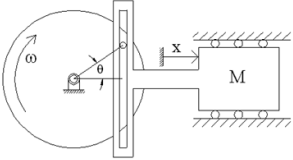
Figure 109. A plot showing the raw data of the friction when rotating the top disc

Adjustment principle	Adjustable Lever	Moving pivot	Adjustable arm			
	Adjustable bar mechanism	5-bar	4-bar (1 slider)	2-3,6+ Bar mechanism?		
	Adjusting path	Turning wheel(s)	Moving bars	Actuated pins generating path	Rotating cams	
	Virtual spring method	Lever				
	CVT	Ball	Double Wheel	Cone	Kopp	Toroidal

	Lock & Move	Specially profiled gears				
Increase traction	Material	Gecko material	Rubber	High surface roughness		
	Geometry	Gear Teeth	Velcro	Flexible teeth	Variable Wedge	
	Bonding (Adhesive/Temperature)	Perfectly polished steel (atomic bonding)	Magnets	Controllable glue Electrical	Controllable glue Mechanical (eg non-Newtonian fluid)	Controllable glue Temperature (eg freezing water)
	Increase normal force	Clamping between 2 surfaces	Clamping with shaft	Use magnets to increase normal force	Pressure	

Adjustment	Electrical Actuators	Linear Spindle Drive	Stepper Motor	Shape memory alloys	Comb drive	Linear induction motor
	Mechanical Actuators	Hydraulic	Pneumatic			
	Mechanical Adjusters	Linkage/Bar mechanisms	Gears	Rope and Pulley	Cams	
Omnidirectional drive		Single layer omniwheel	Multilayer omniwheel	Mecanum wheel	Donut without shape preference	Compliant feet with different materials
Energy Storage	Force/Torque Curve	Constant Force/Torque	Linear Force/Torque	Non-linear Force/Torque		

	Material	Steel	Plastic	Composite	Rubber	
	Material loadcase	Tensile	Bending	Shear	Torsion	Compression
Control	Electrical	Acceleratometer				
	Mechanical	Pendulum				
Sinusoidal path generator	Electrical	Computer				
	Mechanical	Scotch yoke				

Appendix P: Matlab Kinematic & Dynamic Simulation for rigid body model

To simulate the effects of possible friction if a mechanical actuator and sensor would be used (Figure 110), a rigid body model of the system was setup. In order to optimize the generated position output of the slider for the mechanical sensor and controller setup, a genenetic optimizer was used that plotted the output of the slide based on the angular position of the pendulum. To obtain an understanding of the forces on the joints, effects of friction, individual body weights, and dynamic behavior of the system a rigidbody dynamical model was setup (Figure 111). The matlab code for these models can be found in the folder of the attachment under Matlab\RigidBody Simulation.
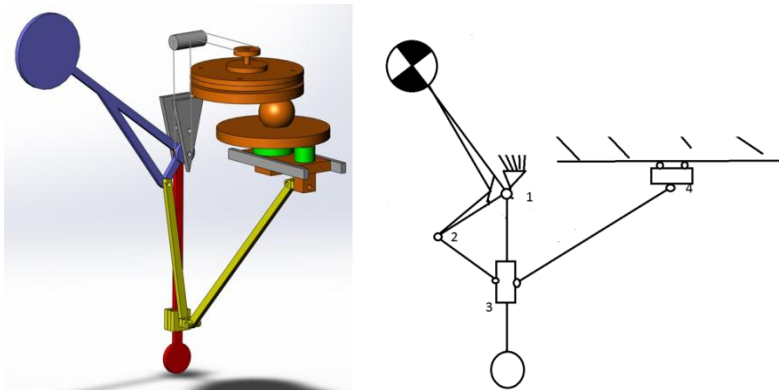
Figure 110 Representation of the mechanical sensor and controller. Left shows a 3d Simulink model, The right shows an abstraction of the model used for simulating in matlab
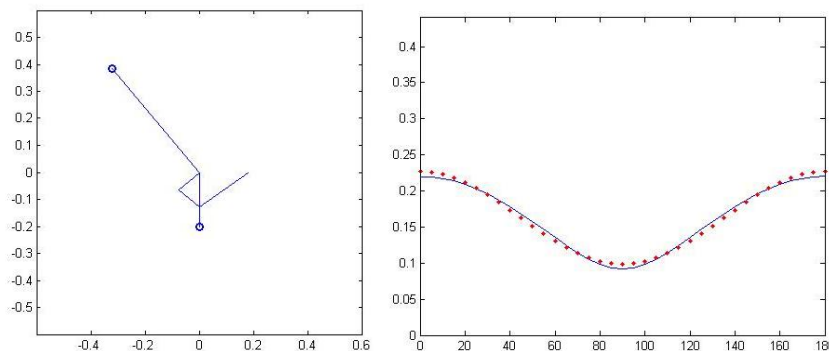
Figure 111 Matlab simulation results
Left: The left picture shows the abstract display of the pendulum with mechanical reference used for the display of the animation of both the dynamic and kinematic simulation
Right: The right picture shows the result of a kinematic simulation trying to track a cosinus.

Appendix O: Literature Research

51

Statically balancing against a rotating external force using elastic elements

Jesse van Dongen

Delft University of Technology
Faculty of Mechanical, Maritime and Materials Engineering
Department of BioMechanical Engineering

Report number: 1307
Student Number: 1316125

Preface

This report displays my literature survey on balancing a pendulum against gravity using elastic elements in the particular case where base of the system is not fixed relative to the gravity orientation. The results discuss the possibility of balancing a pendulum without a fixed vertical reference.

During this literature survey I learned how to search for scientific information, and how to put it into a report. I would like to thank Just Herder from TUdelft , together with everybody at InteSpring BV (especially Giuseppe Radaelli ,Emile Rosenberg and my supervisor Milton Aguirre) for their support in guiding me through the steps of the literature report. Writing has never been my strongest asset, making the creation of this literature review a big struggle for me.

Abstract

An ideal statically balanced device is in static equilibrium throughout its entire working range, has a constant level of energy and can be repositioned in an energy free fashion during quasi-static movement. The ability to move an object without any force allows for higher precision, smaller actuators, and lower power consumption, generating the desire to modify and create systems that are statically balanced [1].

There are multiple ways to make a system statically balanced, the most popular methods use counterweights or springs; counterweights offer simplicity, while spring based solutions generally offer a smaller size and weight package at the cost of more complexity. Another disadvantage of using springs is that a force direction reference is needed. In the case of balancing against gravity, mostly a fixed ground is used for this reference.

However, some systems cannot make use of a fixed ground, while it can still be desirable to balance a system using springs. This generates the research question: is there a system capable of balancing a pendulum utilizing elastic elements without a fixed reference to ground, and if not, how feasible is it to create such a system?

Investigating the issue has identified one main property for the function of such a device: At any position the balancer should be able to change between minimal and maximal torque. In addition, there are two requirements to remain competitive: Adjusting the torque should be energy efficient and force free, and the size and weight of the system should be smaller than that of an equivalent mass counterbalanced system.

To expand the search for a device that holds these properties, a division was made between the ability to adjust energy & the ability to deliver the necessary energy for balancing. These two groups are: energy storage (adjustment by controlling the stiffness in the elastic element), and energy transfer (adjustment by controlling the allowable strain of the elastic element).

Based on these two groups a literature search has been conducted to answer the proposed research question. The results discovered no direct applicable solutions. However, a few energy transfer mechanisms were found that allowed for energy free adjustment when a system was loaded, which fuels the fundamentals of creating a spring balanced pendulum without a fixed reference, encouraging future investigations on the matter.

Table of Contents

Statically balancing using elastic elements against a rotating force

1. Introduction

Recent developments showcase an increased interest in energy efficient actuation. For example, vehicles are being equipped with Kinetic Energy Recovery Systems [2-4], and even within the field of Robotics there is a search for actuators with recoverable energy [5-7] Both in the field of Robotics and Prosthetics, gravitational forces generate a high energy cost to accomplish simple tasks, such as holding an object in space. Although technologies like statically balancing exist, which effectively equate out the effect of gravity within a system, there are various considerations and limitations that need to be taken into account. One of those limitations in the special case of spring based balancers is the requirement of a fixed vertical reference [1]. One particular application where a consistently vertical reference is not available is in the case of balancing on a non-fixed base, such as a human. In this example, this limits the utilization and functionality of spring balanced devices when used for exoskeletons and other systems that can change orientation. This shortcoming drives the creation of a spring balanced system that is able to balance without a fixed vertical reference.

The goal of this literature review is to aid the selection and design of an elastically balanced device without fixed vertical reference. The focus will be on discovering whether such a device already exists, and, if not, identify the properties and feasibility of creating one. An overview is provided for current compliant actuators, or devices with an adjustable output force utilizing elastic elements [7] , adjustable statically balanced systems, including their respective adjustment capabilities, range of motion, efficiency and complexity to assist in concept development & selection.

Before said comparison, an overview will be provided on the basic principles of static balancing, the required properties for a balancer without a fixed vertical reference, and some fundamental information regarding elastic energy storage mechanisms and adjustable transmissions.

2. Method

Problem Analysis

Detailed Problem description: Balancers without fixed reference

When operating a device against external forces, such as those induced by gravity there will be energy costs.

Balancing methods have been created to negate the influence of external forces on a system, lowering the operating energy costs of the system.
Two common methods to balance a system against gravity are balancers based on counterweights or spring mechanisms (See appendix A for more details)

While spring based balancers offer some big advantages over counterweight systems with regard to the systems overall size and weight, they require a fixed vertical gravity reference that can add a lot of complications.

For example, in systems with multiple degrees of freedom, like adding pendula in series, when balanced with springs, a mechanism needs to be attached that passes through the reference of the gravity orientation for each individual pendula. The most common solution utilizes a four-bar mechanism (Figure 1)[8].
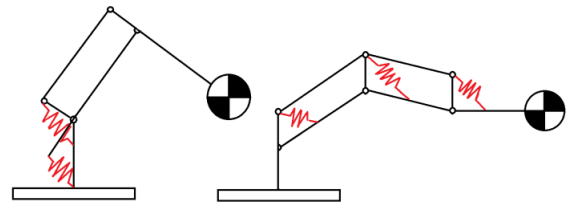
Figure 1: A showcase of 2 multiple degrees of freedom spring based balancers, utilizing four-bar mechanisms to transmit the gravity reference. The left figure shows a design where the springs are mounted on a base, while the right shows a modular design.

Although there are systems that work without balancing every individual link, by balancing the effective center of mass (found through a bar linkage) the system then becomes balanced by directly connecting a spring through that single point [9]. However those systems still require a lot of parts when compared to mass balanced pendula, which can simply be stacked.

Secondly, in systems where there is no location fixed relative to the gravity vector, a new problem surfaces as there is no longer a direct location the balancer can be fixed to. An example of such a case is displayed in Figure 2, while a counterweight based balancer will continue to function when the base is rotated, a spring based balancer will lose its orientation with respect to gravity and lose its ability to balance.
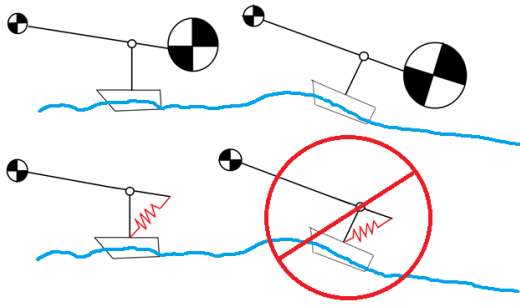
Figure 2: A showcase of a counterweight and spring based balancer when the base is rotated. As the base is a reference for the direction of gravity for a spring based balancer, it will stop functioning when the base is rotated.

A similar issue occurs with balancing systems that can be worn on the human body. A patent from Agrawal et al (Figure 3 left) [10] balances the weight of a human's leg, the orientation of the torso is used as a vertical reference, meaning that if the torso is no longer straight up (e.g. bending forward) the device will no longer show the desired behavior of balancing the leg. As there is no part of the human body that is always vertical, currently having a spring balanced device that always balances correctly requires a connection to the outside world as seen in the patent of Ou Ma et al (Figure 3 right) [11].
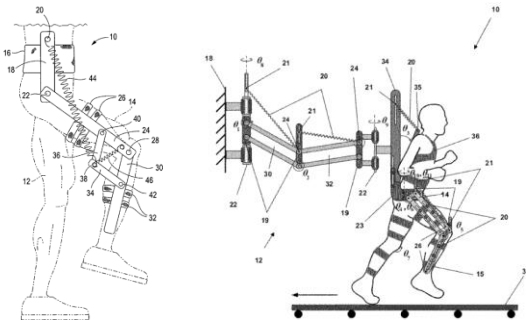
Figure 3:
Left: A spring based gravity balanced orthosis apparatus that balances the weight of a user's leg against gravity. [10]
Right: A wall mounted spring based apparatus for reduced-gravity simulation [11]

In general the advantages of a spring balanced system are often desired in applications where size, inertia or total mass play an important role. Similar criteria are often desired in systems that need to be able to move or be transported, and it is exactly those devices that often do not have a fixed reference to the ground. This creates the demand for a spring balanced system that can still operate without fixed reference.

Properties for an ideal statically spring balanced pendulum without a fixed reference.

When comparing the required moments of an inverted pendulum starting in an upright position relative to the ground on both a horizontal and slanted surface (Figure 4) it can be seen that the sinusoidal balancing function encounters a phase shift with respect to the ground. Notice that the moment curve of the pendulum relative to gravity direction remains unchanged.

With the possibility of a phase shift between 0 and 90° (for instance mounting the pendulum on a vertical wall instead of on the ground),for any angle between the arm of the pendulum and the ground surface, the applied torque should be able to vary from the minimal torque to the maximal torque.
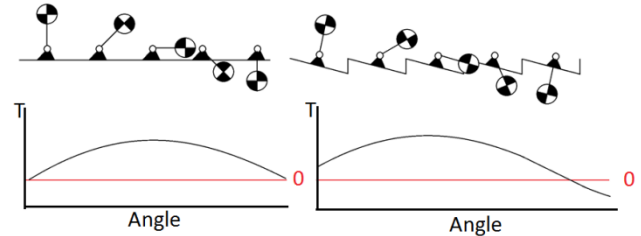
Figure 4: Showcase of the required moments of an inverted pendulum at various positions relative to the ground underneath. On the left the case with a level ground is depicted, while on the right the case with a slanted surface is presented.

This generates the first desired property:

1) At any position the balancer should be able to change between the minimal and maximal torque.

The second property concerns one of the main advantages for statically balanced systems in general; it governs the low force and energy requirements necessary for operation.

If a statically balanced system would require big (energy consuming and heavy) actuators to adjust the system, it would undo its advantageous properties. From which follows, that ideally the adjustment mechanism should adjust the applied torque without any energy cost. This leads to the main desire for such a system:

2) Changing the torque should be energy efficient and ideally force free*

* Note: a restriction exists on the ability to freely change the torque at any position without any energy costs. The average work done by the pendulum should remain zero, as otherwise the search for a perpetual motion device would be initiated.

The major advantage of a spring based balancer over a counterbalanced system is the size and weight. Therefor unless the device can continue to compete on these fields, the use of simpler counterbalanced system would always be preferred, generating the final desire for such a system.

3) The size and weight should be smaller than an equivalent mass counterbalanced system.

With the main property and desires defined, a literature review can be started to look for systems that agree to these requirements.

Subdivision into Energy Storage and Transfer

To compare compliant actuators and statically balanced systems their functioning is separated in 2 parts, Energy Storage and Energy Transfer (Figure 5).
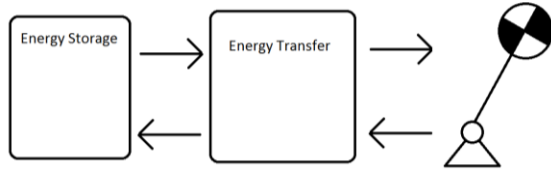
Figure 5: Functional Flow Block Diagram for a system statically balancing an Inverted pendulum.

The energy storage holds a buffer of energy that stores energy when the pendulum loses some of its potential energy, and releases energy when the pendulum needs to gain potential energy. The Energy transfer ensures that the energy from the Energy storage reaches the pendulum and vice versa.
To change the output towards and away from the pendulum, either the energy storage or the energy transfer need to change their throughput (Figure 5). To generate an overview of the possibilities, a search on literature has been conducted on these elements.

As the research focus is on spring based balancers, only the utilization of elastic elements for energy storage will be investigated.

When using an elastic material as energy storage, the amount of energy stored is a function of the deformation applied to the elastic material and the material & geometric properties that give the energy storage element its stiffness.

This generates the notion that the Energy Storage can be controlled by regulating the effective stiffness of the storage, and that the Energy Transfer can be controlled by changing and controlling the actual deformations applied on the elastic material (Figure 6).
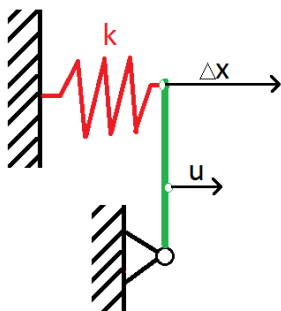
Figure 6: A simple demonstration of the separation in Energy Storage and Energy Transfer for a simple mechanism of a lever attached to a spring that follows Hooke's law . The energy storage defines the spring stiffness (k) affecting the force

generated for a certain spring deflection (Δx) (in the figure the red spring element), while the energy transfer determines the amount of actual spring deflection (Δx) based on an input displacement (u) (in the figure the green lever element).

A short overview will be presented of different types of materials, loading cases and designs for energy storage together with a summation of different balancers and compliant actuators that allow for adjustment of their energy storage mechanism.

For Energy Transfer a short overview will be presented on ideal properties and a short overview of a special type of energy transfer, the continuously variable transmission. Finally, this is followed by different balancers and compliant actuators that allow for adjustment through energy transfer mechanisms.

Method of Search

Search targets for Energy Storage mechanisms

The energy storage purely relates to the elastic energy container that stores energy when not needed and released when it is needed.

Observing the properties for the ideal statically spring balanced pendulum, it can be noted from the first requirement that if adjustment happens through the energy storage mechanism it should be able to change its apparent outwards stiffness at any desired time.

For this reason, first a search will be conducted on various elastic energy storage mechanisms, to show the parameters influencing the general output stiffness. Followed by a search on adjustable static balancers and compliant actuators to obtain an understanding of what devices of this principle currently exist.

Search targets for Energy Transfer mechanisms

Energy Transfer governs the relationship of how much energy is transferred between the internal energy storage and the external output.

From the stated properties for the ideal statically balanced pendulum without a fixed reference, it can be observed from the first point that if adjustment happens through the energy transfer mechanism, it should be able to change its transfer ratio to the desired amount at any desired time. It could also be said that the transfer mechanism or transmission should be continuously variable, which describes a traditional category of transmissions.

Continuously variable transmissions (from here on CVT's) have been in operation since at least since 1877 [12],

with concepts drawn by Leonardo Davinci as early as 1490 [13]

Likewise, the idea of utilizing a CVT for a compliant actuator is not new either. Stramigioli et al [5] describes a conceptual idea of utilizing a CVT to create a "Very Versatile Energy Efficient" (V2E2) actuator that stores energy for any force profile generating negative work on the load.

For this reason, the search for energy transfer mechanisms starts with a brief look at traditional CVTs and their properties, comparing them against the properties needed to statically balance a pendulum using springs. Followed by a search among adjustable static balancers and compliant actuators to show what adjustable systems currently exist.

Search Keywords and Procedure
Utilizing the search targets for energy storage and energy transfer mechanisms, an initial search on articles and patents was started using the search tools made available from the library of the University of Delft.

Figure 7 showcases the process used to go through literature. First, a loop is passed that generates search results, followed by analyzing the found results combined with the criteria to generate a comparison metric, which finally makes it possible to complete a comparison chart.
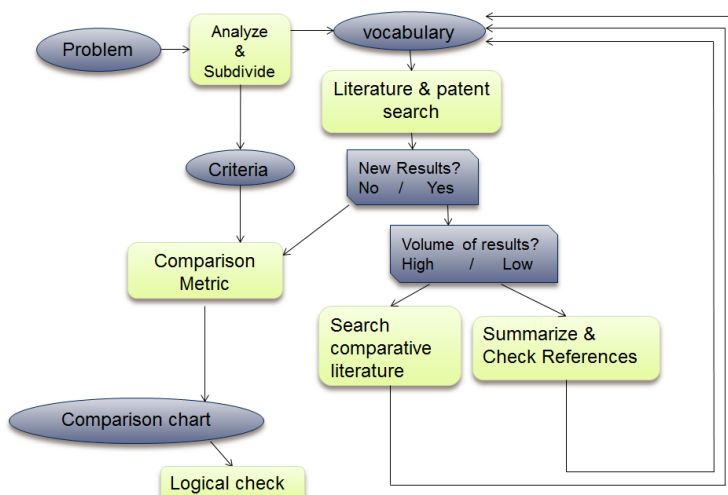
Figure 7: A flow chart describing the used process to go through literature, generate results, and categorize those results.

The most important search terms used to find the desired literature have been:
Compliant Actuator, Variable Stiffness actuator, Adjustable stiffness device, Gravity equilibrator Adjustable lever mechanism, Continuously variable Transmission, Lever transmission, bar mechanism

transmission, joint stiffness control, Adjustable compliance, antagonistic actuator adjustable energy storage, energy free adjustable balancer, force free adjustable balancer, gravity equilibrator, statically balancing, neutral stability, spring to spring balancing, spring force compensation, zero-stiffness.

To make sure that the search covers a broad enough field, references used in scientific articles have been crosschecked for missing papers and results. If a lot of results were found for an item, a search would be started to find technological review papers, to generate an overview from which a selection could be made to narrow down the findings.

This literature research will show personally selected examples out of all the different found solutions and devices, purely to limit the necessary time and space to generate an overview.

Method of Comparison
Based on found literature and the constructed ideal properties for a pendulum without a fixed reference, a list of points has been constructed that will allow for comparison on different solutions. These points are as follows:

- Type of energy adjustment
  Reason: Allows for grouping of similar solutions.

- Elastic range of motion
  Reason: Some devices might work perfect without any available working range, adding the actual range of motion allows for a more thorough comparison. This metric can also be a requirement in the selection process for some applications.

- Ratio of change within the energy adjustment
  Reason: The first ideal property for an ungrounded pendulum requires the ability to generate a sinusoidal torque curve, for this an infinite adjustment ratio is necessary.

- Stiffness range
  Reason: Although gear ratios can be scaled up or down, the range of actual stiffnesses could help in the selection of a compliant actuator for the appropriate scale of work.

5

- Energy Cost of the Adjustment
    Reason: The second ideal property of an unground inverted statically balanced pendulum desires zero energy cost for the adjustment.

- Elastic Element utilized
    Reason: Different elastic elements have different properties in terms of, for instance, the effective use of the material or the actual max allowable rotation.

- Elastic material Utilized
    Reason: Different materials have different inherent properties the elastic range and the actual stiffness can depend on the material utilized

- Shape Characteristic of the stiffness curve
    Reason: Different applications require different stiffness curves. Although curves can easily be changed by cams and other transmission ratios that generally adds to the complexity.

- Average Standard error in amplitude modulation between different stiffnesses
    Reason: When the goal is to control a device with adjustable stiffness it is desirable that the adjustment only multiplies the effective amplitude of the stiffness curve.

- Estimation of the number of parts used
    Reason: To obtain an approximation of the complexity, an assumption on the number of parts has been made for every device.

3. Results

Authors note: Various devices have been found, during the search for technologies and devices. In order to maintain readability most of the analysis, comparison and research have been placed in the appendices. The following chapter provides a summary on the key findings of the different categories

Background search on elastic energy containers and continuously variable transmissions
Elastic Energy Containers
A search on elastic elements and their fundamental properties has been conducted to generate an understanding of the working principles that stiffness adjusting devices might use. This research generated

possible parameters that can be adjusted to change the stiffness.

In general, properties that could be adjusted seem to be in the form of engaging active material (changing length/coils/amount of springs), changing the effective material usage (changing the loading method, changing second moment of inertia), changing material properties (electricity, heat). For the full detail of the comparison of different spring types, shapes and materials a detailed write up can be found in Appendix B: Background Research on energy storage and transfer mechanisms

Continuously Variable Transmissions
Continuously variable energy transfer mechanisms or Continuously Variable Transmissions (CVT) are special transmissions that within a given range can freely adjust their transmission ratio. This special group of transmissions is mostly desired in categories where varying torque and speed requirements are needed, like in the transportation industry.

Of different categories within CVTs, traction drives (due to the need of continuous variability, traditional fixed gearings cannot be utilized) and overrunning clutch designs (working principle of an adjustable lever arm) can be considered the most promising categories, as energetic losses are presented in forms of friction. This means that there are no energy losses when the system is not in operation, contrary to the other categories.

The range of Adjustment of different CVTs varies. Although using a combination of power split mechanisms and end gearings it is possible to adjust the total gearing range upwards or downwards, allowing for the possibility of making any CVT an IVT (Infinitely variable Transmission) or the ability to freely change from a fixed transmission ratio, to one with a blocked input and freely rotatable output.

The utilization of most CVTs is for continuous motion, this limits the options for CVTs that can energy efficiently change their transmission when not rotating. Most traction CVTs change their gearing ratio over multiple rotations, while overrunning clutch designs generally only work in a single direction.

However, as quasi static operation differs from continuous motion, a possible space is generated for new designs, for instance, by utilizing a limited range of motion or unbalanced loading scenarios. For a more detailed comparison on different CVTs please refer to Appendix B: Background Research on energy storage and transfer mechanisms

Search on balancers and stiffness actuators changing the energy container

Found solutions that adjust the energy container can be grouped in a few categories. Out of these categories only one group generated some viable results. A short summary on these groups will be presented, however, a more detailed description analysis on found literature can be found in Appendix C: Results of Literature. The defined categories are:

1. Devices that adjust the pretension of a system [14-20]

Devices in the first category appear to change the apparent stiffness at the cost of tensioning or relaxing the spring. Generating a group of solutions that require energy to be added or removed from the system to adjust it.

2. Devices that change the active part of the spring element [21-26]

Devices in the second category can often change the active part of the spring theoretically at no energy cost; however, this adjustment can generally only happen when the system is at rest. A loaded system would cause the elastic element to deform, requiring either the adjustment device to adapt to the changed shape, or force the spring back to its original shape when adapting. Making these devices cost energy to adjust when not in their neutral position.

3. Devices that change how the system is loaded [27, 28]

The third category shows more interesting results. Most devices of this kind change the second moment of inertia for bending in different ways. Unfortunately this did not bring any better results than the second group, due to only allowing energy free adjustment in a single position. In this group however there was a single device that could be used for adjustment at any position in an energy free fashion.

The virtual spring method [28] uses the effect of superposition by changing the orientation of springs to generate different net result forces without changing the length of the springs, which would release or require additional energy (Figure 8Figure 9).
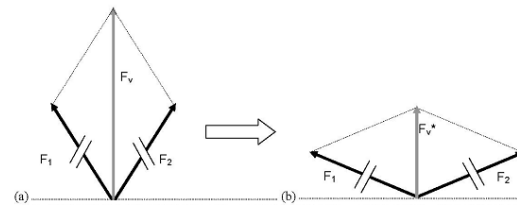
Figure 8: Utilizing the method of superposition on 2 forces of the same size, allows for creation of a resultant force of a different sizes. [28]
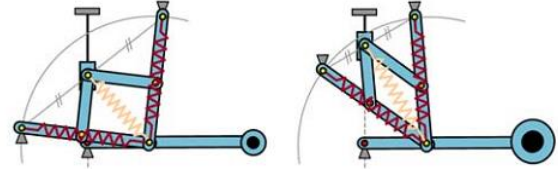
Figure 9: Applying the concept of superposition on a statically balanced pendulum, enforcing an arc for the springs through a pantograph allows for a change of resultant balancing force without changing the stored energy within the spring. [28]

Although this device uses a pantograph which only allows the spring to be adjusted over a single arc, meaning that the device can only be adjusted in an energy free fashion at a single position. However, if a method would be found that changed the arc radius depending on the spring length, it would become possible to adjust at any position, making the virtual spring method the only found method within the adjustment of energy storage that appears to generate a possibility for energy free adjustment in all positions.

Search on balancers and stiffness actuators changing the transmission ratio.

Solutions found for changing the transmission ratio have been grouped in 4 categories. A summary of the findings within these categories will be presented, however, for the detailed evaluations and explanations of these systems please refer to Appendix C: Results of Literature

1. Pendulum based adjustable balancers [7, 29-34]

Devices in the first category are based upon adjusting parameters (A.B.C in Figure 10) of a traditional pendulum.
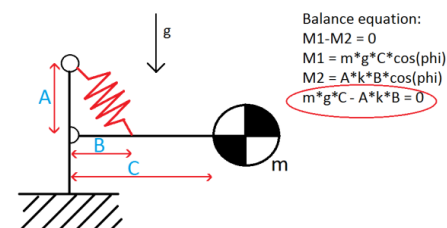
Figure 10: A pendulum counterbalanced by a zero-free-length spring, including a balancing equation for the required mounting position and spring stiffness.

7

Adjusting these parameters usually changes the length of the spring creating an energy requirement or dissipation. For this reason only solutions that can adjust in an efficient matter were evaluated.

Two types of solutions were found that offered methods to adjust in an energy efficient fashion. The first method makes use of a secondary spring that delivers the energy needed for adjustment [30, 31]. Although these devices can only be adjusted in a single position, another spring could be used to allow for efficient adjustment in different positions[29]. However this requires the system to go back to a predetermined configuration to change the position where the device can be adjusted.

The second method, the simultaneous displacement method [7, 32-34], uses the change of 2 parameters at the same time, such that the spring length does not get changed. This, depending on the implementation, can theoretically allow for adjustment at any position.

2. Path adjusting balancers [15]

The second category describes devices that are forced to follow a path or track, where the path equates a certain stiffness pattern, changing this path allows for a different stiffness pattern to be followed. The only device found in literature making use of an adjustable path was the "parallel type variable stiffness actuator" [15]. Only changing the future path allows for energy free adjustment of such a system.

3. Lever CVT based stiffness actuators [35-41]

The third category describes seesaw like devices that use an adjustable lever arm or pivot point to change their transmission ratio. Most of these devices can only be adjusted in an energy free fashion at a neutral load. However, two devices were found that could be used to change the transmission ratio at any position.

The variable stiffness rotational actuator (Figure 11) [40] and the variable stiffness actuator from the university of Twente (Figure 12) [35] Both of these devices control two degrees of freedom instead of one, allowing them to change the leverage at any position without changing the in or output angle.
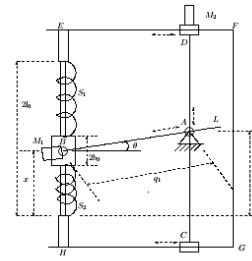
Figure 11: Schematic of the VSRA's working principle. The pivot point of the spring setup can move on a 2d plane allowing the pivot to change such that the output of rotation and the length of the springs do not change when adjusting the lever arm. [40]
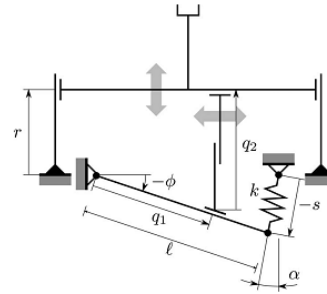
Figure 12: Showcase of the working principle of the vsaUT, by controlling both q1 and q2 at the same time, the lever arm can be adjusted at different heights and set angles even when loaded. [35]

4. Other CVT based stiffness actuators [42]

The fourth and final category describes devices that use a method similar to traditional continuously variable transmissions as the core functionality. Only one device was found within this category, the continuously variable transmission variable stiffness actuator (Figure 13) [42].
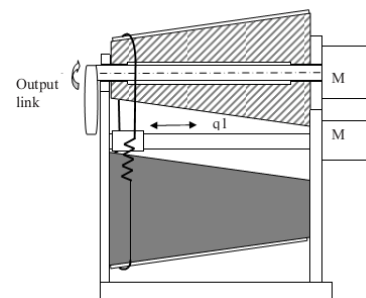
Figure 13: A schematic view of the CVTvsa, a double cone CVT connected not with a regular transmission belt but with an elastic element. [42]

In this device the adjustment happens by changing the elastic belt to the left or right, which changes the effective position on the cones and thus, changing the in- and output-ratio. The novelty of this device is that a single degree of freedom is needed for the adjustment, while from then on the transmission ratio is constant.

A comparison chart that summarizes all of the results found based on the defined metrics follows this section.

Evaluation Table
Table 1: Comparison of various stiffness adjusting mechanisms

Category	Name	Range	Ratio	Adjustability	Adjustment	Elastic Element	Elastic Material	Characteristic	Avg Std Error	Parts
Pretension	VS-Joint [14]	14°	Inf - 1.3	0-7 to 38-51 Nm/deg	Full cost	Compression Spring	Springsteel	progressive	18%	11
Pretension	PVSA [15]	55°	Inf	0-0.9 Nm/deg	Energy free in neutral	Linear Coil Springs	Springsteel	progressive	5%	6
Pretension	Compliant VSA [16]	12-24°	4x	0.2-0.8 Nm/deg	Full cost	Leafspring	Aluminium 7075-T6	linear	7%	6
Pretension	APVSEA [17]	10-100°	10x	0.1-1.0 Nm/deg	Full cost	Linear Coil Springs	Springsteel	linear	7%	9
Pretension	BIJSC [18]	60°	73x	0.011-0.807 Nm/deg	Full cost	Linear Coil Spring + Quadratic profile	Springsteel*	linear	2%	7
Pretension	AMASC [19]	NA	7x	2500-18000 N/m	Full cost	Leaf spring + Logaritmic cam	Fiberglass	linear	1%	11
Pretension	AWCM [20]	60-100°	Inf	0.000-0.008 Nm/deg	Full cost	Linear Coil Spring + quadratic cam	Springsteel	linear	1%	6
Adjustable k	Jack spring actuator [21]	NVT.	Inf	Kinitial - Inf Nm	Energy free in neutral	Linear Coil Spring	Springsteel	linear	NA	2
Adjustable k	Adjustable chair [22]	360°	Inf	Kinitial - Inf Nm	Energy free in neutral	Linear Coil Spring	Springsteel	sinusoidal	NA	6
Adjustable k	Energy Free adjustable gravity equilibrator [23]	360°	Inf	Kinitial - Inf Nm	Energy free in neutral	Linear Coil Spring	Springsteel	sinusoidal	NA	6
Adjustable k	AAC [24]	2-10°	8x	0.07-0.57 Nm/deg	Energy free in neutral	Leafspring	Springsteel	sinusoidal	4%	6
Adjustable k	AVSEA [25]	0-40°	Inf	0.085 - Inf Nm/deg	Energy free in neutral	Leafspring	Springsteel	linear	1%	12
Adjustable k	Rotatable beam, changing the bending moment of inertia. [27]			stepped	Energy free in neutral	bending beam	Steel	linear	NA	2
Adjustable k	VSASF [26]	120°	7x	5-35 Nm/deg	Energy free in neutral	normally loaded belt	Rubber	progressive	NA	11
Adjustable k	Virtual spring method [28]	360°	Inf	Kinitial - Inf Nm	Energy free at lock	Linear Coil Spring	Springsteel	sinusoidal	NA	9
Pendulum based	Adjusting the A and/or B parameter	360°	Inf	0-Unknown kg	Full cost	Linear Coil Spring	Springsteel	sinusoidal	NA	5
Pendulum based	ASD[43]	360°	Inf	0-Unknown kg	Full cost	Linear Coil Spring	Springsteel	sinusoidal	15%	4
Pendulum based	Simultanious Displacement [30] [31]	360°	Inf	0- Unknown kg	Energy free at lock	Linear Coil Spring	Springsteel	sinusoidal	NA	3
Pendulum based	MACCEPA 1 & 2 [32, 33]	45°	Inf	0-3.5e-4 Nm/deg	Energy free at lock	Linear Coil Spring	Springsteel	sinusoidal	2%	6
Pendulum based	MACCEPA 1 & 2 [32, 33]	45°	Inf	0-1.6e-3 Nm/deg	Energy free at lock	Linear Coil Spring	Springsteel		31%	6
Pendulum based	Balancing using a storage spring for adjustment in a single position [30, 31]	360°	Inf	0-Unknown Kg	Energy free at single position	Linear Coil Springs	Springsteel	sinusoidal	NA	8
Pendulum based	Balancing using a storage spring for multiple positions [29]	360°	Inf	0-Unkown Kg	Energy free at lock	Linear Coil Springs	Springsteel	sinusoidal	NA	11
Lever based	Compact VSA [41]	20°	Inf	0-60 Nm/deg	Energy free in neutral	Linear Coil Springs	Springsteel	progressive	NA	5
Lever based	VSRA: [40]	10°	Inf	0-23e-3 Nm/deg	Energy free at load	Linear Coil Springs	Plastic	linear	1%	5
Lever based	Awas [38, 39]	6°	14x	1.6-22 Nm/deg	Energy free in neutral	Linear Coil Springs	Springsteel	linear	4%	5
Lever based	HDAU Hybrid Dual Actuator Unit [37]	30°	31x	0.07-2.2 Nm/deg	Energy free in neutral	Linear Coil Springs	Springsteel	linear	16%	4

| Lever based | vsaUT [35, 36] | 10° | Inf | 1000-Inf N/m * | Energy free at load | Linear Coil Springs | Springsteel | linear | NA | 6 |
| CVT based | CVTvsa [42] | 360° | 4x | Unknown | Energy free at load | Normally Loaded Belt | Rubber | Aprox linear | NA | 4 |

4. Discussion

Although the literature research showed no existing systems for balancing a pendulum without fixed reference, the results made it likely that such a device could be designed.

Looking at the adjustment section of Table 1, a few devices can be adjusted in an energy free fashion while fully loaded, namely the VSRA, vsaUT and the CVTVSA. The first 2 systems use a lever based CVT transmission, while the latter uses an adapted traditional double cone CVT transmission.

The ability to freely adjust output force when the system is under load, make it likely to assume that by connecting these devices with an appropriate controller it should be possible to balance a pendulum.

Looking into the principle why the VSRA and vsaUT which can be adjusted without any energy cost, shows that adjusting the lever arm with 2 degrees of freedom instead of one makes it possible to change the lever arm without changing the output or spring length.
The CVTVSA shows that while traditional CVT's cannot be adjusted at zero speed, that by adding an additional degree of freedom perpendicular to the direction where the driving force is applied, allows for the ability to adjust at zero speed.

Looking at the range of adjustment, it can be seen that lever based systems have a relatively small operating range of 10-30°, while most pendulum and CVT based solutions have a theoretical range of 360°. With a lot of existing CVTs the low amount of solutions give the impression that the field of CVTs for a quasi-static environment has not been fully explored yet.

At the section comparing elastic material and elements, there appears to be very little variation between the balancers. As most devices utilize regular coil springs made out of spring steel, this could allow for possibly smaller and lighter devices by utilizing composite or rubber springs.

In general all necessary components appear to exist. This means that the creation of a spring balanced pendulum without a fixed base is mostly an issue of design optimization.

For this reason, the next step would be to use this information as a tool for creating a proof of concept to validate the hypothesis that it is possible to balance a spring balanced pendulum without a fixed reference in an energy free fashion.

If that hypothesis is indeed true, next steps could be made in attempting to apply these properties into actual devices, while considering properties such as cost, complexity, size and weight in the design problem, to compete with other types of balancers.

5. Conclusion

The objective of this literature survey was to identify whether devices currently exist that could balance a pendulum using elastic elements without a fixed vertical reference, and if not to generate the knowledge to evaluate the feasibility, of creating one.

To evaluate the feasibility of creating such a device, an analysis of the problem was made. This analysis found that a device should be capable of adjusting the output stiffness at any possible position. To stay competitive this adjustment should happen in an energy efficient matter, at low mass & size constraints.

Using an alternative design approach, the problem was separated to generate two possible solution paths: adjusting the energy storage or adjusting the energy transfer mechanism.

A search on a wide selection of variable stiffness actuators and adjustable pendulums, together with the results of the analysis, allowed for categorizing found results within a table (Table 1).

No results found no devices that could balance a pendulum while allowing energy efficient adjustment of the output torque at any position. However a few devices like the VSRA, vsaUT and CVTVSA can freely adjust output stiffness at any time. This strengthened the authors believe that when combined with a pendulum would allow for a reference free balancer to be made.

It was observed that most of the devices were heavy compared to regular spring based balancing devices, as most concepts used regular spring steel coil springs instead of more compact and lighter rubber or coil springs, this implies that there is a lot of room for improvement, if these devices would be optimized for weight and size reduction.

It was also discovered that there are a large amount of CVTs designed for continuous operation when compared to the few CVTs that can adjust efficiently in quasi static operation. This generates an opportunity do explore and develop new efficient CVTs for use within a quasi-static operation.

The main advantage of CVTs over lever based designs is the increased range of motion with a single degree of adjustment. This is advantageous for pendulum balancers as this simplifies the possible control methods.

In conclusion, the literature research did not show an energy efficient compliant actuator for balancing an ungrounded pendulum, however results found principles of operation that could make it feasible to develop such an actuator. Similarly results identify a gap in technology; possibly opening a new field for energy efficient actuation.

References

1. Herder, J.L., *Energy-free systems: theory, conception and design of statically balanced spring mechanisms.*, in *Department of Biomechanical Engineering*. 2001, Delft University of Technology: Mekelweg 2, 2628 CD Delft, The Netherlands.
2. Boretti, A., *Comparison of fuel economies of high efficiency diesel and hydrogen engines powering a compact car with a flywheel based kinetic energy recovery systems.* International Journal of Hydrogen Energy, 2010. **35**(16): p. 8417-8424.
3. Boretti, A.A., *Improvements of vehicle fuel economy using mechanical regenerative braking.* International Journal of Vehicle Design, 2011. **55**(1): p. 35-48.
4. Walsh, J., T. Muneer, and A.N. Celik, *Design and analysis of kinetic energy recovery system for automobiles: Case study for commuters in Edinburgh.* Journal of Renewable and Sustainable Energy, 2011. **3**(1).
5. Stramigioli, S., G. van Oort, and E. Dertien, *A concept for a new Energy Efficient Actuator.* 2008 Ieee/Asme International Conference on Advanced Intelligent Mechatronics, Vols 1-3, 2008: p. 671-675.
6. Visser, L.C., R. Carloni, and S. Stramigioli, *Energy-Efficient Variable Stiffness Actuators.* Ieee Transactions on Robotics, 2011. **27**(5): p. 865-875.
7. Van Ham, R., et al., *Compliant Actuator Designs Review of Actuators with Passive Adjustable Compliance/Controllable Stiffness for Robotic Applications.* Ieee Robotics & Automation Magazine, 2009. **16**(3): p. 81-94.
8. Lin, P.Y., W.B. Shieh, and D.Z. Chen, *Design of a Gravity-Balanced General Spatial Serial-Type Manipulator.* Journal of Mechanisms and Robotics-Transactions of the Asme, 2010. **2**(3).
9. Agrawal, S.K. and A. Fattah, *Gravity-balancing of spatial robotic manipulators.* Mechanism and Machine Theory, 2004. **39**(12): p. 1331-1344.
10. Agrawal, S., *Gravity balanced orthosis apparatus*. 2005.
11. Ou Ma, J.W., *Apparatus and method for reduced gravity simulation*. 2009.
12. Norman H. Beachley, A.A.F., *Continuously variable transmissions: Theory and practice*. 1979: Lawrence Livermore Laboratory.
13. Birch, S. *Audi takes CVT from 15th century to 21st century* Tech briefs 2000 22nd jan 2013]; Available from: http://www.aei-online.sae.org/automag/techbriefs_01-00/03.htm.
14. Wolf, S. and G. Hirzinger, *A new variable stiffness design: Matching requirements of the next robot generation.* 2008 Ieee International Conference on Robotics and Automation, Vols 1-9, 2008: p. 1741-1746.
15. Nam, K.H., B.S. Kim, and J.B. Song, *Compliant actuation of parallel-type variable stiffness actuator based on antagonistic actuation.* Journal of Mechanical Science and Technology, 2010. **24**(11): p. 2315-2321.
16. Palli, G., et al., *Design of a Variable Stiffness Actuator Based on Flexures.* Journal of Mechanisms and Robotics-Transactions of the Asme, 2011. **3**(3).
17. Wang, R.J. and H.P. Huang, *An Active-Passive Variable Stiffness Elastic Actuator for Safety Robot Systems.* Ieee/Rsj 2010 International Conference on Intelligent Robots and Systems (Iros 2010), 2010.
18. Migliore, S.A., E.A. Brown, and S.P. DeWeerth, *Biologically inspired joint stiffness control.* 2005 IEEE International Conference on Robotics and Automation (ICRA), Vols 1-4, 2005: p. 4508-4513.
19. Hurst, J.W., J.E. Chestnutt, and A.A. Rizzi, *The Actuator With Mechanically Adjustable Series Compliance.* Ieee Transactions on Robotics, 2010. **26**(4): p. 597-606.

20. Kilic, M., Y. Yazicioglu, and D.F. Kurtulus, *Synthesis of a torsional spring mechanism with mechanically adjustable stiffness using wrapping cams.* Mechanism and Machine Theory, 2012. **57**: p. 27-39.

21. Hollander, K.W., T.G. Sugar, and D.E. Herring, *Adjustable Robotic Tendon using a 'Jack Spring'(TM).* 2005 Ieee 9th International Conference on Rehabilitation Robotics, 2005: p. 113-118.

22. N. Vrijlandt, J.L.H., *Seating Unit for supporting a body or part of a body*, L. Hoffman & Baron, Editor. 2004: NL.

23. van Dorsser, W.D., et al., *Energy-free adjustment of gravity equilibrators by adjusting the spring stiffness.* Proceedings of the Institution of Mechanical Engineers Part C-Journal of Mechanical Engineering Science, 2008. **222**(9): p. 1839-1846.

24. Rodriguez, A.G., N.E.N. Rodriguez, and A.G.G. Rodriguez, *Design and validation of a novel actuator with adaptable compliance for application in human-like robotics.* Industrial Robot-an International Journal, 2009. **36**(1): p. 84-90.

25. Wang, R.J. and H.P. Huang, *Mechanically stiffness-adjustable actuator using a leaf spring for safe physical human-robot interaction.* Mechanika, 2012(1): p. 77-83.

26. Tonietti, G., R. Schiavi, and A. Bicchi, *Design and control of a variable stiffness actuator for safe and fast physical human/robot interaction.* 2005 IEEE International Conference on Robotics and Automation (ICRA), Vols 1-4, 2005: p. 526-531.

27. T. Sugar, K.H., *Adjustable stiffness leaf spring actuators*, USPTO, Editor. 2009: US.

28. Wisse, B.M., et al., *Energy-free adjustment of gravity equilibrators using the virtual spring concept.* 2007 Ieee 10th International Conference on Rehabilitation Robotics, Vols 1 and 2, 2007: p. 742-750.

29. Duval, E.F., *Mechanical Arm Including A Counter-Balance*, USPTO, Editor. 2008: USA. p. 1-82.

30. Barents, R., et al., *Spring-to-Spring Balancing as Energy-Free Adjustment Method in Gravity Equilibrators.* Journal of Mechanical Design, 2011. **133**(6).

31. Barents, R., et al., *Spring-to-Spring Balancing as Energy-Free Adjustment Method in Gravity Equilibrators.* Proceedings of the Asme International Design Engineering Technical Conferences and Computers and Information in Engineering Conference, Vol 7, Pts a and B, 2010: p. 689-700.

32. Van Ham, R., et al., *MACCEPA: the actuator with adaptable compliance for dynamic walking bipeds.* Climbing and Walking Robots, 2006: p. 759-766.

33. Vanderborght, B., et al., *MACCEPA 2.0: Adjustable Compliant Actuator with Stiffening Characteristic for Energy Efficient Hopping.* Icra: 2009 Ieee International Conference on Robotics and Automation, Vols 1-7, 2009: p. 179-184.

34. J.L. Herder, R.B., B.M. Wisse, W.D. van Dorsser, *Efficiently variable zero stiffness mechanisms.* Workshop on Human-Friendly Robotics, 2011. **2011**.

35. Visser, L.C., et al., *Modeling and Design of Energy Efficient Variable Stiffness Actuators.* 2010 Ieee International Conference on Robotics and Automation (Icra), 2010: p. 3273-3278.

36. Visser, L.C., R. Carloni, and S. Stramigioli, *Variable Stiffness Actuators: a Port-based Analysis and a Comparison of Energy Efficiency.* 2010 Ieee International Conference on Robotics and Automation (Icra), 2010: p. 3279-3284.

37. Kim, B.S. and J.B. Song, *Hybrid Dual Actuator Unit: A Design of a Variable Stiffness Actuator based on an Adjustable Moment Arm Mechanism.* 2010 Ieee International Conference on Robotics and Automation (Icra), 2010: p. 1655-1660.

38. Jafari, A., N.G. Tsagarakis, and D.G. Caldwell, *A Novel Intrinsically Energy Efficient Actuator With Adjustable Stiffness (AwAS).* Ieee-Asme Transactions on Mechatronics, 2013. **18**(1): p. 355-365.

39. Ghorbani, R. and Q. Wu, *Adjustable stiffness artificial tendons: Conceptual design and energetics study in bipedal walking robots.* Mechanism and Machine Theory, 2009. **44**(1): p. 140-161.

40. Rao, S., R. Carloni, and S. Stramigioli, *A novel energy-efficient rotational variable stiffness actuator.* 2011 Annual International Conference of the Ieee Engineering in Medicine and Biology Society (Embc), 2011: p. 8175-8178.

41. Tsagarakis, N.G., I. Sardellitti, and D.G. Caldwell, *A New Variable Stiffness Actuator (CompAct-VSA): Design and Modelling.* 2011 Ieee/Rsj International Conference on Intelligent Robots and Systems, 2011: p. 378-383.

42. Cicchitti, L., *Design and Implementation of a variable stiffness actuator*, in *Construzione di Macchine Automatiche e Robot LS*. 2009, Universita di Bologna: Italy.

43. Uemura, M. and S. Kawamura, *A New Mechanical Structure for Adjustable Stiffness Devices with Lightweight and Small Size.* Ieee/Rsj 2010 International Conference on Intelligent Robots and Systems (Iros 2010), 2010.

44. Tolou, N., et al., *Stiffness Compensation Mechanism for Body Powered Hand Prostheses with Cosmetic Covering.* Journal of Medical Devices-Transactions of the Asme, 2012. **6**(1).

45. Soemers, H., *Design Principles for precision mechanisms*. 2010, Enschede: T-pointprint.

46. Dieter Muhs, H.W., Manfred Becker, Dieter Jannasch, Joachim Voßiek, *Roloff / Matek Maschinenelemente*. 4th ed. 2005, Den Haag: Academic Service. 270-310.

47. Beek, A.v., *Advanced engineering design, lifetime performance and reliability*. 2006, Delft: Delft University of Technology. 500.

48. Hibbeler, R.C., *Mechanics of Materials, Sixth Edition*. 2005, Singapore: Prentice Hall.

49. Cool, J.c., *Werktuigbouwkundige Systemen*. 2003, Delft: DUP Blue print.

50. Cuypers, M.H., *Continu variabele transmissies. Deel 1 : theoretisch en praktisch bekeken.* Aandrijftechniek, 1985. **8**(1): p. 10-15.

51. Chen, T.F., D.W. Lee, and C.K. Sung, *An experimental study on transmission efficiency of a rubber V-belt CVT.* Mechanism and Machine Theory, 1998. **33**(4): p. 351-363.

52. Chen, T.F. and C.K. Sung, *Design considerations for improving transmission efficiency of the rubber V-belt CVT.* International Journal of Vehicle Design, 2000. **24**(4): p. 320-333.

53. Francis, R., *Pushing Belt Drive Efficiency.* PTdesign, 1998. **March 1998**: p. 33-36.

54. Lee, D.W. and C.K. Sung, *On the efficiency analysis and improved design of a rubber V-belt CVT.* International Journal of Vehicle Design, 1997. **18**(2): p. 119-131.

55. Zhu, C., et al., *Experimental investigation on the efficiency of the pulley-drive CVT.* International Journal of Automotive Technology, 2010. **11**(2): p. 257-261.

56. Michael A. Kluger, D.R.F., *An Overview of Current CVT Mechanisms, Forces and Efficiencies.* SAE Technical Paper 970688, 1997.

57. Benford, H.L. and M.B. Leisling, *The Lever Analogy: A New Tool in Transmission Analysis.* SAE Technical Paper, 1981(810102): p. 429-437.

58. Cuypers, M.H., *Continu variabele transmissies. Deel 2 : theoretisch en praktisch bekeken.* Aandrijftechniek, 1985. **8**(2): p. 33-35.

59. Cuypers, M.H., *Continu Variabele transmissies. Deel 3.* Aandrijftechniek, 1985. **8**(3): p. 49-53.

60. Yamamoto, T., K. Matsuda, and T. Hibi, *Analysis of the efficiency of a half-toroidal CVT.* Jsae Review, 2001. **22**(4): p. 565-570.

61. Carbone, G., L. Mangialardi, and G. Mantriota, *A comparison of the performances of full and half toroidal traction drives.* Mechanism and Machine Theory, 2004. **39**(9): p. 921-942.

62. Younes, Y.K., *A Design Scheme for Multidisk Beier Traction Variators.* Journal of Mechanical Design, 1992. **114**(1): p. 17-22.

63. Takaki, T. and T. Omata, *100g-100N finger joint with load-sensitive continuously variable transmission.* 2006 Ieee International Conference on Robotics and Automation (Icra), Vols 1-10, 2006: p. 976-981.

64. Takaki, T. and T. Omata, *Load-sensitive continuously variable transmission for robot hands.* 2004 Ieee International Conference on Robotics and Automation, Vols 1- 5, Proceedings, 2004: p. 3391-3396.

65. English, C. and D. Russell, *Implementation of variable joint stiffness through antagonistic actuation using rolamite springs.* Mechanism and Machine Theory, 1999. **34**(1): p. 27-40.

66. English, C.E. and D. Russell, *Mechanics and stiffness limitations of a variable stiffness actuator for use in prosthetic limbs.* Mechanism and Machine Theory, 1999. **34**(1): p. 7-25.

Appendix A: Basic Information about static balancing

Static Balancing and its advantage

An ideal statically balanced device is in static equilibrium throughout its working range, got a constant level of energy and can be moved energy free in a quasi-static situation [1]. A visualization to obtain a better understanding of the subject can be made using marbles under the effect of gravity.
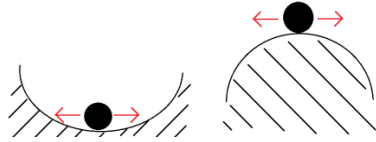

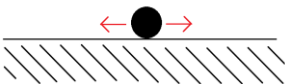Figure 14: A visualization of marbles in a stable (left) and unstable (right) equilibrium.

Figure 15: A visualization of a marble in equilibrium that is neither stable nor unstable.

When a marble is placed on top of a hill (Figure 14) it won't immediately fall down. However if a small perturbation occurs the marble will fall down the hill. If a marble is in a gully (Figure 14) and a small perturbation occurs it will move back to its original position.

This preference for the marble to go towards or away from a certain position means that marble is not in static equilibrium at all positions, in this case due to the influence of gravity. The energy levels of the marble are not constant either due to the different heights over the trajectory meaning that there are different states of potential energy.

When a marble is placed on flat ground (Figure 15) it can be placed anywhere without wanting to change to a different position, meaning it's always in a static equilibrium. A constant height over the trajectory ensures a constant potential energy level. In quasi static movement where the velocity and acceleration are effectively zero, it won't require any force to move the system from the left to the right.

The ability to move an object without any force allows for higher precision, smaller actuators, and lower power consumption [1], generating the desire to modify and create systems that are statically balanced. As gravity is a common phenomenon that gives devices a preferred position, gravity balancing is a popular and commonly applied method of statically balancing. If there would be no gravity then the marbles in all 3 pictures could be placed anywhere in the figure and stay there. Although this research will focus on the case of gravity equilibration all sorts of

forces can be balanced, like for instance undesired internal stiffness'[31, 44].

For simplicity most forms of balancing will be described through the usage of an inverted pendulum with one degree of freedom (Figure 16). With an inverted pendulum, a moment should be created around its base that counteracts the moment generated by the forces of gravity.
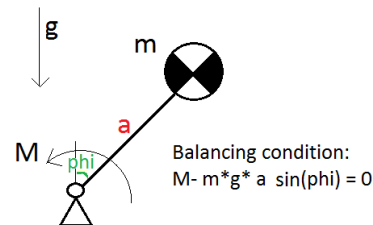

Figure 16: An inverted pendulum under the influence of gravity, including a balancing equation for the required torque (M) with respect to the pendulums angle with gravity (φ) to keep the pendulum from having any preferred position.

Balancers utilizing counterweights

There are multiple ways to compensate against gravity but the most popular way throughout history has been through counterweights. Typical applications (Figure 17) range from big devices such as bridges, cranes and elevators to smaller devices such as desk lamps and pick-up arms.

Figure 17: Various systems that are balanced against gravity by the usage of counterweights.

Balancing by counterweights (Figure 18) works by mounting a mass (m2) such that it generates a force or moment that counteracts the force or moment generated by gravity on the original mass (m1).
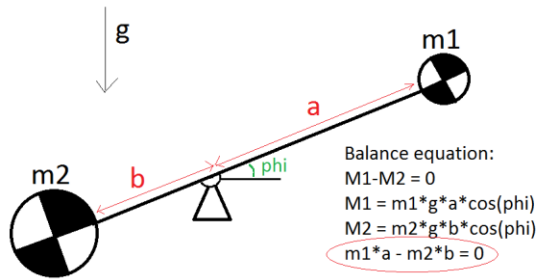
Figure 18: An inverted pendulum under the influence of gravity, counterbalanced by a secondary mass, including a balancing equation for the required ratios of mass and distance.

This means that counterweights require an additional mass for the counterbalance, meaning that the total mass and inertia of the moving system increases which means a higher force is required for acceleration. Counterweight balanced systems are generally bulky compared to the unbalanced system as there needs to be additional space for the counterweight.

However the simplicity of such a system requiring no addition of energy to place it in any position makes it a popular and often cheap choice for gravity equilibration. If the downfalls are not a problem for a desired application then it's mostly advised to go for this method.

Spring balancers with a fixed reference

Another way to statically balance devices is through the usage of elastic elements such as springs. Although more complex in its execution, spring based balancers can often store more energy in their spring within a smaller size and weight package, than equivalent counterbalanced systems.

Balancing by the use of springs (Figure 20, Figure 19), generally works through the utilization of special zero-free-length springs that have a linear relation between force and its actual length rather than just its extension. This allows for the creation of a sinusoidal torque curve that counteracts the gravity induced torque (Figure 16). In order to obtain the correct phase in the counter torque placement of the spring attachment points relative to the pendulum joint and the gravity vector is critical (For example in Figure 20 the mounting point should be perfectly vertical above the pendulum joint)
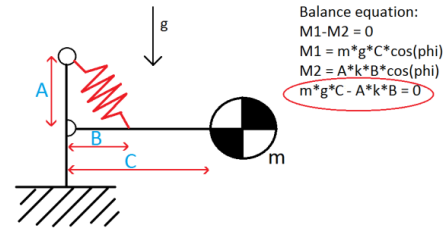

Figure 20: A pendulum counterbalanced by a zero-free-length spring, including a balancing equation for the required mounting position and spring stiffness.
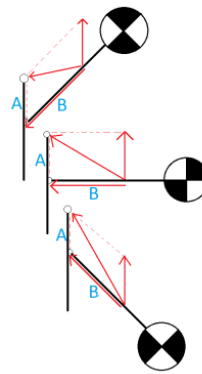

Figure 19: On the left a figure is shown of an inverted pendulum in multiple positions.

If a zero-free-length spring is used, the spring force becomes:

F = k*Lspring

Decomposing the forces into a force alongside the arm (b) and a force parallel to (a). Will then be

F||a= k*a
Fb = k*b

Although springs with absolutely no initial size in any plane do not exist, Zero-free-length springs can be created through multiple methods

1) Adjusting the pretension (Figure 21) of the spring such that its force/length graph crosses the zero.
2) Placing the spring at a different location (Figure 22 a-b) then where its force is exerted.
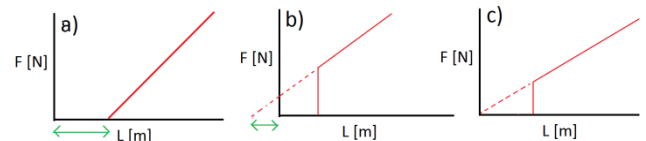3) Using special materials (Figure 23) that initially show a nonlinear force deflection relationship.

Figure 21: A showcase of 3 (red) force/length characteristics with their appropriate zero-force lengths (green) [1]
  a) **a regular spring without pretension and a positive zero-force-length.**
  b) **a pretensioned spring with a negative zero-force-length**
  c) **a pretensioned spring where the pretension is such that it generates a zero-force-length of zero**
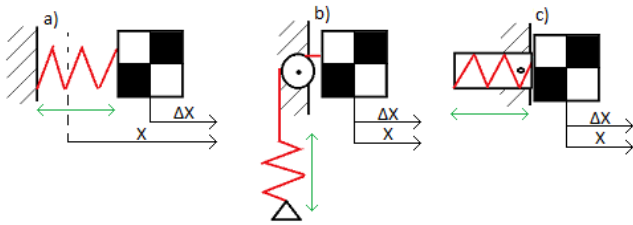
Figure 22: A showcase of 3 different configurations of a 1-dof, mass-spring system. [1, 45]

    a)   **The spring is directly attached to the mass, making the initial spring length add up to the total length.**

    b)   **Using a pulley system the spring is hidden away making the initial length not affect the total length.**

    c)   **By placing the spring attachment points on the same plane even though there is an excess length elsewhere, can make a spring act like as if it got zero-free length**
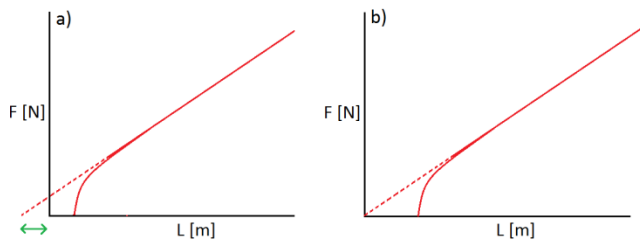

Figure 23: Showcase of two force deflection curves of rubber springs. [46]

    a)   **Natural rubber initially shows a big decrease in stiffness, giving it an effective negative free length.**

    b)   **Adding some stiff material in series with rubber allows for the creation of an effective zero-free-length spring.**

17

Appendix B: Background Research on energy storage and transfer mechanisms

Elastic elements and their properties

Parameters affecting the stiffness

Before looking at various mechanisms that manipulate the stiffness of elastic mechanisms, it is important to overview various types of springs and their working principles in order to understand what variables can be adjusted to manipulate the stiffness.

An overview of different types of springs and their loading conditions is shown in Figure 24 [46].Although the overview is for metal springs different materials could be used to generate similar shapes.
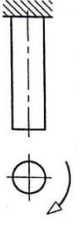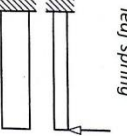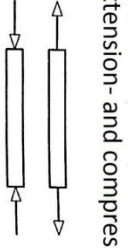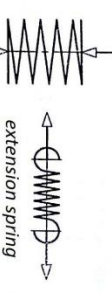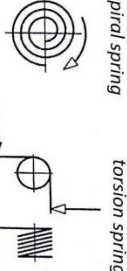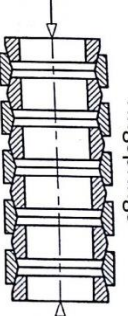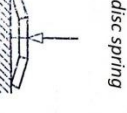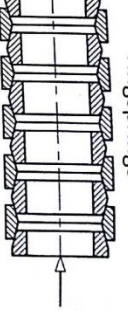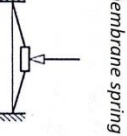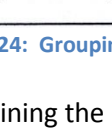

Figure 24: Grouping of metal springs to material load [46]

Combining the basic formulae for force and deflection for some of the coiled and disc shapes generates Table 2 [47]. From the different equations it can be seen that the stiffness can be modified by changing the amount of coils (n), wire dimensions (d), coil

radius (r), shear modulus of elasticity (G), modulus of elasticity (E) and in the case of a spiral spring the effective spring length (l) and for the disc spring the disc width δ.
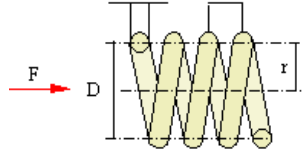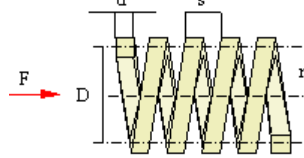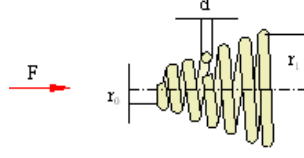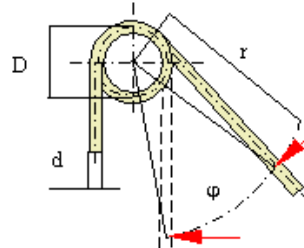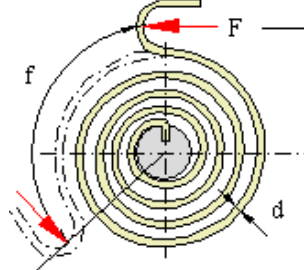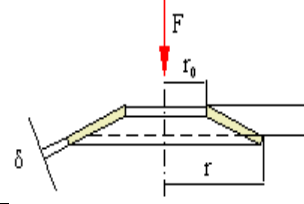
Spring	Stiffness
Cylindrical coilspring Round wire	$F = \dfrac{\pi}{16}\dfrac{d^3}{r}\tau$ $f = \dfrac{64\,n\,r^3\,F}{d^4\,G}$
Cylindrical coilspring Square wire	$F = \dfrac{d^3}{4.8\,r}\tau$ $f = \dfrac{44.9\,n\,r^3\,F}{d^4\,G}$
Conical coilspring Round wire	$F = \dfrac{\pi}{16}\dfrac{d^3}{r_1}\tau$ $f = \dfrac{16\,n\,(r_1+r_0)(r_1^2+r_0^2)\,F}{d^4\,G}$
Torsion spring Round wire	$F = \dfrac{\pi}{32}\dfrac{d^3}{r}\sigma$ $\varphi = \dfrac{2\,D\,\pi\,n}{E\,d}\sigma\dfrac{180}{\pi}$ φ [deg.]
Spiral spring Round wire	$F = \dfrac{\pi}{32}\dfrac{d^3}{r}\sigma$ $f = \dfrac{2\,r\,l}{E\,d}\sigma$ l = eff spring length
Disc Spring	$F = \dfrac{\delta^2}{1 - 2/3\,r_0/r}\sigma$ $f = \dfrac{0.65\,r^2}{E\,\delta\,(1 - 2/3\,r_0/r)}\sigma$

Table 2: Approximate formulae for spring stiffness's of some coiled shaped and disc type springs. [47]

The relationship between force and deflection of a transverse loaded leaf spring can be found in Table.2 [47]. The I in Table 3, stands for the second moment of inertia for which the general formula and some examples of cross-sections can be found in Table 4 [48].

From the relationship between force and deflection it can be seen that the stiffness can be modified for this type of spring by changing either the length (L), modulus of elasticity (E) or the moment of inertia (I)
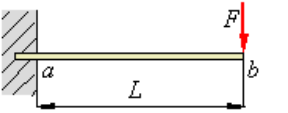
Loading	deflection	slope
	$\delta_b = \dfrac{FL^3}{3EI}$	$\theta = \dfrac{FL^2}{2EI}$

Table 3: Linear formulae of deflection and slope for a transverse loaded beam. [47]
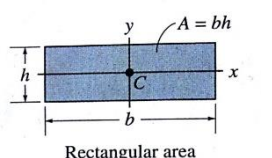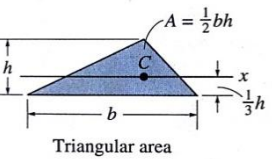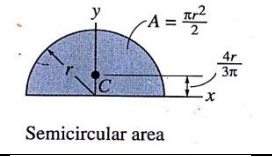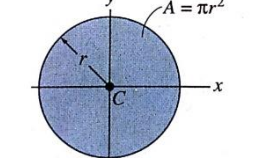
Shape	Moment of Inertia $I_x = \int y^2\, dA$
 Rectangular area	$I_x = \frac{1}{12}bh^3$ $I_y = \frac{1}{12}hb^3$
 Triangular area	$I_x = \frac{1}{36}bh^3$
 Semicircular area	$I_x = \frac{1}{8}\pi r^4$ $I_y = \frac{1}{8}\pi r^4$
 Circular area	$I_x = \frac{1}{4}\pi r^4$ $I_y = \frac{1}{4}\pi r^4$

Table 4: Some examples of the bending moment of inertia for popular shapes over either the x- or y-axis. [48]

The relationship between force and deflection of a normally loaded beam can be found in Figure 25 [47].
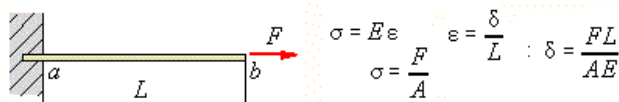
Figure 25: Simple calculation of the extension of a normally loaded tension bar.

From this relationship it can be seen that the beam length (L), area (A) and modulus of elasticity (E) all linearly relate towards the stiffness of the leaf spring.

The relationship between torque and rotation of torsionally loaded beam can be found in Table 5 [47]

From this it can be seen that the stiffness is determined linearly by the Shear modulus of elastiticity (G), rotational moment of inertia (I_p) and the length of the torsion rod (L).
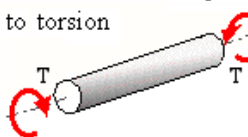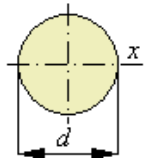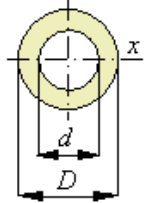
Cross section	Torsion
Elementary equations for uniform beams subjected to torsion	$T = S_t\,\tau_{max},\quad S_t = \dfrac{I_p}{r}$ $I_p = I_x + I_y$ $\varphi = \dfrac{TL}{GI_p},\quad G = \dfrac{E}{2(1+v)}$
	$I_p = \dfrac{\pi}{32}d^4$ $S_t = \dfrac{\pi}{16}d^3$
	$I_p = \dfrac{\pi}{32}(D^4 - d^4)$ $S_t = \dfrac{\pi}{16}\dfrac{D^4 - d^4}{D}$

Table 5: Torsion bar and the appropriate formulae to calculate the torque necessary to obtain a certain output [47]

Weight based efficiency on elastic elements

One of the properties for the ideal statically spring balanced pendulum without a fixed reference is that the total size and weight should be smaller than an equivalent mass balanced system.

Although in some cases the weight of springs can be negligible to the total weight of a system, when the amount of energy that needs to be stored in the system increases, generally the weight of the system will increase, which is why this section focusses on the weight based efficiency of different elastic elements.

When looking at elastic elements a separation can be made on the intrinsic properties of the used material, and how the material is shaped and loaded as a spring. Which follows from that the amount of energy per volume can be calculated with: $W/V = \alpha * \sigma^2/E$, "$\alpha$" gives an indication of how efficiently the material is used, the Young's modulus (E) is an intrinsic property of utilized material, the material stress (σ) depends on the loading condition and is limited by the elastic limits of the material. The energy per volume can easily be transformed into the energy to weight ratio through dividing by the density (δ) of the material.

A showcase of different utilizations of material for a few common spring types can be seen in Figure 26 [49]
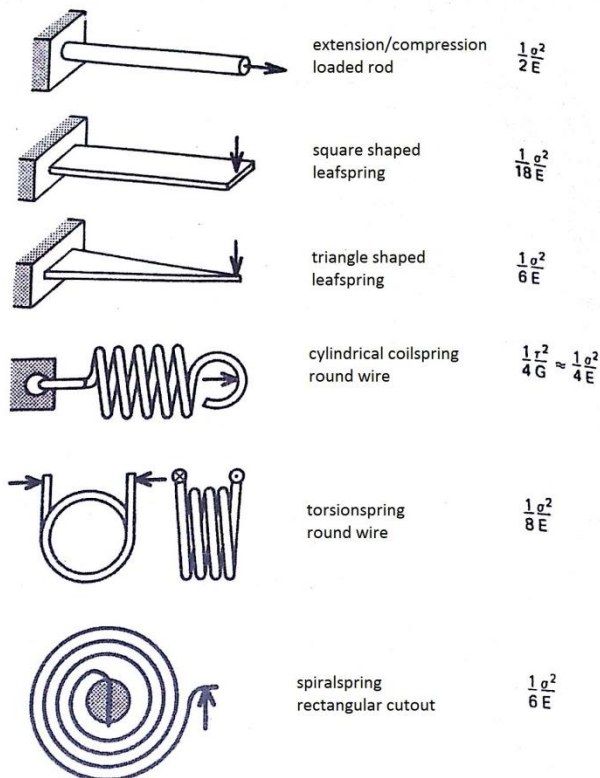
Figure 26: Comparison of different spring types and the amount of energy per volume $W/V = a*\sigma^2/E$. [49]

In the energy to weight ratio, the young modulus, maximum allowable stress and density depend on the material. Table 6 [49] shows a comparison of some different configuration of springs and material and their respective energy to weight ratio.

material	springtype	α	σ max [MN/m^2]	E [GN/m^2]	ρ [kg/m^3]	W/m [J/kg]
Springsteel	coilspring	1/4	1200	210	7800	200
wood	leafspring	1/6	120	27	600	150
rubber	tensile rod	1/2	2.5	0.0015	1200	1800
carbonfiber	leafspring	1/12	2000	110	1500	2100
aramidfiber	leafspring	1/12	2000	100	1500	2100
glassfiber	leafspring	1/12	2000	54	2500	3000

Table 6: Comparison table showcasing the energy to weight ratio (W/m = ($\alpha *\sigma^2$)/(E*δ)) in spring steel and some non-metal spring materials. Note: for the leaf springs a triangle shaped leaf spring is assumed, for composites it is assumed that only 50% is filled with fibers hence the halving of α [49]

From Table 6 it can be seen the energy to weight ratio can improve tenfold over regular steel coil-springs, by carefully selecting materials. This means that if there is a desire to maximize the amount of energy with a weight constraint that alternative materials such as rubber and glass-fiber should be looked at over traditional coil springs.

Continuously Variable Energy Transfer mechanisms

Before looking at various elastic mechanisms that manipulate their output force through an adjustable transmission ratio, it is important to have an understanding on various types of existing continuously variable transmissions.

CVT's can get divided in five categories [12] [50]
1. Hydrostatic
2. Traction drive (V-belt and Rolling contact)
3. Overrunning clutch (Lever types)
4. Electric
5. Slipping clutch

With these categories it is important to note that for a passive system that energy losses must generate an increased operating effort (e.g. friction), rather than utilizing energy from the finite energy storage and possibly depleting it. This makes the usage of Hydrostatic, Electric and Slipping clutch designs undesirable. For that reason only Traction and Overrunning clutch designs will be discussed further. (Although it should be noted that the energy losses could possibly be counteracted by accounting for the inefficiencies by charging more energy than necessary)

Traction Drive CVTs
Traction drive is a term applied to any device which transmits power through adhesive friction between two objects loaded against each other [12].
The group of traction drives can be further separated into 2 groups, rolling contact traction drives and belt traction drives [12].

Belt Drive CVTs
The most famous belt drive CVTs are the variating pulley (Figure 27) and double cone (Figure 28) drives.
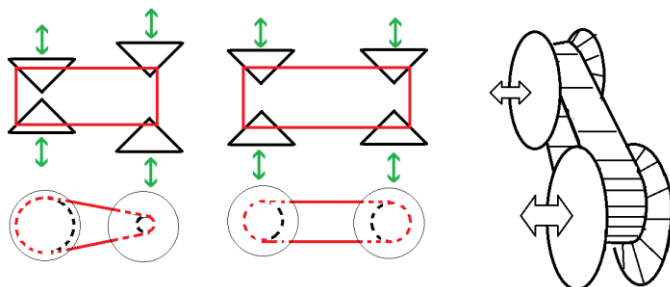

Figure 27: Variating pully CVT belt drive
The variating pulley belt drive is able to adjust the generated input and output force by moving sets of conical pulleys further apart or closer together. This makes the drive belt catch on to the pulley at different diameters allowing for adjustment of the transmission ratio.
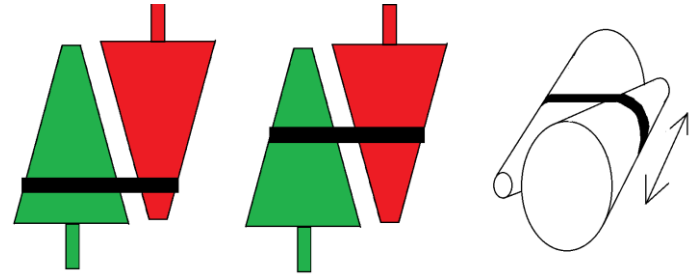
Figure 28: Double cone CVT belt drive
The Double Cone belt drive is able to adjust the generated input and output speed by adjusting a drive belt over 2 conically shaped pulleys. This means that the effective used diameter of the input and output shaft changes allowing the adjustment of the transmission ratio.

Efficiency:
Normally during power transmission, the belt undergoes cyclic tension and compression deformation when it is bent on and off the pulleys. This results in torque loss due to the bending hysteresis, that depends on the elastic properties and the magnitude of flexure of the belt [51, 52].

These effects make the selection of belts highly dependent on different load cases, pulley sizes as well as maintenance [53].

Overall the efficiency of a well set up belt driven CVT ranges from 90-97 % efficiency [51, 53-56] .

Amount of necessary parts:
The minimum amount of parts for variating pulley system to function equals 8. 4 conical pulleys, 2 shafts, a housing and a belt.
For a double cone belt drive in the most simple form 6 parts are necessary: Input cone, output cone, 2 shafts and a housing, connecting belt.
However once again that does not include the parts necessary to actually adjust the gear ratio.

Ability to adjust ratio when the device is not rotating
Belt drives adjust their ratio by applying a force on the belt, which makes the belt slowly shift towards a desired set point. For this to work the CVT's should be rotating.

Range:
Both belt type CVT's allow for full 360° rotations. Although they do not allow for one wheel to freewheel (an infinite ratio). If that would be desired a power split could be added to the system (more on that later)

Lever equivalent

Every transmission can be analyzed using lever analogy. Which can make the the torque and speed calculations easy and improves the ability to visualize the results and effects of gear tooth ratios [57]. For that reason the lever equivalent of every discussed CVT will be displayed.

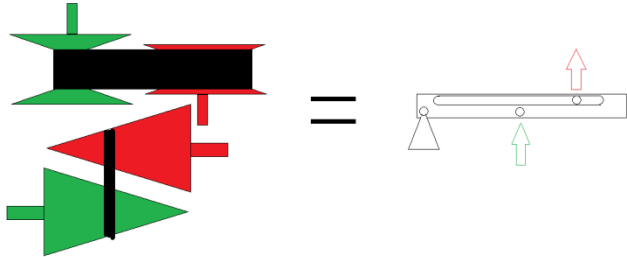Figure 29 shows the lever equivalent of the variating pulley belt drive and the double cone drive.

Figure 29: lever equivalent of the variating pulley belt drive and the double cone belt drive.

Rolling contact traction drives

Rolling contact traction drives transmits power through adhesive friction between two objects loaded against each other [12]. The difference between belt drive CVT's is that rolling traction CVT's utilize traction wheels or balls instead of a belt.

Unlike traction drives with a set transmission ratio, there is a lot of diversity with continuously variable traction drives [58]. For this reason only a small selection of all the different rolling contact traction drives will be shown here.

The chosen selection are CVT's that seem to reoccur the most in literature [12, 50, 56, 58, 59]
Namely: Wheel CVT (Figure 30), Ball CVT (Figure 31), Half Toroidal CVT (Figure 32), Full toroidal CVT(Figure 33), Milner CVT (Figure 34), Kopp CVT (Figure 35), Nutating traction drive (Figure 36), Beier CVT drive (Figure 37).
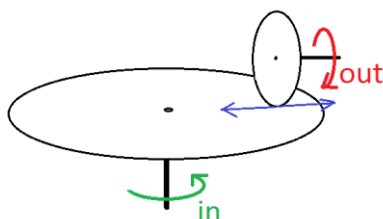
Figure 30: Wheel CVT
The wheel CVT works through a set of double wheels with one wheel placed 90° ontop of the other. By variatating the distance of one wheel towards the center of the other wheel the effective gearing ratio can be adjusted.
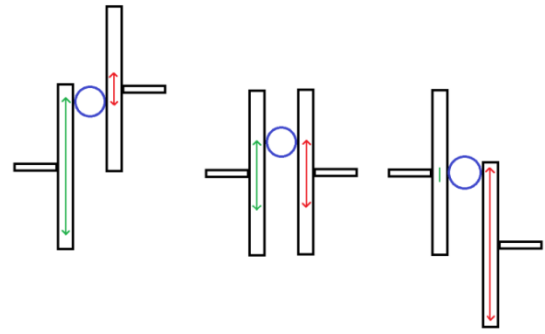
Figure 31: Ball CVT
The ball CVT works by placing a ball between two wheels connected to an in and output shaft. By moving one shaft up or down the relative position of the ball on the wheels changes, generating a different gearing ratio between the in and output wheel.
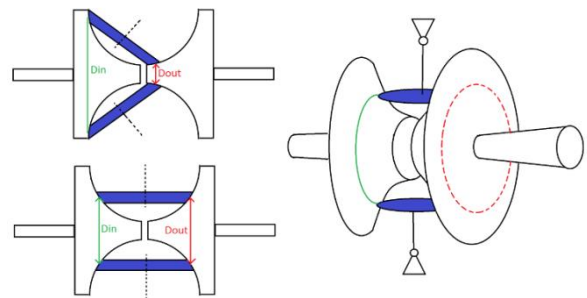
Figure 32: Half Toroidal CVT
The half toroidal CVT works by moving a disc between 2 wheels. Those wheels are shaped such that from a single point of rotation the disc can contact both wheels at different diameters allowing for a change of transmission ratio without having to move the actual driven wheels.
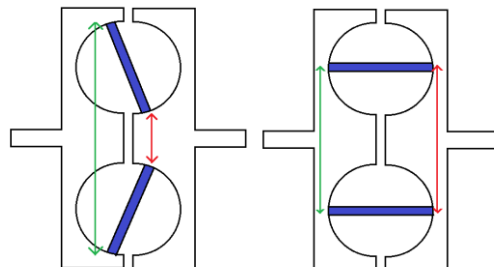
Figure 33: Full toroidal
The half toroidal CVT works by moving a disc between 2 wheels. Those wheels are shaped such that from a single point of rotation the disc can contact both wheels at different diameters allowing for a change of transmission ratio without having to move the actual driven wheels.
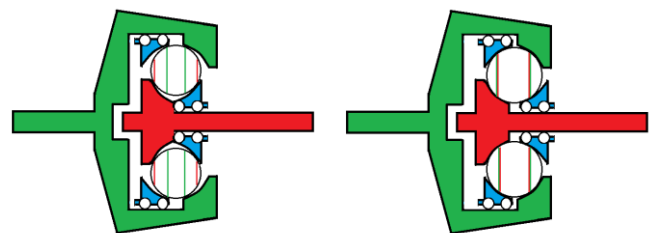
Figure 34: Milner CVT
The milner CVT works by moving moving little widges (blue in the drawing) to the left or the right. This pushes the balls up or down on the structure, making the inner and outer shaft effectively connect to the ball at a different circumference changing the output ratio. Of the CVT.
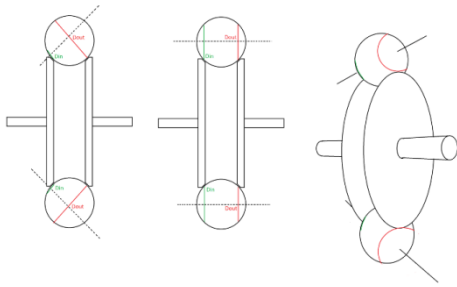
Figure 35: Kopp CVT
The kopp CVT functions by changing the center of rotation on a ball that connects an input and output wheel. Rotating the center of rotation effectively changes the radius around the ball that the in and output shaft follow, and with that change the transmission ratio.
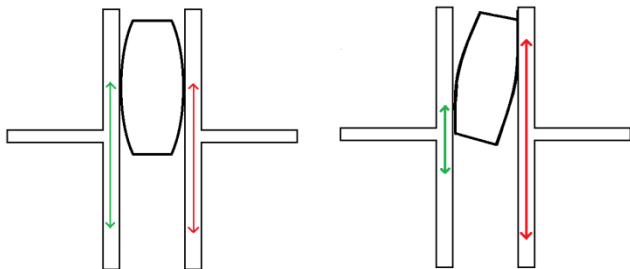
Figure 36: Nutating Traction drive
By placing a barrel shaped object between two wheels, and adjusting the angle of rotation of said barrel it becomes possible to alternate the contact point on the wheels effectively connecting the wheels at different diameters which changes the gearing ratio.

Figure 37: Beier CVT drive
The beier CVT drive works by meshing one set of wheels into another set of wheels changing the effective radius on one of the wheels and with that the gear ratio. The speciality of the concept lies in the utilization of multiple discs, that for a single compressive force generates multiple contact points. Allowing for high torque throughput for a relativel low compression force.
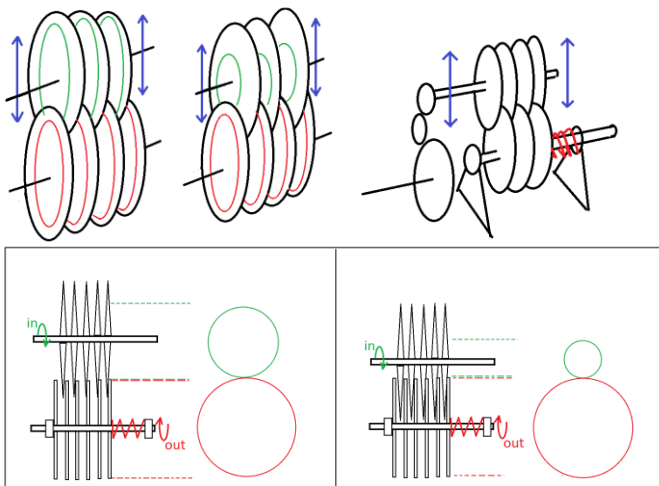
Efficiency
The key components introducing non-negligible energy losses with a friction CVT are spin and slip losses and not neglect able losses in bearings [58]

Since there is no relative speed difference between the in- and output shaft when operating quasi-statically spin should be neglect able.

Table 7 gives a general overview of efficiencies of various rolling contact traction drives. Formulae that can be used to predict the efficiency can be found in [58].

Traction Type	Efficiency
Wheel	93-96% [50]
Ball	75-90% [58]
Half Toroidal	90-97% [56, 60] [61]
Full Toroidal	88-97% [58] [61]
Milner	75-90%*
Kopp	75-90% [58]
Nutating	75-96% [56]
Beier	93-96% [62]

Table 7: Showcase of various efficiencies of rolling traction drives. *Due to the similar functioning of the Milner and the Kopp traction drive it is assumed that the efficiency of the Milner traction drive will be approximately the same as the Kopp CVT.

Range:
All of the noted CVT's can be used for a range of over 360° degrees. Although only the wheel and ball CVT by default allow for the usage of an infinite range. To obtain an infinite range with the others the addition of an additional device such as a power split mechanism should be utilized to generate an infinitely variable transmission.

Amount of necessary parts
To generate an overview of the amount of necessary parts Table 8 has been set up.

Type of CVT	# parts			
Wheel	4	2 shafts	2 wheels	
Ball	5	2 shafts	2 wheels	1 ball*
Half Toroidal	6	2 shafts	2 toroidal wheels	1 disc*
Full toroidal	6	2 shafts	2 toroidal wheels	1 disc*
Milner		2 shafts	2 balls	2 guides
Kopp CVT	6	2 shafts	2 balls	1 ball*
Nutating	5	2 shafts	2 wheels	1 barrel*
Beier	5	2 shafts	3 wheels*	

Table 8: Showcase of a summation of parts for various rolling contact traction drives.
* The number denotes a minimum amount to function. Adding more parts, generates more contact points, and with the same normal force allows for a higher torque throughput.

23

Ability to adjust ratio when the device is not rotating

For all devices beside the ball type CVT, adjusting happens by putting a force on the adjustment mechanism which changes the ratio over a certain range of rotation. Instantaneous change would require for the force transmitting member to slip, requiring high forces as these CVT's are designed to transmit energy through traction.

Lever equivalent

Every transmission can be analyzed using lever analogy. Which can make the the torque and speed calculations easy and improves the ability to visualize the results and effects of gear tooth ratios [57]. For that reason the lever equivalent of every discussed CVT will be displayed.

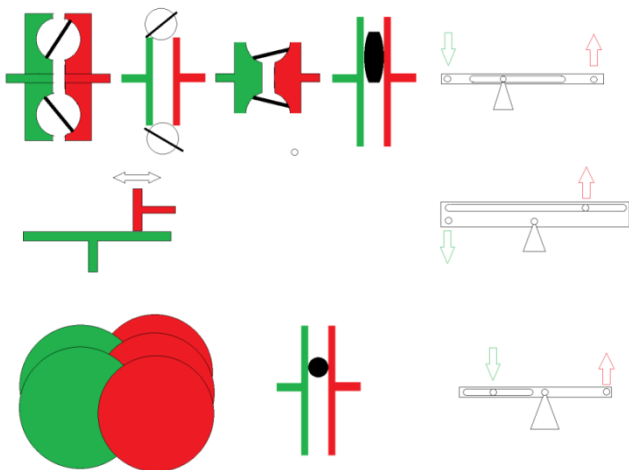Figure 38 shows the lever equivalent for a wide selection of rolling contact traction drives.

Figure 38: Overview of the lever equivalent for various rolling contact traction drives.

Overrunning clutch CVTs

Overrunning clutch or Epicyclic CVT's make use of adjustable mechanisms with a limited range, and through a ratchet or a swashplate generate a full cyclic motion. Some popular examples within this category are the Zero-max CVT (Figure 39) and the Benitez's ratcheting CVT (Figure 40).
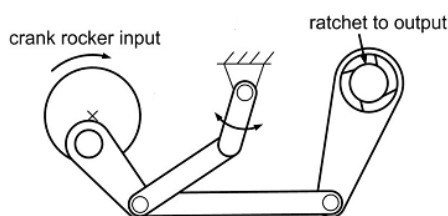

Figure 39: The zero-max CVT utilizes an adjustable four-bar mechanism to transfer an adjustable force from input to output. A ratcheting mechanism changes the small stroke of the four-bar mechanism into a single forward motion. By adding multiple devices together at an offset phase will allow for the generation

of an output that will approach linearity. However due to the ratchet the system only works in a single direction.
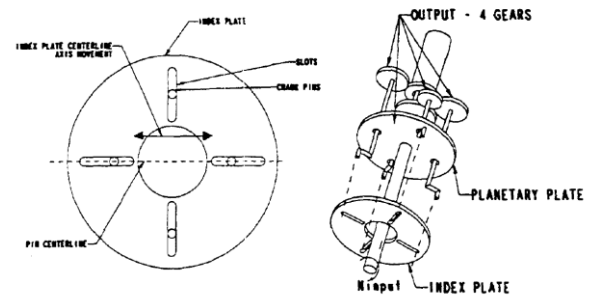
Figure 40: The benitez ratcheting CVT. The index plate rotates in a swirling motion off centered from the input shaft. This makes the pins in the index plate move up and down similar to a scotch-yoke, a ratcheting gear set at the back transforms this sinusoidal motion back in a roughly linear output speed.

Efficiency:

The advantage of variable geometry CVT's is the lack of slip due to all parts being fixed. However to generate a linear output there is often a requirement for a lot of devices put together in parallel.Besides that variable geometry CVT's are often not dynamically balanced, causing various vibrations into the system.

Literature for variable geometry based CVT's showcases an efficiency of 85-93% [56]

Range:

The range of epicyclic and overrunning clutch designs is 360° The range of adjustment of a zero-max CVT is in the order of 4x.

Amount of necessary parts:

The zero-max CVT requires 1 input wheel, 5 links and a ratcheting bearing. Making for a total of 7 parts

Ability to adjust ratio when the device is not rotating:

Overrunning clutch or Epicyclic CVT's can be adjusted when the device is not running. As it generally relates to adjusting the length of a lever arm.

Lever equivalent:

Every transmission can be analyzed using lever analogy. Which can make the the torque and speed calculations easy and improves the ability to visualize the results and effects of gear tooth ratios [57]. For that reason the lever equivalent of every discussed CVT will be displayed.

Figure 41, shows the lever equivalent for the overrunning clutch CVT's.

Figure 41: Overview of the lever equivalent for both the zero max and benitez overrunning clutch CVT's.

The next step would be looking into various compliant actuators in order to see and know what methods and adaptations have been used before.
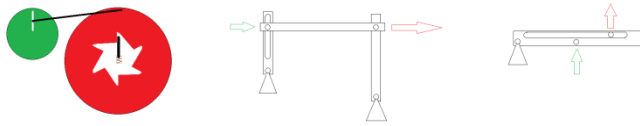
An direct utilization of a lever equivalent of the zero-max CVT can be found in the five bar linkage CVT (Figure 42) that has been discussed by Takaki et Al [63, 64]
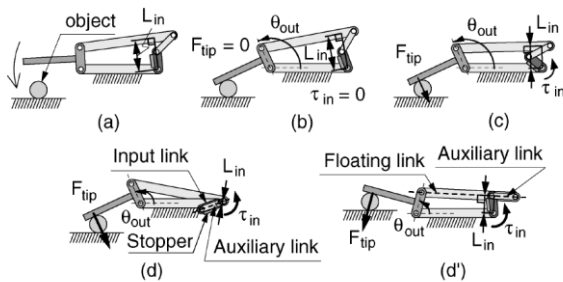
Figure 42: Showcase of the Five-bar linkage CVT under various positions and transmission ratios.

CVT Evaluation:

The ability of a CVT to match any input speed to a desired output speed generated a lot of research and products within the Production and Transport industry, the previous showcase is only a very small selection of all the patents and products created.

These devices however are often designed to operate in a continuous motion and at a high speed, with their primary competition against multi-gear gearboxes.

In the case of a spring balanced inverted pendulum, the competition is against a simple counterweight, in terms of mass, complexity and weight. And unlike the vehicular and production industry it should be possible to change the ratio even when the device operates in a quasi-static operation rather than in continuous fashion.

From the above solutions none of the previously shown CVTs are directly applicable; however this does not mean that existing CVTs cannot be modified or adopted for quasi-static operation. The different set of requirements and goals could generate completely different solutions.

The requirements for simplicity and limited weight could point into the direction for lever type CVT's. The requirements for energy free adjustment could point in the direction of a ball type CVT's.

Appendix C: Results of Literature

Adjusting the Energy Storage
Changing the Energy Storage through Pretension

VS-Joint [14]

Functioning:

The VS (Variable Stiffness) joint (Figure 43) is essentially a system where coil springs are kept together by 2 plates. Through a stiff connection the top plate is connected to a disc with a cam profile underneath the bottom plate. Through wheels the bottom plate is able to move over the cam profile, which effectively changes the height of the bottom plate. The height difference between the top and bottom plate changes the compressing the springs, resulting in a higher required force to move the system over a prescribed distance or a change of perceived stiffness.
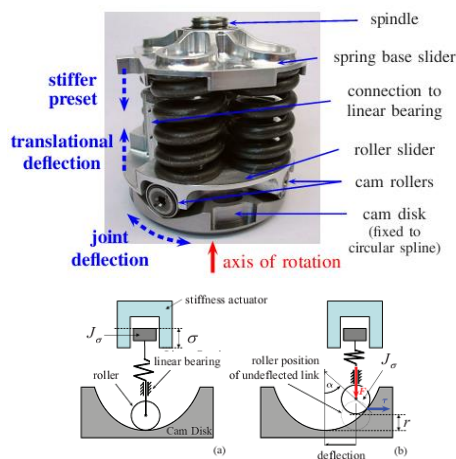

Figure 43: The VS Joint [14]
The top figure shows an assembled prototype of the VS joint. The bottom figure displays the working principle.

Range of motion & Adjustability:

The VS joint got a maximal range of 14° for all stiffness settings in both directions, with the actual stiffness range depending on the provided cam profile.
The stiffness can be adjusted between 0-7 Nm/deg in the neutral position, and 38-51 Nm/deg in the location of maximal deflection (Figure 44).
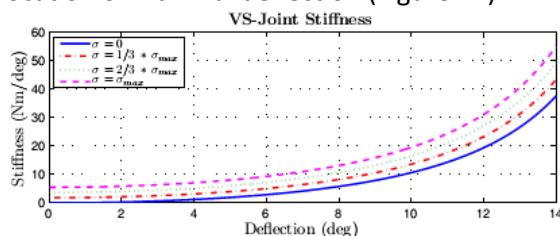
Figure 44: Adjustability of the stiffness in the VS-Joint [14]
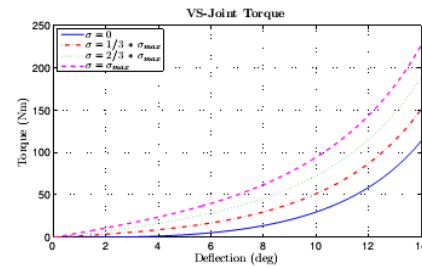
Figure 45: The Torque deflection curve of the VS-joint [14]

Analyzing the stiffness curve (Figure 45Figure 46) shows that at the different stiffness setting there is not only a change in amplitude, but a change in curvature as well. Table 9 displays the standard error between different lines.

Figure 46: On the top a figure showcasing the relative magnification between different lines of the stiffness curve. On the bottom the figure showcases the polynomial data fit on top of the original data.

	Standard error (σ / ц)
Line4/Line3	4%
Line4 /Line2	12%
Line3/Line2	8%
Line4/Line1	33%
Line3/Line1	30%
Line2/Line1	21%

Table 9: This table showcases for the VS-Joint how closely 2 lines are a pure amplitude magnification, the lower the value the more 2 lines being a pure amplitude modulation.

Efficiency:

The VS-joint is adjusted by moving the spring base slider downward to pretension the spring. This means that the potential energy that gets stored within the spring needs to be supplied when changing the preset.

Number of components:

The VS joints seems to have the following parts, Top plate, bottom plate, cam-disc, 3 wheels, 3 springs, spindle, accounting for a total of 11 parts.

PVSA [15]

Functioning:

The PVSA (parralel type variable stiffness actuator) , has two rotatable cams with a profile that looks like a circle with the top flattened out (Figure 47Figure 48). Together these cams generate a path that the a follower spring on the output link has to follow. Rotating these cams changes how steep the path is, resulting in more or less compression of the follower spring when the output arm is moved, resulting in a change of the perceived output stiffness.
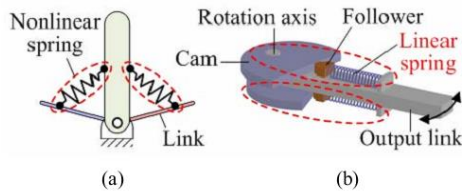
Figure 47: Working principle of the PVSA [15]
a: Showcase of the principle of using antagonistic springs to change the stiffness by rotating 2 links.
b: Showcase of the PVSA using the double cam mechanism.
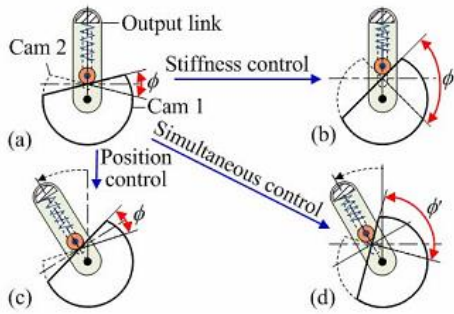
Figure 48: Working principle of the PVSA mechanism [15]
a to b: By rotating the set of cams from position a to position b it can be seen that the slope the cam has to follow changes increasing the effective stiffness that is felt on the output link.
c: a showcase that rotating both cams in the same direction changes the neutral position of the arm.
d: carefully controlling both the stiffness and neutral position allow you to actuate a device with a desired amount of stiffness.

Range of motion & Adjustability

The PVSA got a maximal range of 55° in both directions for the lowest stiffness and around 20° in both directions for high stiffness setting. The stiffness ranges from 0-0.9 Nm/° (Figure 49)
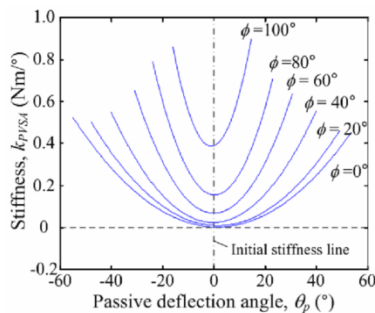
Figure 49: Showcase of the stiffnesses over varying output link positions, graphed for different cam rotation settings. [15]

Analyzing the stiffness curve (Figure 50Figure 51) shows that at the different stiffness setting while there is not a pure change in amplitude, the change in curvature remains relatively small.

Table 10 displays the standard error between different lines.
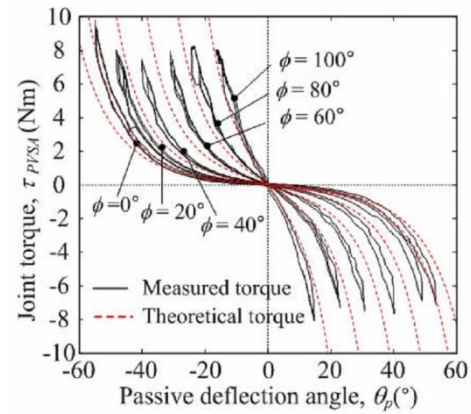
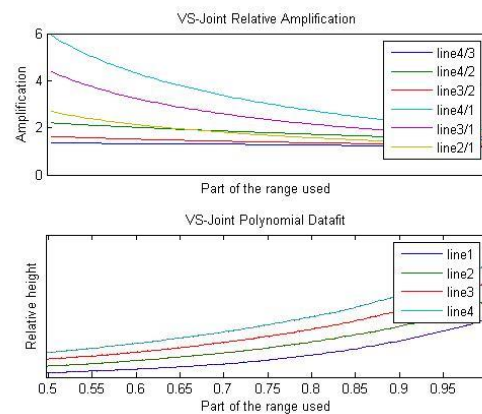Figure 50: The Torque deflection curve of the PVSA [15]
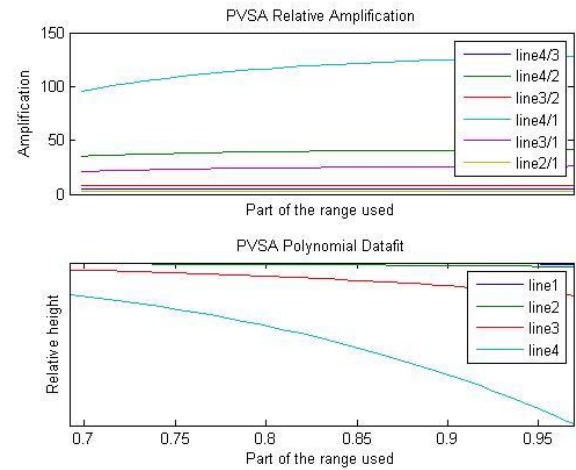
Figure 51: On the top a figure showcasing the relative magnification between different lines of the stiffness curve. On the bottom the figure showcases the polynomial data fit on top of the original data.

Standard error (σ / ц)	
Line4/Line3	2%
Line4 /Line2	4%
Line3/Line2	2%
Line4/Line1	7%
Line3/Line1	5%
Line2/Line1	4%

Table 10:
This table showcases for the PVSA how closely 2 lines are a pure amplitude magnification, the lower the value the more 2 lines show a constant amplitude magnification.

Efficiency

The stiffness is controlled partly by pretension of the spring and partly by the slope generated by the cams.

In case the center of rotation of the cam-discs collides with the following tip on the spring, changing the stiffness with the cams wouldn't cause any change of the spring length and happen without any energy cost.

The further away the spring tip is from the center of rotation of the cams the more energy will be wasted to adjust the stiffness (Figure 52).

$$dL_{spring} = c-a$$
$$c = a / \cos \theta$$
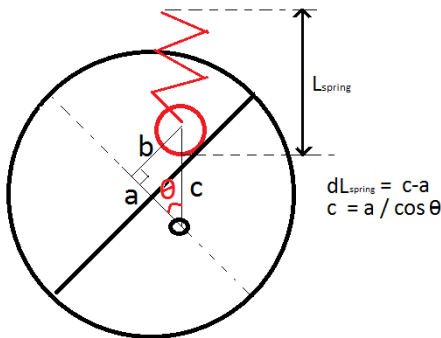
Figure 52: A small calculation of the PVSA showing that to make the length of the spring not change during rotation, that the length 'a' should approach zero.

Number of Components

The simplest version of the PVSA appears to have, 2 cam discs, 2 cam followers, an output link, and a shaft. Giving it a total of 6 parts.

Antagonistic variable stiffness actuators [16, 65, 66]

When designing machines that are safe to use within a human environment, designers often look at nature for inspiration. The way how humans and animals change their stiffness using an antegonistic pair of muscles resulted in the usage of many designs trying to mimic that. [16]

Antegonictic variable stiffness actuators can be devided into three control categories (Figure 53) [65].

- Antegongonistic actuators and springs (Configuration 1).

- Seperated position and stiffness actuator, with the position actuator behind the spring (Configuration 2).

- Seperated position and stiffness actuator where the actuator is placed in front of the spring (Configuration 3).
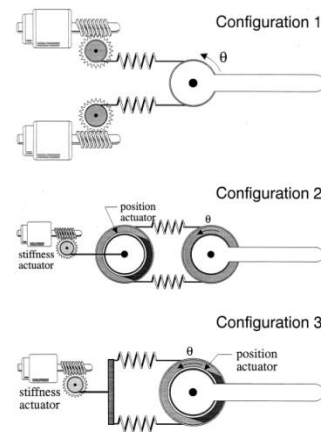
Figure 53: 3 different configurations configurations of antegonistic variable stiffness actuators. [65]
Configuration1: Antegonistic actuator and springs
Configuration2: Position actuator and separated stiffness actuator.
Configuration3: Position actuator moved to the joint side of the springs. [65]

Compliant VSA [16]

Functioning:

The Compliant VSA (Figure 54) (Compliant Variable stiffness actuator) is an antagonistic variable stiffness actuator of configuration 1

The Compliant VSA works by 2 actuators working in union (Figure 54 Top). The neutral position of the system is at the average of the angle of the 2 actuators.

If the angle of the actuators is the same the VSA will be at its lowest stiffness setting, if the actuators are rotated in opposite directions it will be at its maximal stiffness setting. Carefully controlling both actuators then allows for control over position and stiffness.
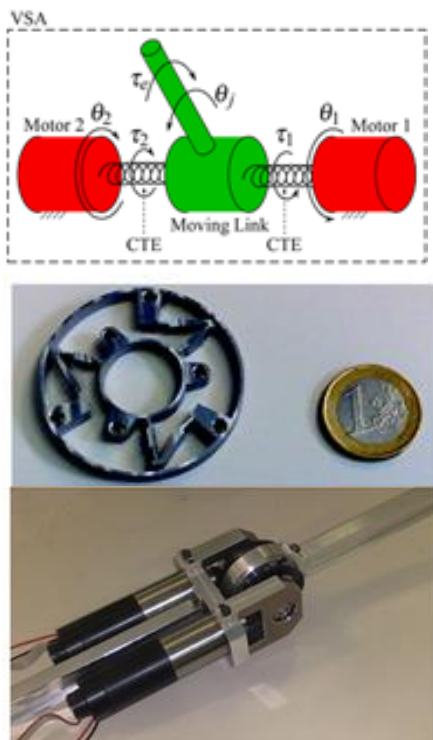

Figure 54: The Compliant VSA [16]
Top picture: showcases a schematic of the working principle.
Middle picture: showcases the utilized compliant spring
Bottom picture: showcases a sample of a working model.

Range of Motion & Adjustability

The compliant vsa got a maximal range of 12-24 degrees depending on the stiffness at both the minimal and maximal stiffness the maximal range is equal to 12 degrees. The stiffness can be adjusted between 0.2-0.8 Nm/deg, equivalent to a range of factor 4.

Analyzing the stiffness curve (Figure 55Figure 56) shows that at the different stiffness setting while there is not a pure change in amplitude, the change in curvature remains relatively small. Table 11 displays the standard error between different lines.

Figure 55: The stiffness curve of the Compliant VSA, for different values of the commanded stiffness. [16]

Figure 56: On the top a figure showcasing the relative magnification between different lines of the stiffness curve. On the bottom the figure showcases the polynomial data fit on top of the original data.

	Standard error (σ / ц)
Line4/Line3	1%
Line4 /Line2	2%
Line3/Line2	1%
Line4/Line1	2%
Line3/Line1	4%
Line2/Line1	4%

Table 11:
This table showcases for the Compliant VSA how closely 2 lines are a pure amplitude magnification, the lower the value the more 2 lines show a constant amplitude magnification.

Efficiency

The Compliant VSA's stiffness is adjusted tensioning the springs. This means that the potential energy that gets stored within the spring needs to be supplied when changing the preset.

Number of Components

In the most simple configuration the Compliant VSA needs 2 springs, 2 input shafts, housing and a pendulum, so 6 parts.

APVSEA [17]
Functioning:
The Active-Passive Variable Stiffness Elastic Actuator (APVSEA) (Figure 57), in an antegonistic actuator of configuration 3.

A motor (Motor 2 in the figure), compresses the springs, increasing the effective stiffness, where the other motor (Motor1) drives a spindle mounted changing the neutral position.

Another similar device is described in [Design of New Variable Stiffness Actuator and Application for Assistive Exercise Control].
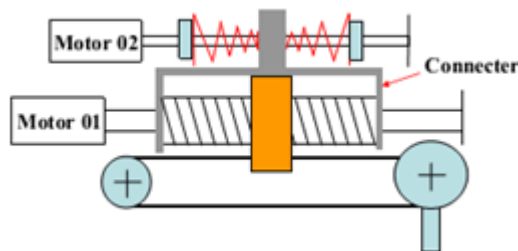
Figure 57: A concept of an Active-Passive Variable Stiffness Elastic Actuator. [17]

Range of Motion & Adjustability
The APVSEA got a range of motion of 100° in its lowest stiffness up to 10° at its highest stiffness. The stiffness can be adjusted between 0.1- 1.0 Nm/deg (interpolated from Figure 58).

Figure 58: Stiffness curve of the APVSEA showcasing the applied torque over the angular deflection for various spring pretensioning presets. [17]

Analysing the stiffness curve (Figure 58Figure 59) shows that at the different stiffness setting while there is not a pure change in amplitude, the change in curvature remains relatively small. Table 12 displays the standard error between different lines.
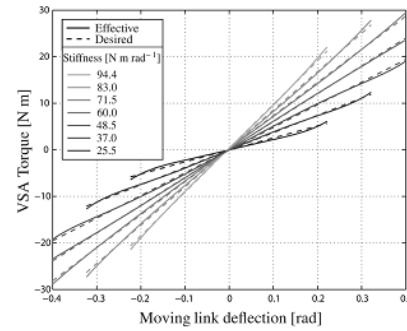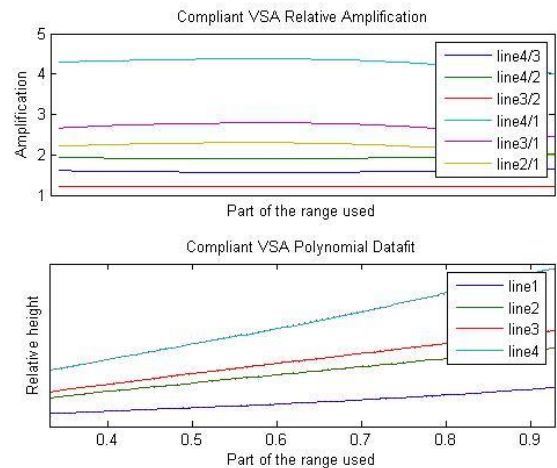

Figure 59: On the top a figure showcasing the relative magnification between different lines of the stiffness curve. On the bottom the figure showcases the polynomial data fit on top of the original data.

Standard error (σ / ц)	
Line4/Line3	7%
Line4 /Line2	11%
Line3/Line2	5%
Line4/Line1	4%
Line3/Line1	5%
Line2/Line1	9%

Table 12:
This table showcases for the PVSA how closely 2 lines are a pure amplitude magnification, the lower the value the more 2 lines show a constant amplitude magnification.

Efficiency
The Apvsea is adjusted by compressing the antagonistic springs. This means that the potential energy that gets stored within the spring needs to be supplied when changing the preset.

Number of Components
For the APSEA you need at least, 2 springs, 1 connector, 1 spindle, 2pullies, 2 shafts, housing and a band. So in total 9 parts.

BIJSC [18]
Functioning:
The biologically inspired joint stiffness control mechansim (BIJSC) (Figure 60). Is an antegonistic actuator of configuration 1. The BIJSC showcased that the utilization of quadratic springs (generated by combining linear springs with a cam profile) allows for the creation of a linear stiffness curve of torque over angular displacement.
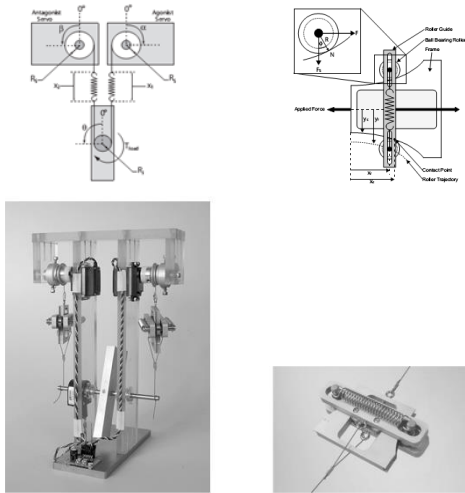
Figure 60: Figures of the BIJSC [18]
Top left: General working model of the BIJSC showing an antagonistic actuator of configuration 1
Top right: Showcase of the spring and cam setup to generate a quadratic stiffness curve.
Bottom left: Assembled prototype of the BIJSC.
Bottom right: Assembled prototype of the device to generate a quadratic stiffness curve.

Range of Motion & Adjustability
The BIJSC was tested up to an angle of 60° in both directions for all of its stiffness settings. The stiffness can be adjusted between 0.011- 0.807 Nm/deg.
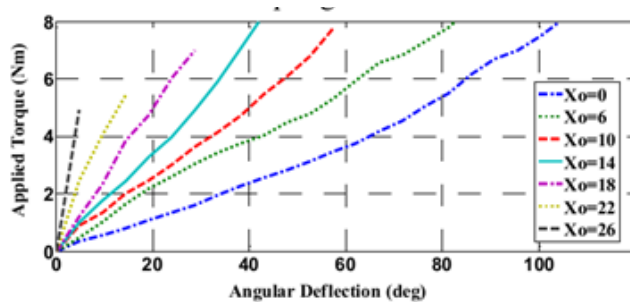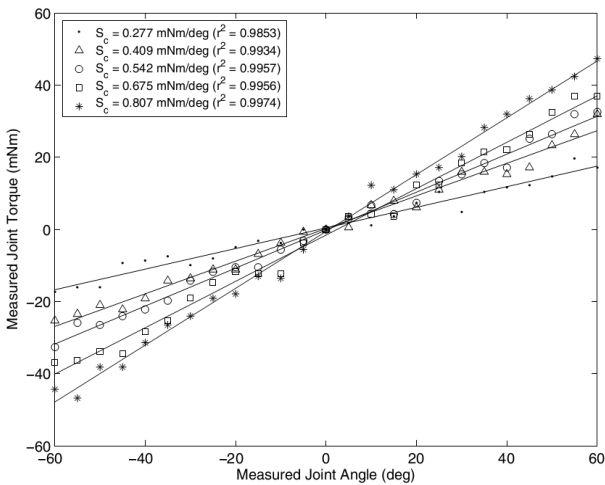

Figure 61: Stiffness curve of the BIJSC showcasing the applied torque over the angular deflection for various spring pretensioning presets. [18]

Analyzing the stiffness curve (Figure 61Figure 62) shows that at the different stiffness setting shows that the system shows nearly pure amplitude modulation. Table 13 displays the standard error between different lines.
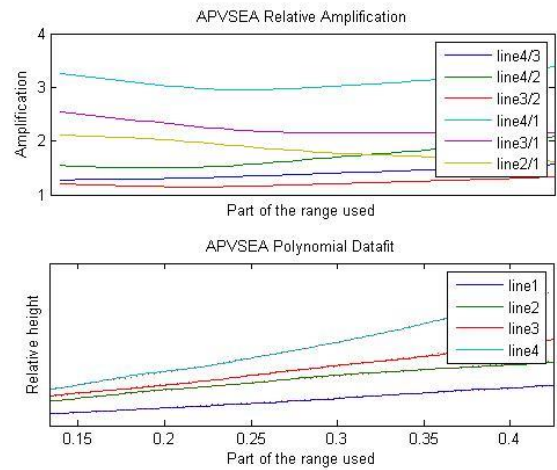

Figure 62: On the top a figure showcasing the relative magnification between different lines of the stiffness curve. On the bottom the figure showcases the polynomial data fit on top of the original data.

Standard error (σ / ц)	
Line4/Line3	1%
Line4 /Line2	1%
Line3/Line2	2%
Line4/Line1	2%
Line3/Line1	3%
Line2/Line1	2%

Table 13:
This table showcases for the PVSA how closely 2 lines are a pure amplitude magnification, the lower the value the more 2 lines show a constant amplitude magnification.

Efficiency
The BIJSC is adjusted by pulling the antagonistic springs. This means that the potential energy that gets stored within the spring needs to be supplied when changing the preset.

Number of Components
In the simplest version without the mechanism to generate a quadratic force relationship, the BIJSC requires 2 springs, 2shafts, rope, housing and a pulley, so in total 7 parts.

AMASC [19]

Functioning:

The Actuator with Mechanically Adjustable Series Compliance (AMASC) (Figure 63) is an antagonistic actuator of Configuration 2, meaning that the amasc got a separate actuator for controlling the basic equilibrium point, and the initial pretension.

What makes the AMASC special is that the desired stiffness curve is generated due to a pair of snail cams with a logarithmic transmission ratio connected to a set of linear springs. Which generates a linear force deflection curve at the output.
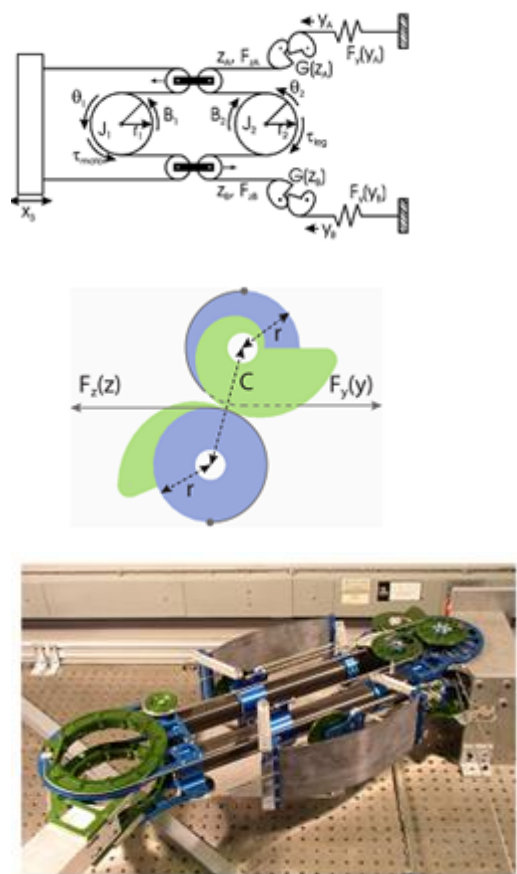
Figure 63: The Antagonistic actuator with mechanically adjustable series compliance. [19]
Top: The cable routing diagram of the AMASC. (Note J1,J2 are freely rotatable but pinned with G free floating). X3 is actuated to change the stiffness, θ1 is actuated to change the position.
Middle: A showcase of the configuration of the pulley setup that sits in between the springs and actuators generating the desired stiffness curve..
Bottom: A showcase of the AMASC prototype.

Range of Motion & Adjustability

The AMASC springs are able to deflect 0.06 meter and can be adjusted in stiffness by a factor 7 from 2500N/m to 18000N/m

Analyzing the stiffness curve (Figure 64Figure 65) shows that at the different stiffness setting shows that

the system shows nearly pure amplitude modulation. Table 14 displays the standard error between different lines.
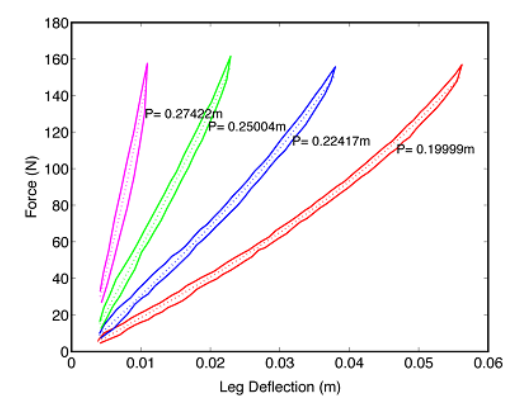
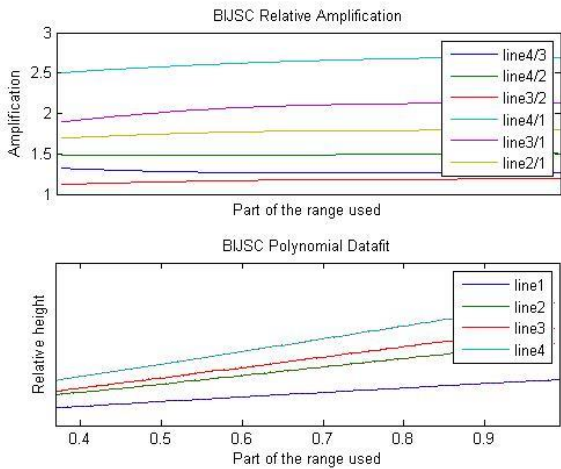**Figure 64: The force deflection curve of the AMASC [19]**

Figure 65: On the top a figure showcasing the relative magnification between different lines of the stiffness curve. On the bottom the figure showcases the polynomial data fit on top of the original data.

Standard error (ơ / ɥ)	
Line2/Line1	1%
Line3 /Line1	1%
Line3/Line2	2%

Table 14:
This table showcases for the AMASC how closely 2 lines are a pure amplitude magnification, the lower the value the more 2 lines show a constant amplitude magnification.

Efficiency

The AMASC is adjusted by moving a platform that in the end pulls the antagonistic springs. This means that the potential energy that gets stored within the spring needs to be supplied when changing the preset.

Number of Components

In its most simple form without the pullies for linearization of the forces the AMASC requires 2 springs, and 6 pulleys, movable platform, a housing and some rope. So 11 parts.

AWCM [20]

Functioning:

The AWCM (antagonistic wrapping cam mechanism) (Figure 66Figure 67) is an antagonistic variable stiffness actuator of configuration1.

Instead of placing the actuators at the base of the device they are placed alongside the to-be actuated arm. The cam profile is designed such that the spring characteristic is perfectly quadratic generating a linear rotational stiffness relationship.

Moving the cams together in opposite directions tensions the springs generating a higher stiffness curve. While changing the cams in the same direction will change the neutral position of the antagonistic setup.
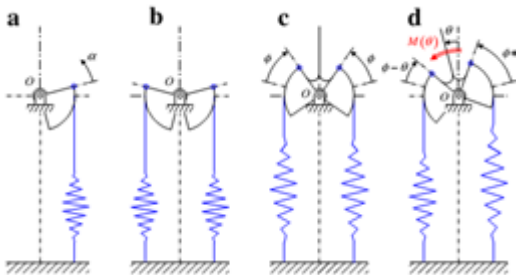
Figure 66: Antagonistic set-up of two quadratic springs for an adjustable stiffness torsional spring mechanism [20]
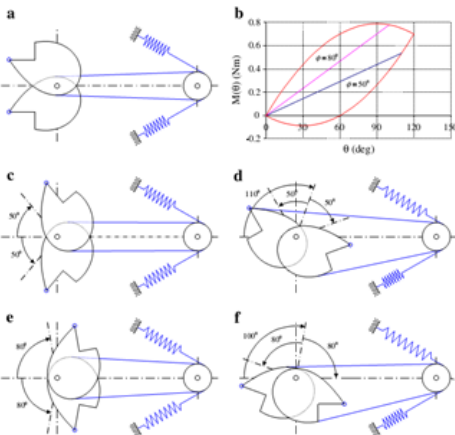
Figure 67: Antagonistic set-up of two linear springs, combined with a quadratic cam mechanism for an adjustable stiffness torsional spring mechanism with linear characteristic. [20]

Range of Motion & Adjustability

The AWCM can be used up for a range of up 100 degrees At its minimal and maximal stiffness the range is approximately 60 degrees.
The stiffness can theoretically be adjusted to anywhere within the red enclosure in Figure 68. Generating a range of –2 to 8 mNm/deg realistically the minimum would be bound above zero as cables are not able to submit compression forces.

Analyzing the stiffness curve (Figure 68Figure 69) shows that at the different stiffness setting shows that

the system shows nearly pure amplitude modulation. Table 15 displays the standard error between different lines.
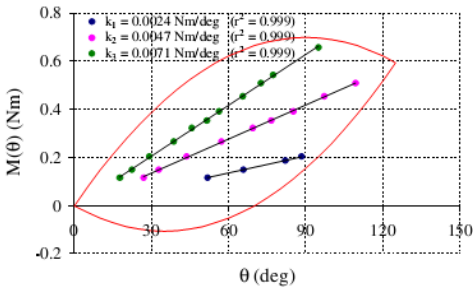

Figure 68: Experimental results of the prototype for three different adjusted stiffness values, the red circle shows the theoretically possible stiffnesses. [20]
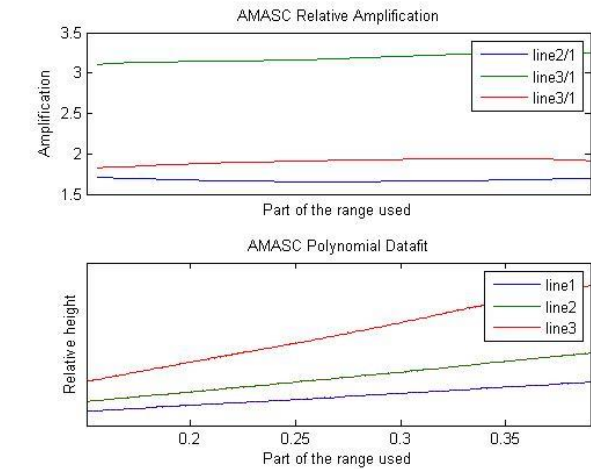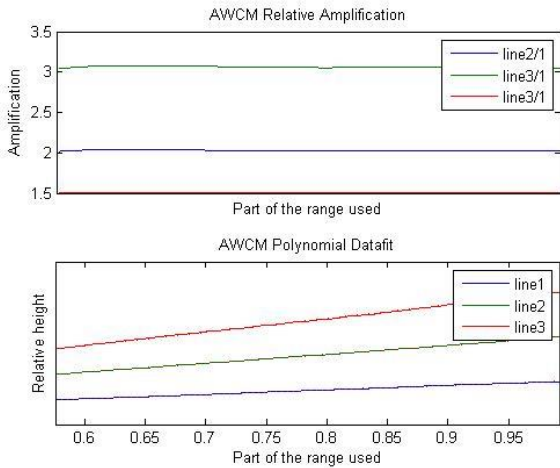

Figure 69: On the top a figure showcasing the relative magnification between different lines of the stiffness curve. On the bottom the figure showcases the polynomial data fit on top of the original data.

	Standard error ($σ / ч$)
Line2/Line1	0.3%
Line3 /Line1	0.3%
Line3/Line2	0.2%

Table 15:
This table showcases for the AWCM how closely 2 lines are a pure amplitude magnification, the lower the value the more 2 lines show a constant amplitude magnification.

Efficiency

The AWCM is adjusted by pulling the antagonistic springs. This means that the potential energy that gets stored within the spring needs to be supplied when changing the preset.

Number of Components

In the most simple configuration, 2 springs, 1 shaft, a housing and 2 wrapping cams are required resulting in 6 total parts.

Changing the Energy Storage through Adjustable Stiffness

While there are a lot of concepts that change the effective stiffness by adjusting the pretension, there were no direct gravity equilibrators found utilizing this method.

Rather than changing the pretension to change the effective stiffness of a system, changing the actual stiffness of a spring, does show more applications within statically balancing.

Stiffness type adjustments of springs.

When looking through literature, a distinction can be made between stiffness type adjustment by adding or removing more active parts of the elastic element(s), or by changing properties of the material or its configuration.

Adding or removing active parts of the elastic element.

Jack spring actuator [21]
Functioning
The adjustable jack spring actuator (Figure 70) works by engaging and disengaging one or more coils of a coil spring, by the use of a spindle. Effectively increasing the stiffness or decreasing the stiffness.
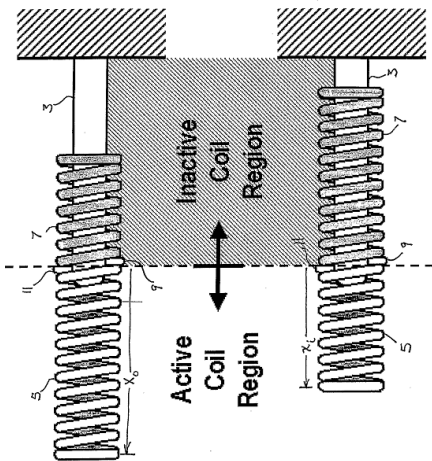
Figure 70: A showcase of a jack spring actuator where the amount of active coils are varied. [21]

Range of Motion & Adjustability
For determining the range of motion and possible stiffnesses it is important to understand how coil springs work (Figure 71).
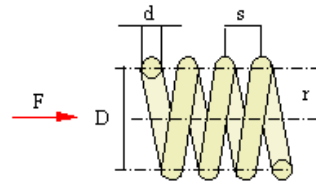
Figure 71: This figure [47] showcases a simple formula for the spring deflection "f" using the amount of active coils "n", radius of the spring "r' force applied on the spring "F", diameter of a wire "d" and the shear modulus "G". Since stiffness is denoted as force over displacement the stiffness of a spring can be described with.

Spring stiffness (k) = F/f = d^4*G / (64*n*r^3). Clearly showing the inverse linear relationship with coils and stiffness.

This means that depending on the amount of coils in the base spring and required deflection it would theoretically be possible to change the stiffness from 0 (infinite coils) to infinite (no coils).

Efficiency
When the spring is not under tension, the spindle would be able to freely rotate and with that engage or disengage the amount of active coils within the spring. However when when the spring is tensioned beside frictive forces, additional energy would be required when adjusting for a higher stiffness, as with the same elongation a spring with a high spring stiffness contains more energy than one with a low spring stiffness.

Number of Components
In the most simple configuration the jack spring actuator consists of 2 parts, a coil spring and the coil engagement spindle.

Adjustable chair [22]

Functioning:

This adjustable chair (Figure 72) shows a chair that statically balances the user to be able to change their height without any force within a certain range.
A four bar mechanism makes sure that the seating part of the chair always remains horizontal with respect to the ground, and a wire attached between a spring and a lever ensures an effective zero-free-length spring.

The main point of interest in this patent is the ability to change the the spring stiffness by engaging more or less coils of the base spring with a spindle (see the jack spring actuator), allowing the user to adjust the chair to fit to their body weight.
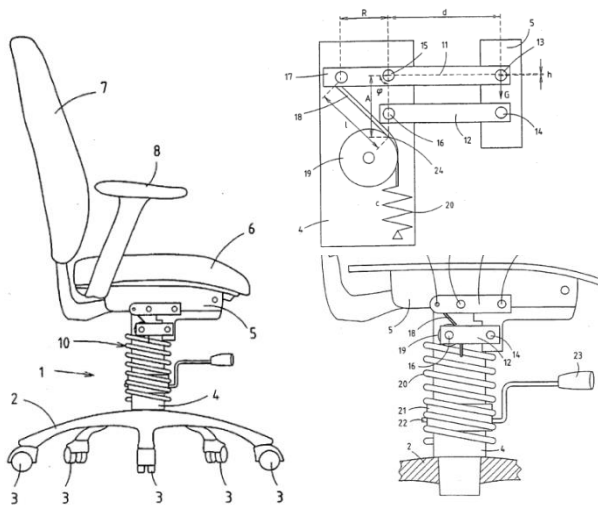

Figure 72: Showcasing an adjustable chair by Niels vrijlandt et al. [22] The left side shows a general overview of the chair, while on the top right the four bar mechanism that generates the constant gravity counteracting force. The bottom right shows the spring combined with an threaded spindle, that can be used to engage or disengage more or less active coils.

Range of Motion & Adjustability

The range of motion if parts would not collide with each other in this system would be 360°.
Like the jack spring actuator the stiffness would be possible to adjust from very little to very high depending on the selected spring, a note should be made that if too few coils are activated of the spring that the maximal range would decrease, unless the spring gets plastically deformed.

Efficiency

When the spring is not under tension, the spindle would be able to freely rotate and with that engage or disengage the amount of active coils within the spring. However when when the spring is tensioned beside frictive forces, additional energy would be required when adjusting for a higher stiffness, as with the same elongation a spring with a high spring stiffness

contains more energy than one with a low spring stiffness.

Number of Components

In the simplest configuration this entire system requires 2 parts for the stiffness adjustment (spring and spindle) combined with 4 bars to generate the constant upwards force.

Energy Free adjustable gravity equilibrator [23]

Functioning

In the Energy Free adjustable gravity equilibrator (Figure 73) a coil spring is used with a spindle to change the effective amount of engaged coils and thus spring stiffness (see the jack spring actuator), a wire and pully system ensures an effective zero-free-length.
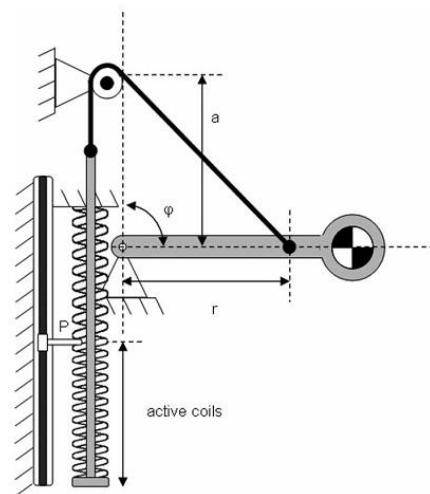
Figure 73: A drawing of the working principle of the Energy Free adjustable gravity equilibrator. [23]

Range of Motion & Adjustability

The range of motion if parts would not collide with each other in this system would be 360°.
Like the jack spring actuator the stiffness would be possible to adjust from very little to very high depending on the selected spring, a note should be made that if too few coils are activated of the spring that the maximal range would decrease, unless the spring gets plastically deformed.

Efficiency

When the spring is not under tension, the spindle would be able to freely rotate and with that engage or disengage the amount of active coils within the spring. However when the spring is tensioned beside frictive forces, additional energy would be required when adjusting for a higher stiffness, as with the same elongation a spring with a high spring stiffness (basically the spring potential should be overcome)

Number of Components

In the most simple configuration, the energy free adjustable gravity equilibrator requires 2 parts for the stiffness adjustment, a spring and a spindle, and 4 parts for the constant upwards force a pulley, rope, housing and a pendulum.

AAC [24]

Functioning:

The AAC (Actuator with adaptable compliance) (Figure 76) utilizes leaf springs to change stiffness.

Beside balancing mechanisms where the stiffness can be adjusted by activating or deactivated coils this balancing mechanism utilizes bendable beams as the elastic elements, where changing the effective beam length modifies the stiffness.

Modelling a beam using a single finite element (Figure 74) gives: Vmax = -PL^3 / 3 EI,   Stiffness K = P/Vmax = - 3 EI/L^3 Showing that the stiffness of a beam is inversely related to the length of a beam to the power 3rd (for small angles of deflection).
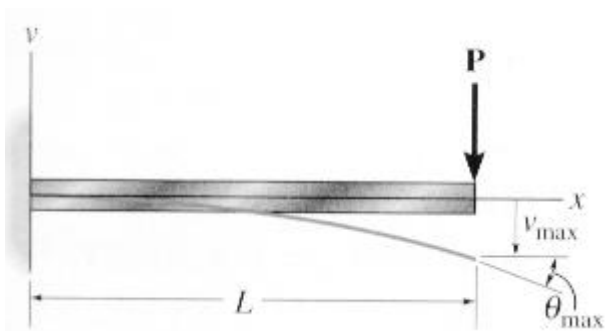

Figure 74: A showcase of a bending beam [48]

In the case of the AAC the length of the effective part of the beam is adjusted by the usage of rollers (Figure 75), by moving the rollers towards the tip of the less elastic material is utilized increasing the stiffness.

To set the neutral position the entire structure is raised and or lowered.
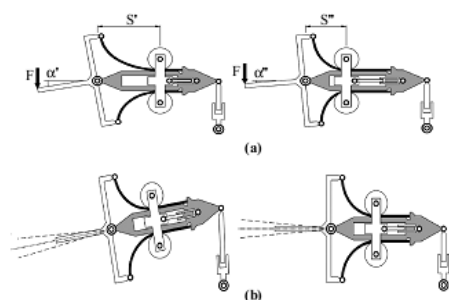
Figure 75: A showcase of the functioning of the AAC [24]

Figure 76: Assembled prototype of the AAC actuator. [24]

Similar as when modifying the spring stiffness with coil springs this only happens in an energy free fasion when there is no load applied to the system. If a load is applied to the system it will cost energy to increase the stiffness by shortening the length. This can easily be visualized by the beam having to be straightened out by the rollers.

Range of Motion & Adjustability

The range of motion of the end tip is between 2 and 10 degrees, relatively in the highest and lowest stiffness setting. The stiffness varies between 0.07 and 0.56 Nm/deg in between the lowest and highest stiffness setting.

Figure 77: Angular stiffness profile for the Actuator with adaptable compliance, showcased for multiple roller positions [24]

Analyzing the stiffness curve (Figure 77) shows that at the different stiffness setting shows that the system shows nearly pure amplitude modulation (Figure 78). Table 16 displays the standard error between different lines

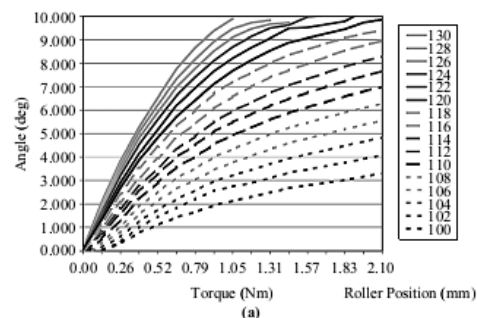**Figure 78: On the top a figure showcasing the relative magnification between different lines of the stiffness curve. On the bottom the figure showcases the polynomial data fit on top of the original data.**

	Standard error (σ / ų)
Line4/Line3	4%
Line4 /Line2	6%
Line3/Line2	1%
Line4/Line1	8%
Line3/Line1	4%
Line2/Line1	3%

Table 16:
This table showcases for the AAC how closely 2 lines are a pure amplitude magnification, the lower the value the more 2 lines show a constant amplitude magnification.

Efficiency
Similar as when modifying the spring stiffness with coil springs this only happens in an energy free fasion when there is no load applied to the system. If a load is applied to the system it will cost energy to increase the stiffness by shortening the length. This can easily be visualized by the beam having to be straightened out by the rollers.

Number of Components
In the simplest case the AAC needs 2 rollers, 2 springs, a base and an arm. So in total it sums up to 6 parts.

AVSEA [25]
Functioning:
The AVSEA (Figure 79) (Active Variable Stiffness Elastic Actuator) is a device able to modify the output position and output stiffness.

The stiffness is modified by changing the effective length of a bending beam by motor 02 (for more details see the AAC).

The bending beam holds a casing for the spindle of motor 1 which then adjusts the neutral position of the output link.
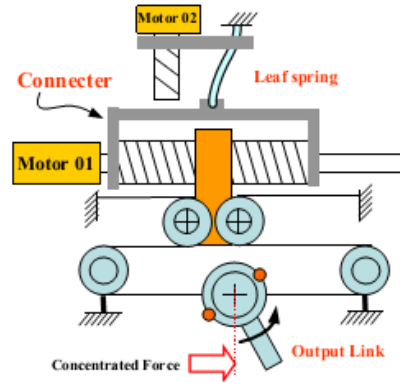
Figure 79: A systematic drawing of the functioning of the avsea. Motor 2 drives a spindle that adjust the active length of the leaf spring adjusting the stiffnes of the output link, where motor 1 drives a spindle that adjusts the neutral position of the output link. [25]

Range of Motion & Adjustability
The max deflection is roughly 40 degrees which decreases to zero at the maximum stiffness.
The stiffness can be adjusted from 0.085 Nm/deg towards theoretically infinite stiffness (spring length of 0).
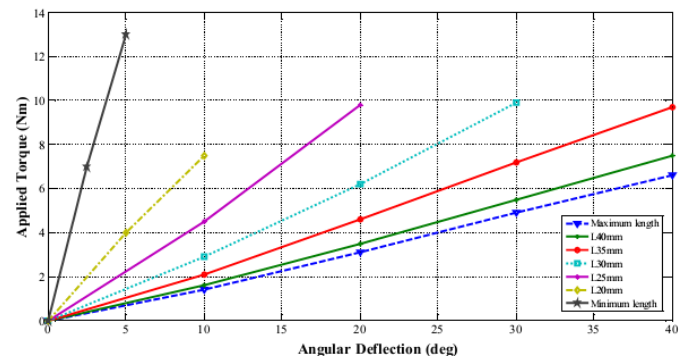
Figure 80: Showcase of the angular stiffness curve of the AVSEA for various active spring lengths. [25]

Analyzing the stiffness curve (Figure 80) shows that at the different stiffness setting shows that the system shows nearly pure amplitude modulation (Figure 81). Table 17 displays the standard error between different lines
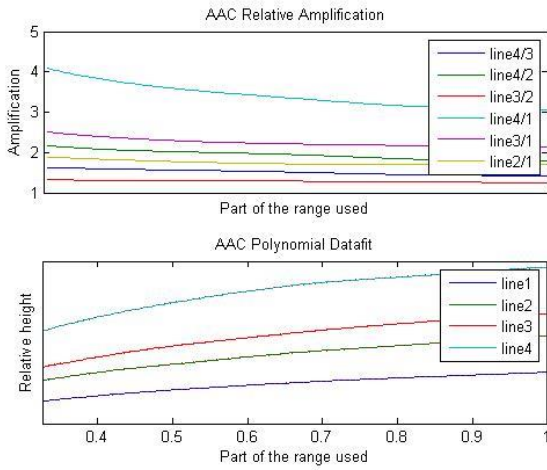
Figure 81: On the top a figure showcasing the relative magnification between different lines of the stiffness curve. On the bottom the figure showcases the polynomial data fit on top of the original data.

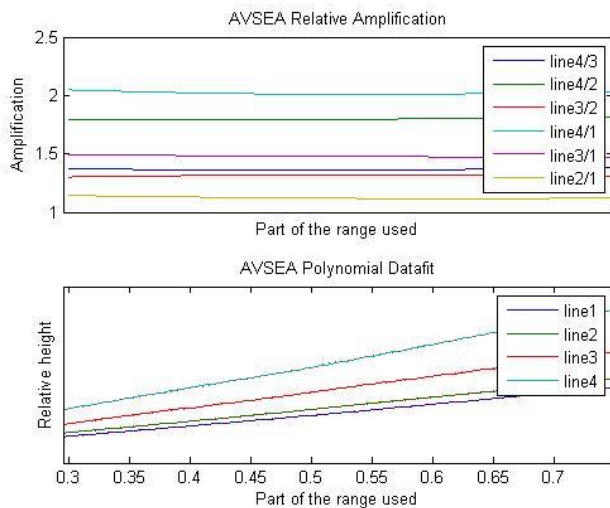|	Standard error (σ / ц)
Line4/Line3	1%
Line4 /Line2	1%
Line3/Line2	1%
Line4/Line1	1%
Line3/Line1	1%
Line2/Line1	1%

Table 17:
This table showcases for the AAC how closely 2 lines are a pure amplitude magnification, the lower the value the more 2 lines show a constant amplitude magnification.

Efficiency

Similar as when modifying the spring stiffness with coil springs adjustment only happens in an energy free fasion when there is no load applied to the system. If a load is applied to the system it will cost energy to increase the stiffness by shortening the length. This can easily be visualized by the beam having to be straightened out by the rollers.

Number of Components

In the showcased figure there are the following parts. 1 cable, 1 arm, 4 pullies, 2 spindles, 1 spring, 1 housing, 2 spindle arms. Accounting for 12 parts

Rotatable beam, changing the bending moment of inertia. [27]
Functioning

The stiffness of a single finite element bending beam is equal to "K = P/Vmax = - 3 EI/L^3" Which means that the stiffness is linearly dependant on the bending moment of Inertia (Figure 82). This patent (Figure 83) showcases a rotatable rod , that allows for the

selection of different bending moments of inertia, generating a compliant and stiff beam depending on its orientation. To prevent buckling a spring is added to the outside of the rotating rod.
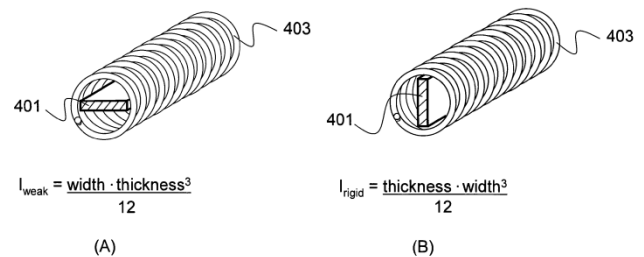

$$I_{weak} = \frac{width \cdot thickness^3}{12} \qquad I_{rigid} = \frac{thickness \cdot width^3}{12}$$

(A) (B)

Figure 82: Calculated bending moment of inertia for 2 configurations of a rod. [27]
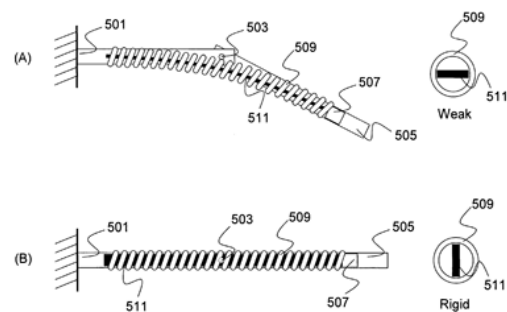
Figure 83: Sideways showcase of the rods being loaded at the end point with the same force at different settings of bending stiffness. [27]

Range of Motion & Adjustability

In order to prevent out of plane buckling the rod can only be used in 2 configurations stiff (high width low thickness) and compliant (low width, high thickness).

The total range of movement depends on the configuration and the used material's max allowable stress. Based on the information in this patent nothing can be said about this particular configuration.

Efficiency

When the device is not loaded beside friction there should be no issues in rotating the rod in terms of energy usage. When the device is loaded the stiffness cannot be changed due to the chance of out of plane buckling

Number of Components

A spring and a rod together count up to 2 parts.

VSASF [26]

Functioning:

The VSASF (Variable Stiffness Actuator for Safe and Fast Physical Human/Robot Interaction) (Figure 84), changes its stiffness by varying the active length of elastic material, however unlike previous examples it does so by loading the elastic material in the normal direction rather than loading it in bending or torsion.
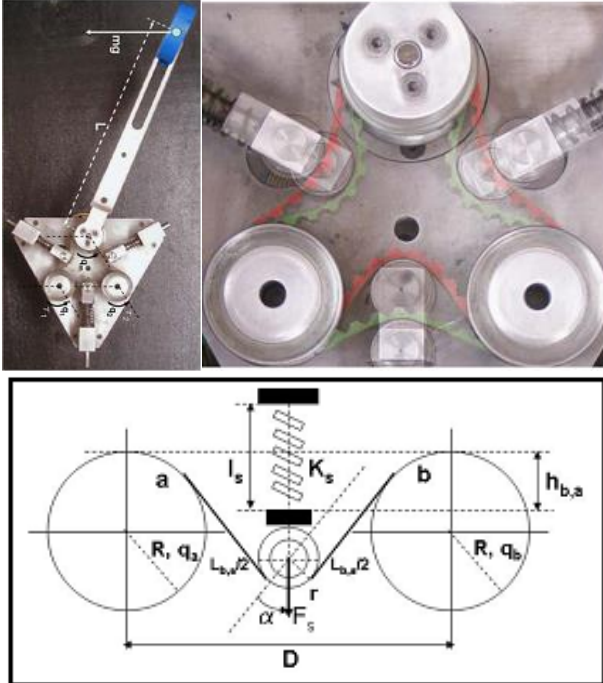

Figure 84:
Top left: Showcase of the VSAF protype [26]
Top Right: Showcase of stiffness adjustment system
Bottom: Schematic of the stiffness adjustment system [26]

In the triangle configuration on the top right (Figure 84) it can be seen that the system can adjust the rubber band such that there is either more elastic material on the top part of the triangle (green) or more elastic material on the bottom part of the triangle (red). (the top pulley is the rotatable arm, the bottom pullies are used to move material from the top to the bottom section).

This means either an increase in stiffness (less total length of elastic material on top) or a decrease in stiffness (increase of total length of elastic material on the top. (see the formula in Figure 85)

$$\delta = \int_0^L \frac{N}{EA}\, dx.$$

Figure 85: Formulae showing the elastic elongation due to a normal load [48]

Asuming a constant load at the end of the beam, with no variation in E modulus or Thickness, gives that the extension of a normally loaded rod is equal to dx = FL/EA resulting in a stiffness of.

K = F/dx = EA/L Meaning that there is a inversely linear relationship between the length of a normally loaded rod and its stiffness.

Range of Motion & Adjustability

The range of motion of the VSASF was not discussed in the literature. Nor was the material of the belt mentioned. Asuming the belt is made of natural rubber an extension of up to 150% will remain approximately linear[Harris' Shock and Vibration Handbook (5th Edition)/mechanical properties/ch 33 mechanical properties of rubber]. This would equal a rotation of approximately 120 degrees in both directions.

The stiffness can be adjusted from 5 Nm/deg to 35Nm/deg (Figure 86)
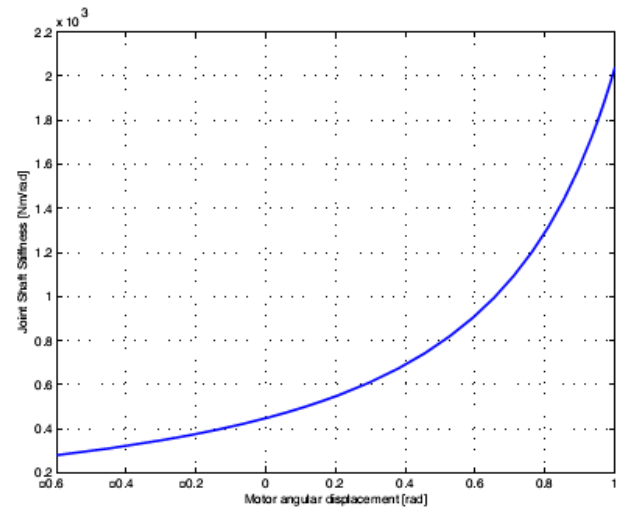
Figure 86: A showcase of the joint shaft stiffness at its neutral position for different at different settings of the stiffness adjusting motor pullies. [26]

Efficiency

When the belt is nut under tension it can easily be adjusted in length and should hardly cost any force or energy (assuming zero bending stiffness).
However to go from a low stiffness to a high stiffness when under load would require that the difference in potential energy is supplied in some way to the system.

Number of Components

The VSASF requires 3 pullies, an elastic drivebelt, and 3 belt tensioners together with a housing and 3 shafts. In total 11 parts.

Virtual spring method [28]

Functioning

B. M. Wisse et Al that by the utilizing super position on force vectors (Figure 87) of multiple zero free length springs, that it is possible to have a spring appear as if it got a variable basic stiffness.

By moving the springs such that they do not get extended in length, it becomes possible to adjust without the cost of energy (Figure 88). (Although one should note that this means that changing from a low stiffness to a high stiffness, that effectively the spring length will be reduced to keep a constant amount of energy).

Utilizing hook's ideal spring theory ($E=1/2*k*u^2$) shows that a spring with a 4 times higher stiffness, would need to decrease 50% in length to obtain a neutral amount of energy. Placing that in the balancing equation $A*B*k = m*g*C$ shows by the linear dependency upon A,B and k, that even if the length gets increased that the stiffness decreases double as fast resulting in a decrease of the total balanced force, which is why this method was placed in the adjustable stiffness section rather than adjustable transmission ratio.
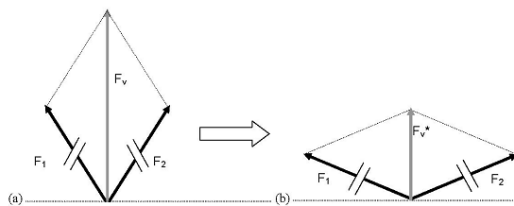

Figure 87: Utilizing the method of superposition on 2 forces of the same size, allows for creation of a resultant force of a different sizes. [28]
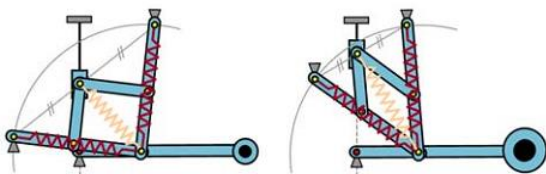

Figure 88: Applying the concept of superposition on a statically balanced pendulum, enforcing an arc for the springs through a pantograph. [28]

Range of Motion & Adjustability

As long as parts do not collide a spring balanced pendulum should work for a full 360°
As shown by the method of superposition (Figure 87) if 2 forces of equal size are pointed in opposite direction then no force is exerted while if they align both forces can be added up together.

Efficiency

Adjustment can happen in a force & energy free method (when neglecting friction losses) at any position of the arm, however the arc that needs to be followed in order to not extend the spring differs for every setting. With a fixed pantograph (Figure 88) adjustment can only happen in a single position.

Number of Components

The minimum amount of parts consists of a pendulum, 4 bars, 2 springs, housing and sliding guidance. Making 9 parts.

Adjusting the Energy Transfer

While it is possible to change the output of the direct energy storing mechanism, it is also possible to adjust the generated force by means of a transmission between the input and output.

This group can be divided in pendulum based adjustable transmission ratios, and other transmission methods (like (snail) cams, pullies and gears and continuously variable transmissions)

Pendulum based adjustable transmission ratios.

Adjusting the A and/or B parameter

Balance equation:
M1-M2 = 0
M1 = m*g*C*cos(phi)
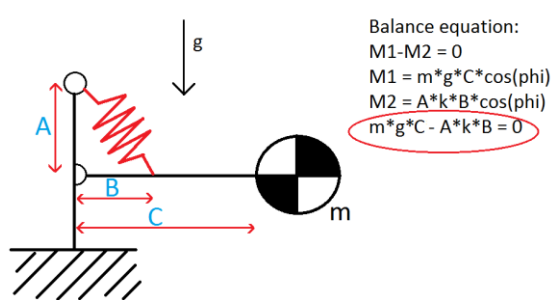M2 = A*k*B*cos(phi)
m*g*C - A*k*B = 0

Figure 89: A showcase of an inverted spring balanced pendulum and the accompanying balance equation

When looking at the balancing equation for a default spring balanced inverted pendulum (Figure 89), it directly shows that it becomes possible to adjust the balancing properties by adjusting the lengths of A and/or B.

It is a quite common way to be able to adjust the balancing force of a device like in the Adjustable Stiffness Device (ASD) from Mitsunori et Al [43] (Figure 90)
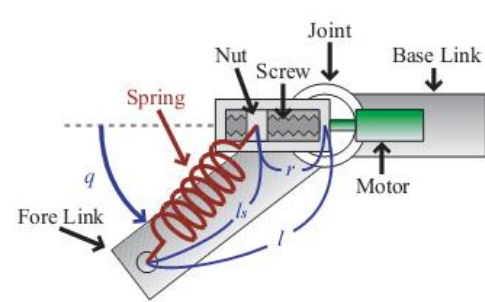

Fig. 2.   Proposed Mechanism

Figure 90: : Visualization of the working method of the Adjustable stiffness device. [43]

Range of Motion & Adjustability

The range of motion of traditional spring balanced inverted pendulums is 360 degrees as long as parts don't collide.

With essentially an infinitely available adjustment of the "to be balanced force" limited by the available size and selected spring.

Analyzing the stiffness curve (Figure 91), after doing a polynomial data fit (Figure 92) shows that at the different stiffness settings that the system is a bit off from pure amplitude modulation, which is most likely attributed to non-ideality of the utilized spring. Table 18 displays the standard error between different lines
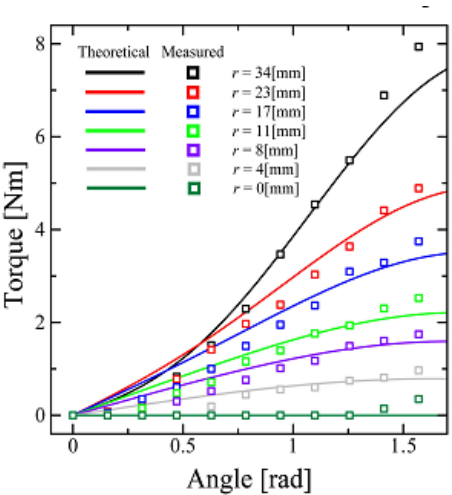

Fig. 6.   Experimental Results

Figure 91: The angular stiffness curve of the ASD balancer [43]
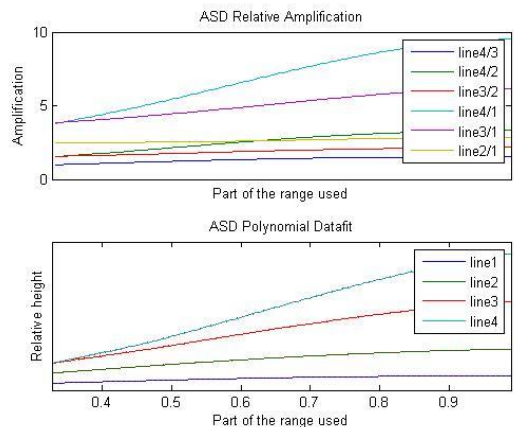
Figure 92: On the top a figure showcasing the relative magnification between different lines of the stiffness curve. On the bottom the figure showcases the polynomial data fit on top of the original data. [43]

	Standard error (σ / ɥ)
Line4/Line3	13%
Line4 /Line2	21%
Line3/Line2	10%
Line4/Line1	26%
Line3/Line1	15%
Line2/Line1	5%

Table 18:
This table showcases for the AAC how closely 2 lines are a pure amplitude magnification, the lower the value the more 2 lines show a constant amplitude magnification.

Efficiency

While there are a lot of concepts utilizing this method to great success, adjustment requires a change of length in the utilized spring generating an effective energy cost due to changes in potential energy.

Number of Components

The ASD requires 5 parts, namely 2 links, 1 spring, housing and a spindle.

General Note:

Due to the inherent cost of energy when adjusting Pendulum based balancers using A and/or B adjustment, only a single example has been presented.

There are however some systems that can adjust the variation with hardly any force.

Adjusting both the A&B parameters
Functioning:

One way to stop the springs from changing length when adjusting is by choosing parameters A&B such that during adjustment the spring remains at a constant length

Just L. Herder et Al [34] describes this type of system as systems utilizing the simultaneous displacement method (Figure 93). A method of how to possibly implement that is shown in Figure 94.
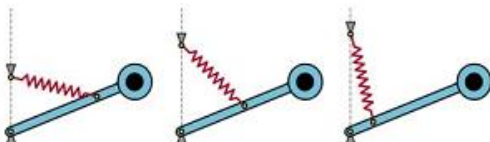
Figure 93: A showcase of the virtual displacement method, Adjusting the vertical and pendulum mounted spring attachment points at the same time such that the spring doesn't get extended. [34]
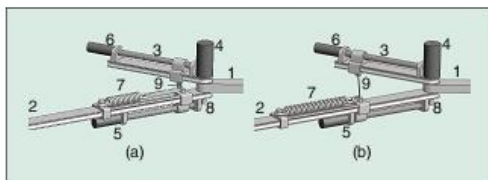
Figure 94: A design of 2 arms connected by a spring, where the spring adjustment points can be modified by a spindle drive. Allowing to effectively control possible ratios of A&B when balancing for a certain weight. [7]

Range of Motion & Adjustability:

The range of motion of traditional spring balanced inverted pendulums is 360 degrees as long as parts don't collide.

With essentially an infinitely available adjustment of the "to be balanced force" limited by the available size and selected spring.

Efficiency

Adjustment can happen in a force & energy free method (when neglecting friction losses) at any position of the arm; however the total length of spring is different for every position of the arm. With a fixed bar adjustment can only happen in a single position.

Number of Component

In the most simple configuration 3 parts are needed, 1 spring, 1 pendulum and a base to mount the spring on.

MACCEPA 1 & 2 [32, 33]
Functioning

The Maccepa (Mechanically Adjustable Compliance and Controllable Equilibrium Position Actuator) 1&2 allow for actuation with 2 degrees of freedom, allowing to adjust the applied moment arm of the system the system such that the moment gets increased while the spring length stays constant (Figure 95Figure 96). On the top of the figures it can be seen that 2 spindle drives directly regulate the spring attachment points. In the maccepa figures it can be seen that the angle of an arm can be adjusted together with a spindle drive connected to the spring itself. Allowing again by adjusting both actuators correctly at the same time that the spring doesn't get extended.
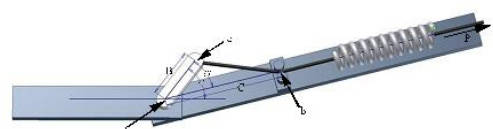
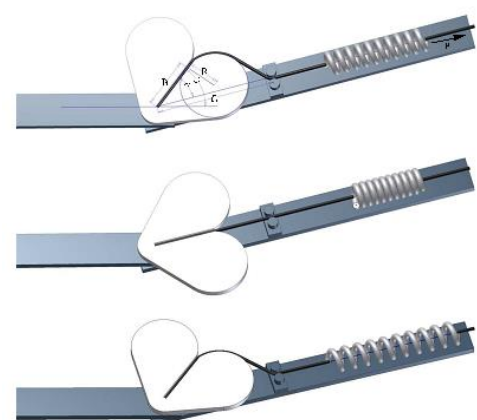**Figure 95: A visualization of the working principle of the MACCEPA 1. [32]**

Figure 96: A visualization of the working principle of the MACCEPA 2. [33]

Range of Motion & Adjustability

The MACCEPA is designed for a working range of up to 45 degrees away from the neutral position .

The stiffness of the MACCEPA1 can be adjusted from 0 to 0.02 Nm/rad depending on the pretension and spring adjustment arm (Figure 97).

The stiffness of the MACCEPA2 can be adjusted from 0 to 0.09 Nm/rad depending on the pretension and spring adjustment (Figure 97)
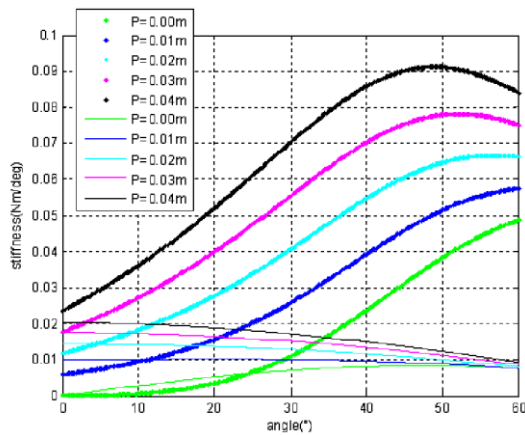

Figure 97: Comparison of the stiffnesses of the MACCEPA1 &2 for different arm angles and pretension settings. [33]
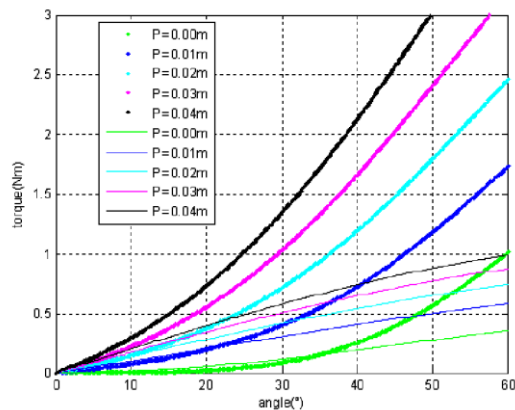

Figure 98: A rotational stiffness curve of the MACCEPA1&2 showcasing the relation between Torque and arm angle relative to the neutral position. The thick line depicts the MACCEPA2 the thin line the MACCEPA1. The different lines show different pretension settings. [33]

Analyzing the stiffness curve (Figure 98) shows that at the different stiffness setting shows that the system shows nearly pure amplitude modulation for the MACCEPA1 but that the additional range of the MACCEPA2 comes at a cost (Figure 99Figure 100). Table 19Table 20 display the standard error between different lines
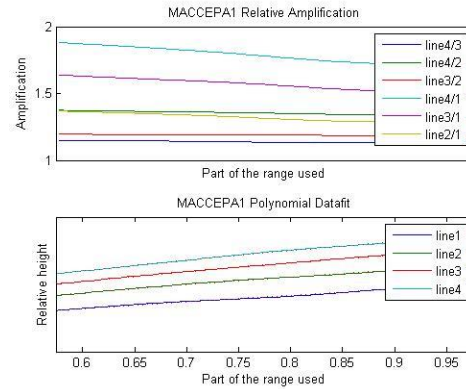

Figure 99: On the top a figure showcasing the relative magnification between different lines of the stiffness curve. On the bottom the figure showcases the polynomial data fit on top of the original data.

MACCEPA1 Standard error (σ / ц)	
Line4/Line3	1%
Line4 /Line2	1%
Line3/Line2	1%
Line4/Line1	3%
Line3/Line1	3%
Line2/Line1	2%

Table 19:
This table showcases for the MACCEPA1 how closely 2 lines are a pure amplitude magnification, the lower the value the more 2 lines show a constant amplitude magnification.
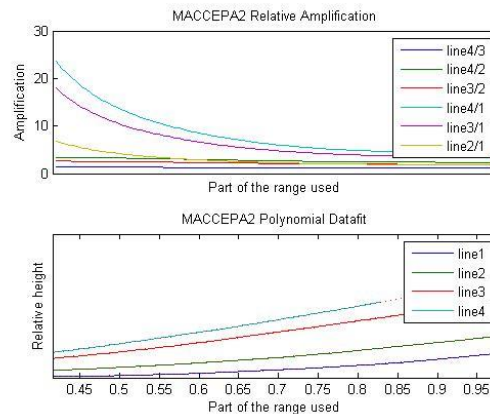
MACCEPA2

Figure 100: On the top a figure showcasing the relative magnification between different lines of the stiffness curve. On the bottom the figure showcases the polynomial data fit on top of the original data.

MACCEPA 2 Standard error (σ / ц)	
Line4/Line3	2%
Line4 /Line2	13%
Line3/Line2	11%
Line4/Line1	59%
Line3/Line1	56%

Line2/Line1	44%

Table 20:
This table showcases for the MACCEPA2 how closely 2 lines are a pure amplitude magnification, the lower the value the more 2 lines show a constant amplitude magnification.

Efficiency

By actuating the angle and pretension at the same time, with correct control it becomes possible to change the angle while not extending the spring. This makes it theoretically possible to change the stiffness without any energy cost.

Number of Components

In the simplest case the MACCEPAs consists of 2 rods, a spring, rope housing and an adjustable arm. In total this equals out to 6 parts.

Balancing using a storage spring for adjustment in a single position [30, 31]

Functioning

The issue with adjusting one of the lengths in a statically balanced system was primarily that while doing so the spring gets extended, resulting in a loss of energy. R. Barents et Al proposed the usage of a storage spring (Figure 101Figure 102), where for a single position of the pendulum (in the described case at a horizontal position), the spring attachment point can be adjusted by exchanging energy from one spring to the other.
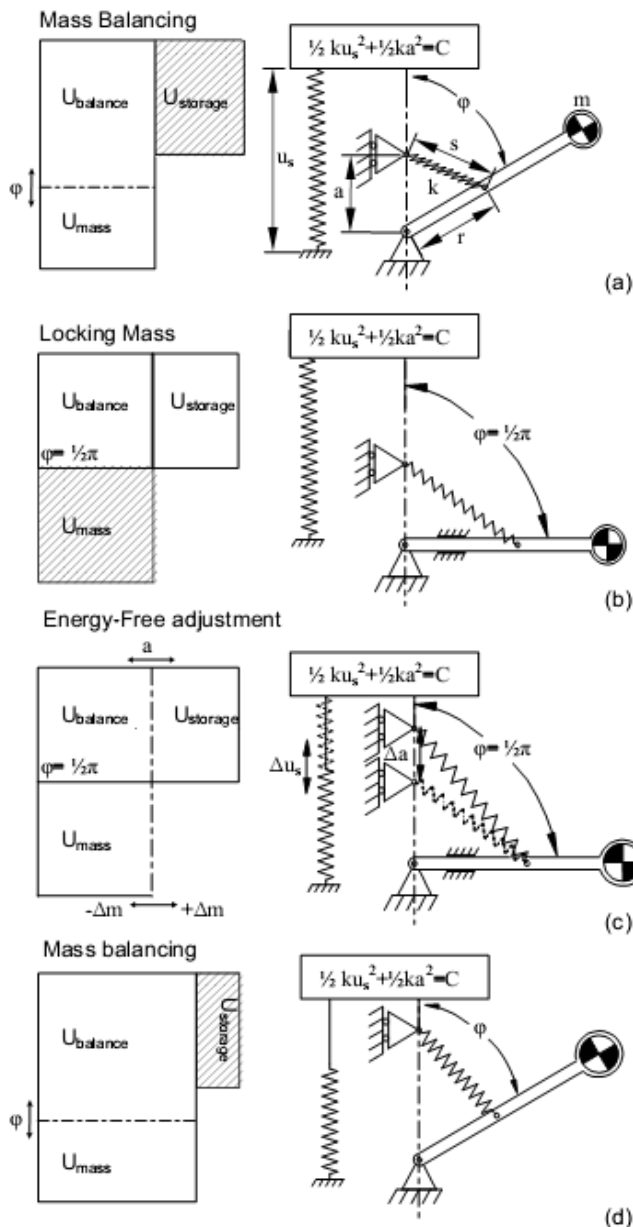
Figure 101: Showcase of the working principle of the storage spring method by R. Barents et Al. [30]
A: Showcase of the regular operating in a statically balanced fasion for a low weight mass.
B: The arm of the pendulum gets locked, and the spring adjustment gets unlocked.
C: With energy from the storage spring the height of spring attachment point can be adjusted. To set the height correctly for a different mass.

D: After the adjustment the height spring attachment point gets locked and the arm gets unlocked the system is now statically balanced for a different end weight.
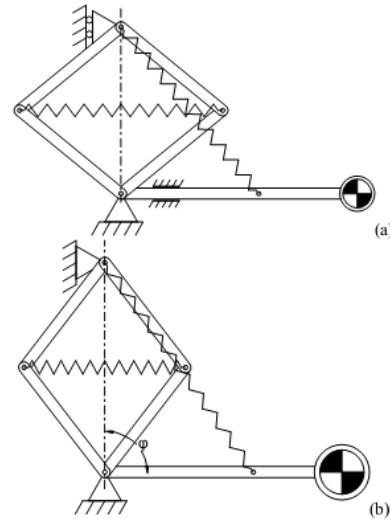
Figure 102: Showcase of the an implementation of the storage spring principle for the usage of weight adjustment at the horizontal position. [30]

Range of Motion & Adjustability

The range of motion of said system is 360° unless parts collide with each other.

The amount of possible adjustment depends on the energy stored within the storage spring. And mechanical properties of the spring and size constraints.

Efficiency

The system is setup such that at a single position the storage spring and the balancing spring keep a constant potential energy allowing energy transfer from one to the other.

In other positions than the one selected for balancing the mass the potential difference of the mass would need to be overcome while adjusting.

Number of Components

In the simplest configuration the system requires 5 bars a housing and 2 springs. Totaling to 8 parts.

Balancing using a storage spring for multiple positions [29]
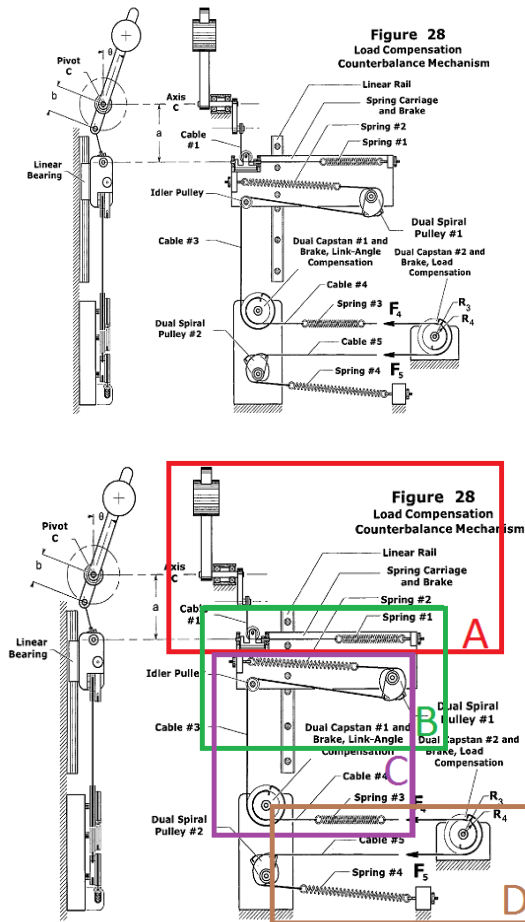### Functioning

Figure 103: Schematic overview of the multiple position adjustable storage spring system. [29]

The balancer using a storage spring for multiple positions (Figure 103) regards a device that initially works the same as the balancer by R.Barents [30] [31] using a storage spring.

- Regular balancer:
Part A of the patent, describes a regular zero free length balancer using a pully and a rope to generate a zero free length spring.

- Force free weight adjustable for a single pendulum angle.

Part B showcases that by attaching the system of A on a rail that the length of A in the balancing equation can be varied (effectively changing the to be balanced mass). As the extension of a spring cost energy, a second spring with a snail cam is added that counterbalances the spring force for a single position of the pendulum.

- Force free weight adjustable balancer, that at a single weight can adjust the pendulum angle.

Part C showcases a system that changes the pretension of the spring of section B, for a single to be balanced weight. This changes the angle of the pendulum where the system can be adjusted. In order to make this adjustment without any cost of energy, a third spring is added that allows the springs in section C to exchange energy with each other.

- Force free weight adjustable balancer, that can be adjusted at any angle with any weight

Part D showcases a system that changes the pretension of the spring of section C, this allows for the angle where the system can be adjusted to happen at different weights.

Range of Motion & Adjustability
The range of motion of said system is 360° unless parts collide with each other.

The amount of possible adjustment depends on the energy stored within the storage spring. And mechanical properties of the spring and size constraints.

Efficiency
for any of the adjusters in B,C,D to work they must have a constant total of potential energy, meaning that if section D gets adjusted to make section C work for a different weight, followed by section B being adjusted to compensate for a different weight. Then in order to change section D again, first B must be moved back to its original position, then C, and only then can D be adjusted again.

This means the system from its base state can adjust for different masses at any angle of the pendulum and will then offer correct balance, however if the mass gets changed again it should then always happen at exactly the same position, until the system is put back to its initial at that same position allowing it to be adjusted in another position again.

Number of Components
In the system there is
1 pendulum, 4 springs, 4 pulleys, a housing and 1 sliding base so 11 parts total

Lever based adjustable transmission ratios

Compact VSA [41]
Functioning:

The compact vsa (compact variable stiffness actuator), utilizes an antagonistic springs setup. Although rather than directly pulling the springs, you effectively pull through a lever (Figure 104) with an adjustable lever arm, allowing you to adjust the effective stiffness.

The specialty of the compact VSA is that instead of using a regular lever, it uses a cam profile (Figure 105) with adjustable pivot, allowing the system to fit a smaller space.
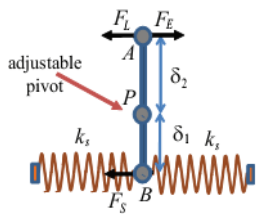

Figure 104: An antagonistic spring setup connected to a lever arm with adjustable pivot point. [41]
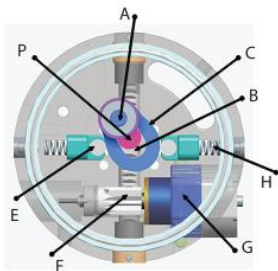

Figure 105: CAD Assembly of the CompactVSA showcasing the use of a cam profile with adjustable pivot generating the different stiffness profiles. [41]

Range of Motion & Adjustability
The Compact VSA can be adjusted for a maximal angular rotation of 0 to 20°. The stiffness can be adjusted from 0 to 60 Nm/deg.

As the different lines in the stiffness curve (Figure 106) heavily intermesh, it is not possible to say something about the linear dependency of the different curves.
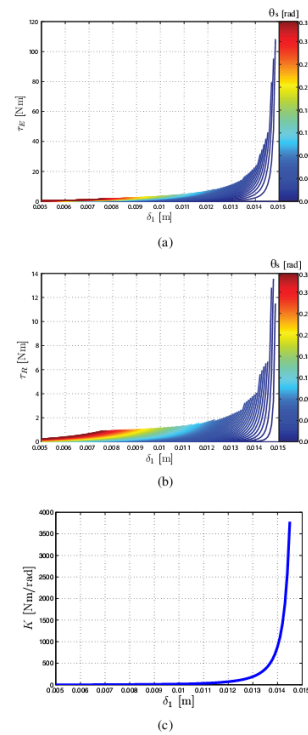

Figure 106 [41]:
    a. **Figure showing the Elastic Torque over Pivot position for angular deflections θ**
    b. **Showcase of the Resistant Torque over Pivot position for angular deflections θ**
    c. **Showcase of stiffness for different pivot positions.**

Efficiency
Adjustment of the cam can happen only in a force free matter when the springs are not tensioned. When under tension changing the pivot would cause the spring to shorten or lengthen, effectively causing the spring to release or store more energy. This stored energy needs to be supplied by the actuation system. Meaning that the system can only be adjusted force free in a single position ($\theta = 0°$)

Number of Components
In the simplest configuration the system requires, 2 springs, 1 cam, 1 adjustable shaft and a housing, so in total 5 parts.

VSRA: [40]

Functioning

The VSRA (Variable Stiffness Rotational Actuator) (Figure 107) is a stiffness actuator that that works by changing the pivot of a lever arm (Figure 108) effectively changing the leverage between in and output.

What makes the VSRA special is that the position of the lever arm is changed using 2 actuators instead of one, allowing to move the pivot in a 2d space. This makes it possible to adjust the stiffness in such a way that the springs do not change in length, and the output angle doesn't get changed. Since adjustment doesn't change the spring length it allows for operation that only requires a low amount of energy.
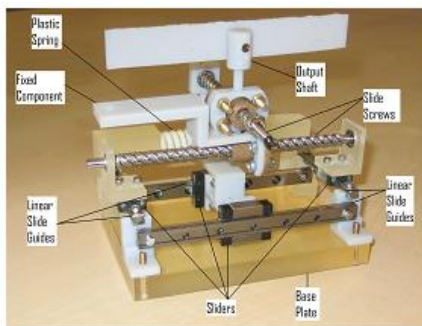

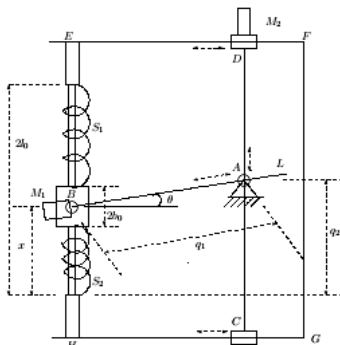**Figure 107: A showcase of the VSRA prototype [40]**

Fig. 2. Schematic of a variable stiffness rotational actuator.

Figure 108: Schematic of the VSRA's working principle. The pivot point of the spring setup can move on a 2d plane allowing the pivot to change such that the output of rotation and the length of the springs do not change when adjusting the lever arm. [40]

Range of Motion & Adjustability

The VSRA got a range roughly from 0 to 9 degrees (Figure 109), while the stiffness can be adjusted from 0 to 23e-3 Nm/degree (Figure 110)
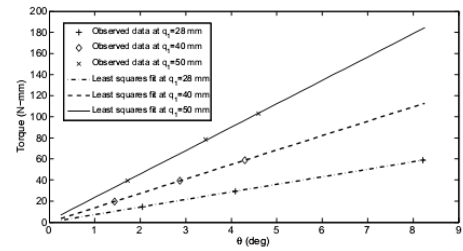

Figure 109: The torque over angular displacement stiffness characteristic of the VSRA [40]
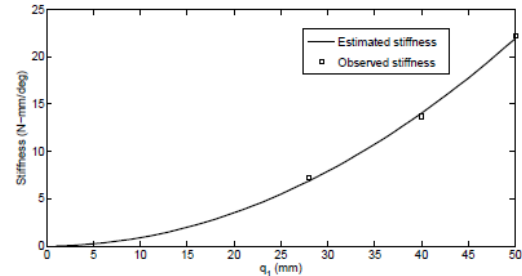

Figure 110: A showcase of different possible stiffness's for different lengths of the moment arm. [40]

Analyzing the stiffness curve (Figure 109), after doing a polynomial data fit (Figure 111) shows that at the different stiffness settings that the system shows nearly pure amplitude modulation, which is most likely attributed to the small range of motion applied. Table 21 displays the standard error between different lines
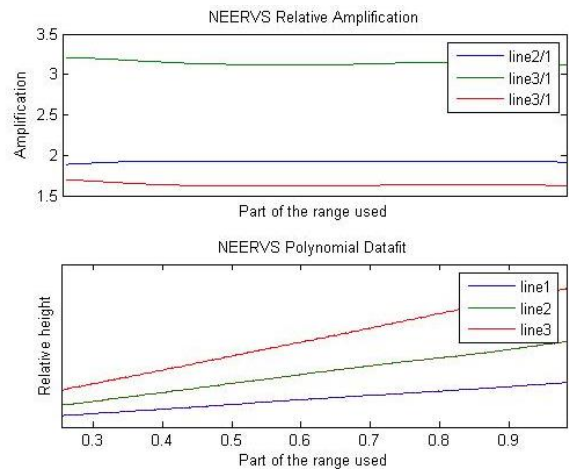

Figure 111: On the top a figure showcasing the relative magnification between different lines of the stiffness curve. On the bottom the figure showcases the polynomial data fit on top of the original data.

Standard error (σ / ҵ)	
Line2/Line1	1%
Line3/Line1	1%
Line3/Line2	1%

Table 21:
This table showcases for the NEERVS how closely 2 lines are a pure amplitude magnification, the lower the value the more 2 lines show a constant amplitude magnification.

Efficiency

As adjusting the stiffness does not change the length of the spring or the angular output of the system. Effectively no work is done. So the primary losses of the VSRA will come from friction losses combined with losses due to the 2 actuators not working perfectly in unison.

Number of Components

In the simplest configuration, you need 2 springs, a lever and a pivot point that can be moved in a 2d space together with a housing. Bringing the system to a total of 5 parts.

Awas [38, 39]

Functioning

The AWAS (Actuator with Adjustable Stiffness) (Figure 112) makes use of an antegonistic pair of springs in combination with an adjustable lever arm to change the output impedance. Different from changing the pivot point in Compact VSA the Awas moves the spring up and down on a lever arm instead of changing the pivot point, although both methods effectively reduce or elongate the length of the arm.
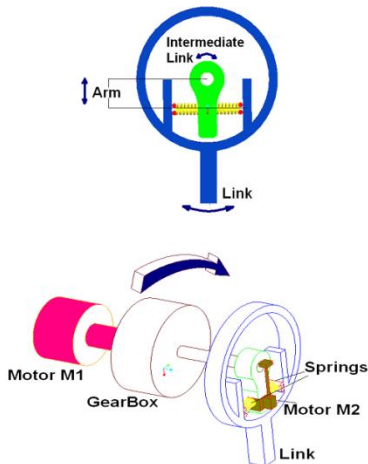

Figure 112: A showcase of the working principle of the AWAS. On the top a series of springs can be seen hold within a casing that can slide up or down on the intermediate link changing the effective stiffness. The bottom figure showcases a possible assembly when coupled with an actuator. [38]

Range of Motion & Adjustability

The AWAS got a maximum angular deflection that varies between 1.2° (maximum stiffness) and 7° (minimal stiffness).

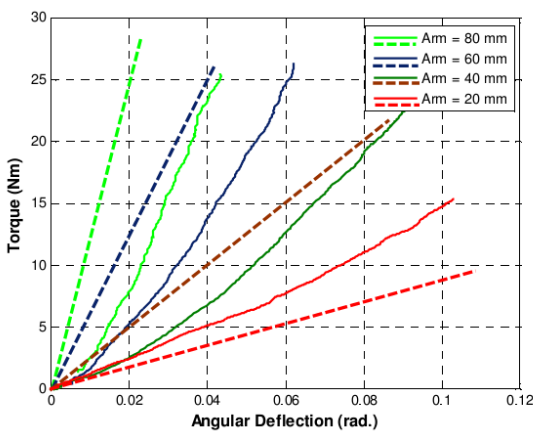With the ability to adjust the stiffness between 1.6 Nm/degree and 21.81 Nm/degree

Figure 113: Showcase of the angular stiffness curve for the AWAS, at different arm lengths. [38]

Analyzing the stiffness curve (Figure 113) shows that at the different stiffness setting shows that the system

shows nearly pure amplitude modulation (Figure 114). Table 22 displays the standard error between different lines
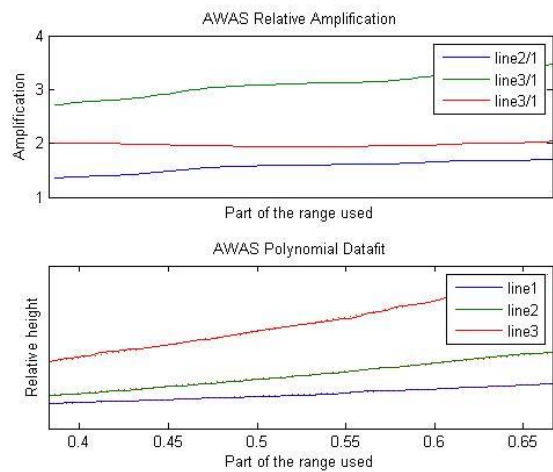

Figure 114: On the top a figure showcasing the relative magnification between different lines of the stiffness curve. On the bottom the figure showcases the polynomial data fit on top of the original data.

Standard error (σ / ц)	
Line2/Line1	6%
Line3/Line1	6%
Line3/Line2	1%

Table 22:
This table showcases for the NEERVS how closely 2 lines are a pure amplitude magnification, the lower the value the more 2 lines show a constant amplitude magnification.

Efficiency

Adjustment of the spring position can happen only in a force free matter when the arm is not angled. When angled changing the spring location cause the spring to shorten or lengthen, effectively causing the spring to release or store more energy. This stored energy needs to be supplied by the actuation system. Meaning that the system can only be adjusted force free in a single position ($\theta = 0°$)

Number of Components

In the simplest configuration the AWAS requires housing, 2 springs and a link and output shaft. Bringing the total to 5 parts

HDAU Hybrid Dual Actuator Unit [37]

Functioning:

The HDAU (Hybrid Dual Actuator unit) works by the effect of an adjustable moment arm (Figure 115). Placing the springs further away from the rotational point generates a bigger moment arm increasing the moment required to rotate the arm, causing a change in the output stiffness.
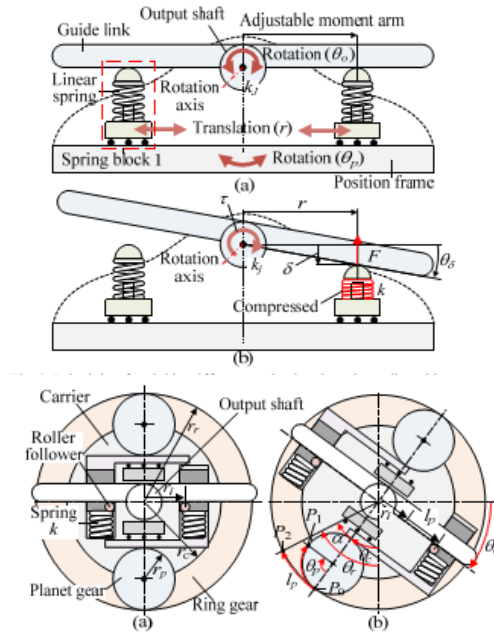

Figure 115: Showcase of the HDAU the top figure shows the working principle by movable placement of the engaging springs changing the moment arm. The bottom figure shows the assembly of the system in compact round casing. [37]

Range of Motion & Adjustability

The maximum operating range of the HDAU is around 30°, the stiffness adjustment ranges from 0.07 ~2.2 Nm/degree. (Figure 117)

Analyzing the stiffness curve (Figure 116) shows that at the different stiffness setting that the system doesn't appear to show pure amplitude modulation (Figure 118). Table 23 displays the standard error between different lines
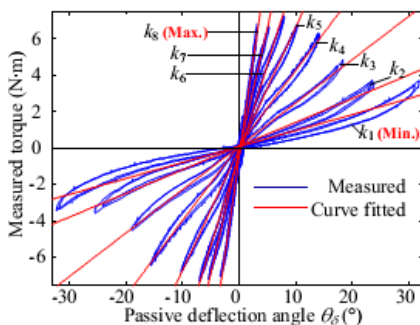

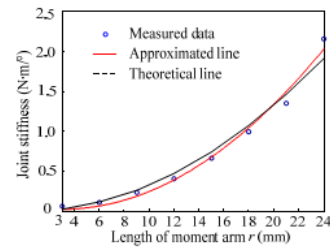Figure 116: Showcase of the stiffness curve for the HDAU[37]

Figure 117: Showcase of the adjustability in stiffness for the HDAU [37]
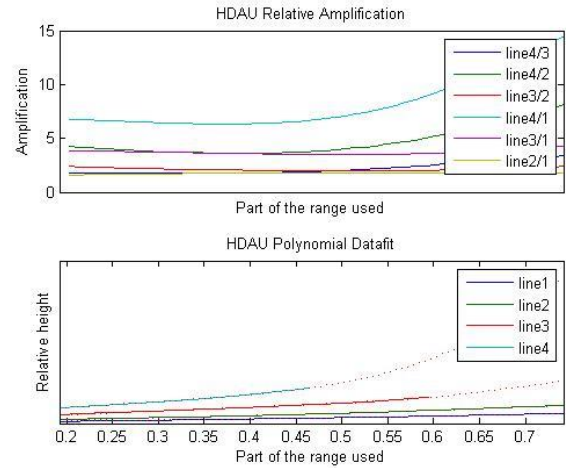

Figure 118: On the top a figure showcasing the relative magnification between different lines of the stiffness curve. On the bottom the figure showcases the polynomial data fit on top of the original data.

Standard error (σ / ц)	
Line4/Line3	24%
Line4 /Line2	27%
Line3/Line2	7%
Line4/Line1	30%
Line3/Line1	5%
Line2/Line1	3%

Table 23:
This table showcases for the HDAU how closely 2 lines are a pure amplitude magnification, the lower the value the more 2 lines show a constant amplitude magnification.

Efficiency

When the lever arm is at a horizontal position the leverage can be adjusted without energy. However when the system is tensioned, and the arm rotated different positions for the springs have a different corresponding length, meaning that said potential should be overcome when adjusting the stiffness while the system is tensioned.

Number of Components

In the simplest configuration the HDAU requires a lever arm with 2 springs together with an output shaft. Bringing the total to 4 parts.

vsaUT [35, 36]

Functioning

The vsaUT (Variable Stiffness actuator from the University of Twente) (Figure 119) shows a variable stiffness actuator that works through an adjustable lever arm.

The novelty of the design is to control 2 degrees of freedom in order to adjust the stiffness (Figure 120Figure 121). This allows for adjustment of the moment arm without changing the length of the spring or inducing a deviation in the output. This means that in the effective stiffness change no work is done.
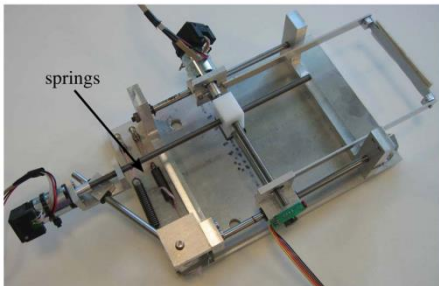

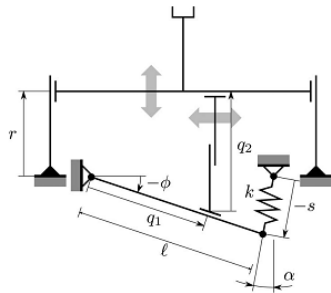Figure 119: A showcase of the assembled prototype of the vsaUT [35]

Figure 120: Showcase of the working principle of the vsaUT, by controlling both q1 and q2 at the same time, the lever arm can be adjusted at different heights and set angles even when loaded. [35]

Range of Motion & Adjustability

The vsaUT was shown to work up to an angle of 9 degrees. The actual stiffness range of the device isn't stated however its output can be changed at least from a stiffness of 2500N/m to 1000N/m (Figure 122)
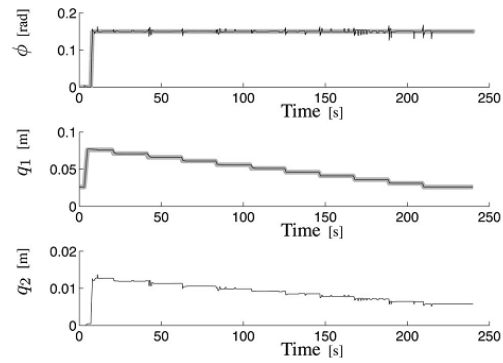

Figure 121: Showcase how the angle which affects the extension of the spring stays constant when changing the position of the moment arm [35]
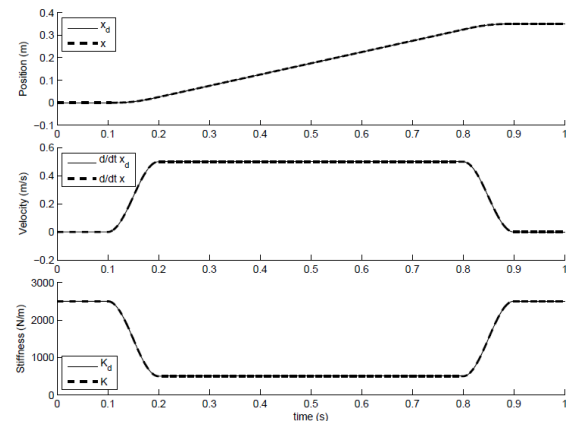
Figure 122: Showcase of the vsaUT being actuated over a small trajectory. [35]

Efficiency

As adjusting the stiffness does not change the length of the spring or the angular output of the system. Effectively no work is done. So the primary losses of the vsaUT will come from friction losses combined with losses due to the 2 actuators not working perfectly in unison.

Number of Components

In the simplest configuration the vsaUT requires a spring, a moment arm, 2 slider mechanisms, a housing and a pivot. Resulting in a total of 6 parts.

Traditional CVT based adjustable transmission
CVTvsa [42]
Functioning
The CVTvsa (Continuously variable transmission based variable stiffness actuator), combines a traditional continuously variable transmission (CVT) with an antagonistic pair of springs in the form of an elastic band (Figure 123).

The CVT similar to a double cone CVT allows changing the relative input and output diameter which effectively changes the gear ratio.

Due to limiting the output range of the CVT a sliding rail can be used to adjust the gear ratio (Figure 124).
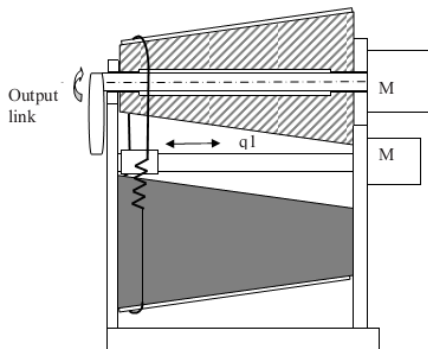

Figure 123: A schematic view of the CVTvsa, a double cone CVT connected not with a regular transmission belt but with an elastic element. [42]
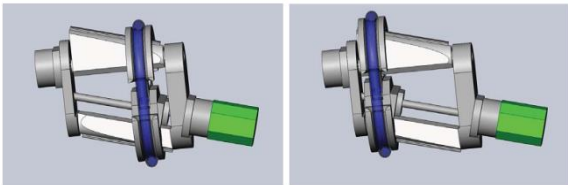

Figure 124: Cad drawing of the CVTvsa showcasing the sliding rail which allows adjusting the ratio without overcoming the friction of the transmission belt. [42]

Range of Motion & Adjustability
The range of motion is not mentioned in the literature although since the half pulleys carrying the rubber are placed on a cone like structure the further the device rotates the further it will deviate from its desired gear ratio. For this reason an assumption will be made that the range is similar to lever type vsa's so in the order of 10°

The stiffness depends on the compliant member which wasn't specified. The ratio change for a cone based CVT is often in the range of 4x [], so that will be assumed for now.

Efficiency
Although it depends on implementation theoretically the adjustment of the CVTvsa happens without extending the springs or the output angle, meaning that there are no energy losses in the form of potential energies.

Number of Components
In its simplest configuration the CVTvsa requires: housing, 2 cone shaped shafts and a rubber belt. Counting all parts results in a total of 4 parts excluding the mechanism to actually change the belt position.

Appendix D: Matlab Code
Code for comparing the amplitude modulation of graphs. (Based on a matlab function by Giuseppe Radaelli)

```matlab
clc;close all;clear all
% warning('off','all');

list = dir('Pictures');
list=struct2cell(list);
% list=list(1,3:end-1)';
list=list(1,3:end)';
nr = size(list,1);
Amount_Of_Images = nr


%%
dataplotding=100;
ni = 4;
Graphs_per_image = ni
samplemax = 200;
for i= 1 : nr*ni
    if (i-1)/ni == round(i/ni)
        nrtje = 2*((i-1)/ni+1)-1;
        figure(nrtje)
        filename = ['Pictures\'
char(list(ceil(i/ni)))]
        image1=imread(filename);
        imshow(image1,'InitialMagnification',
400);
        titles=filename;
        hold on
    else
    end

    % Initially, the list of points is empty.
    xy = [];

    n = 0;
    %Selecting the zero
    if (i-1)/ni == round(i/ni)
    disp('Left mouse button picks zero.')
    [xi,yi,but] = ginput(1);
        plot(xi,yi,'g+')
        zeroxy = [];
        for k = 1:ni
        zeroxy(:,(i+k)-1) = [xi;yi];
        end
    end
    % Loop, picking up the points.
    disp('Left mouse button picks points.')
    disp('Right mouse button picks last point.')
    but = 1;
    while but == 1
        [xi,yi,but] = ginput(1);
        plot(xi,yi,'r.')
        n = n+1;
        xy(:,n) = [xi;yi];
    end
    % Interpolate with a spline curve and finer
spacing.
    t = 1:n;
%    ts = 1: 0.1: n;
    ts = linspace(1,n,samplemax);
    xys = spline(t,xy,ts);

    % Plot the interpolated curve.
    plot(xys(1,:),xys(2,:),'r--');


    % theta=atan2((y(2:end)-y(1:end-1)),(x(2:end)-
x(1:end-1)));
    % theta=-theta;
    % THETA(:,i)=theta;

%    X(:,i)=xys(1,:);
%    Y(:,i)=xys(2,:);

    %eerste waarde op nul zetten
    if (i-1)/ni == round(i/ni)
        xtemp = xys(1,:)-zeroxy(1,i);
```

```matlab
        ytemp = -(xys(2,:)-zeroxy(2,i));
        %maximale & lengte x waarde bepalen
        maxxtemp = max(xtemp);
        xxtemp = xys(1,1);
        yytemp = xys(2,1);
        xxxtemp = dataplotding*xtemp/maxxtemp;
        xxxtemp2 = [xxxtemp; xxxtemp; xxxtemp;
xxxtemp]';
    else
        xtemp = xys(1,:)-zeroxy(1,i);
        ytemp = -(xys(2,:)-zeroxy(2,i));
    end
    %normalizeren door te delen met maximale
waarde x en vermenigvuldigen
    %met 100
    xtemp = dataplotding*xtemp/maxxtemp;
    ytemp = dataplotding*ytemp/maxxtemp;

    % output
    X(:,i)=xtemp;
    Y(:,i)=ytemp;

    order = 5; %order of the fit
    [p, s] = polyfit(xtemp,ytemp, order);
    Output = polyval(p,xxxtemp);
    Correlation= corrcoef(ytemp, Output);
    Ytje(:,i) = Output;
    Ptje(i,:)= p;

    % Combineren
    if i/ni == round(i/ni)
        initialvalue = round(0.55*samplemax);
        finalvalue = round(0.8*samplemax);
        rangetje =initialvalue:finalvalue;
        combinaties = combnk(1:ni,2);
        Temp = [];

        for j = 1: length(combinaties)
            first_value = (i-
(ni))+combinaties(j,1);
            second_value = (i-
(ni))+combinaties(j,2);

            Temp =
Ytje(rangetje,second_value)./Ytje(rangetje,first_v
alue);
            Tomp = Ytje(rangetje,second_value)-
Ytje(rangetje,first_value);
            Temp2(:,j) = Temp;
            Tomp2(:,j) = Tomp;
            Test(j) = std(Temp)*100/mean(Temp);
%relative standard error in %;
            Tost(j) = std(Tomp)*100/mean(Tomp);
%relative standard error in %;
        end
        combinaties;
        RelativeStandardErrorInPercent=[Test'
Tost' combinaties]

        figure((2*i)/ni)

        aa = subplot(2,1,2);
            plot(X(:,i-(ni-
1):i)/dataplotding,Y(:,i-(ni-1):i))
            hold on
            plot (xxxtemp2(rangetje,i-(ni-
1):i)/dataplotding,Ytje(rangetje,i-(ni-1):i),'R:')

xlim([xxxtemp2(initialvalue)/dataplotding,xxxtemp2
(finalvalue)/dataplotding])
            ylim('auto')
            set(gca, 'YTickLabelMode', 'Manual')
            set(gca, 'YTick', [])
            hold off

legend('line1','line2','line3','line4')
%           legend('line1','line2','line3')
            xlabel('Part of the range used')
            ylabel('Relative height')
            title('HDAU Polynomial Datafit')
        bb = subplot(2,1,1);
            plot(Temp2)
```

```matlab
            set(gca, 'XTickLabelMode', 'Manual')
            set(gca, 'XTick', [])
            xlim([0,length(Temp2)])
            xlabel('Part of the range used')
            ylabel('Amplification')

legend('line4/3','line4/2','line3/2','line4/1','li
ne3/1','line2/1')
%
legend('line2/1','line3/1','line3/1')
            title('HDAU Relative Amplification')
%         cc = subplot(3,1,3);
%             plot(Tomp2)
%             set(gca, 'XTickLabelMode', 'Manual')
%             set(gca, 'XTick', [])
%             xlim([0,length(Tomp2)])
%             xlabel('Part of the range used')
%             ylabel('Amplification')
%
legend('line4/3','line4/2','line3/2','line4/1','li
ne3/1','line2/1')
%             title('VS-Joint Relative
Amplification')

    else
    end


end
```